Use of various seeding light sources for seeding FEL

M. E. Couprie, Synchrotron SOLEIL

B. Carré, T. Ruchon, P. Salières: CEA-IRAMIS-SPAM

N. Joly : MPQ, Erlangen University

Seeding and self-seeding at New Fel sources, ICTP, Trieste, italy, 10-12 Dec. 2012

Motivation for seeding

seeding for performing the energy exchange :

=> bunching on the undulator fundamental and harmonics

Low gain case : coherent harmonic generation

High gain case :

- quicker saturation => compactness and cost
- improved stability (intensity, wavelength, jitter) => pump-probe user appplications
- «control» of temporal coherence properties : removal of spikes

Required properties of a seeding source

«Ideally» :

- wide spectral range : tuneability, short wavelength and ultimately handling of «gap scan» (FFDW orbit correction, synchronised change of seed wavelength, undulator gap and monochormator setting)

- Polarised for proper energy exchange in the undulator / adjustable polarisation

- high intensity : power overcoming shot noise *J.Wu et al, Appl. Phys. Lett. 90 (2007) 488*
L. Giannessi et al, FEL04 (2004) 37

cf strategies to reduce shot noise
A. Gover et al. PRL 102, 154801 (2009), A. Nause et al. J. Appl. Phys. 107, 103101 (2010)
V. Linvinenko, Proceeding FEL 09, Liverpool, 2009
D. Ratner et al., PRL 14, 060710 (2011)

- spectral bandwith - adapted to the gain bandwith?

- adjustable pulse duration / Chirp handling?

- repetition rate adapted to the the accelerator's one

Required diagnostics of a seeding source

- power level monitoring

- spectral tuning between the seed and the undulator radiation :
=> monochromator

- temporal synchrotronisation with the electron beam
=> photodiode, streak-camera.... with a radiation output of the electron beam (either undulator spotnaneous emission, or transition radiation in the chicane/ dogleg of injection...)

- proper focus in the undulator
=> telescope

- transverse overlap with the electron beam
=> profile monitor (CCD, Yag screeen, MCP....)

First coherent harmonic generation results

ACO (Orsay, France), 166 MeV

Nd-Yag at 1.06 µm, 20 Hz, 15 MW, 12 ns

=> CHG at 352 nm

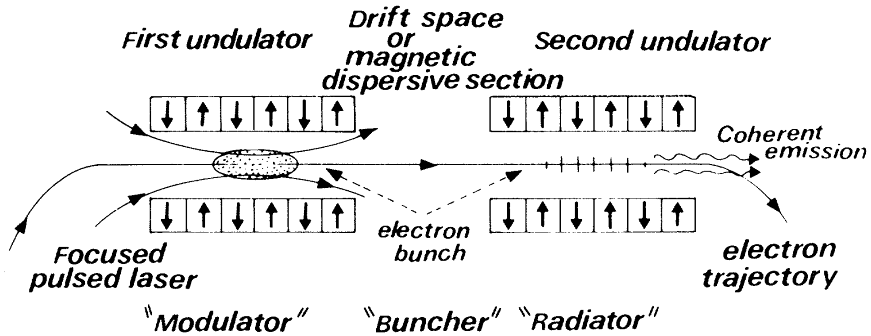

B. Girard, Y. Lapierre, J. M. Ortéga, C. Bazin, M. Billardon, P. Elleaume, M. Bergher, M. Velghe, Y. Petroff, *Opitcal frequency multiplication by an optical klystron*, Phys. Rev. Lett. 53 (25) 2405-2408 (1984)

352 nm
$R_3 = 3$

352 nm
$R_3 > 100$

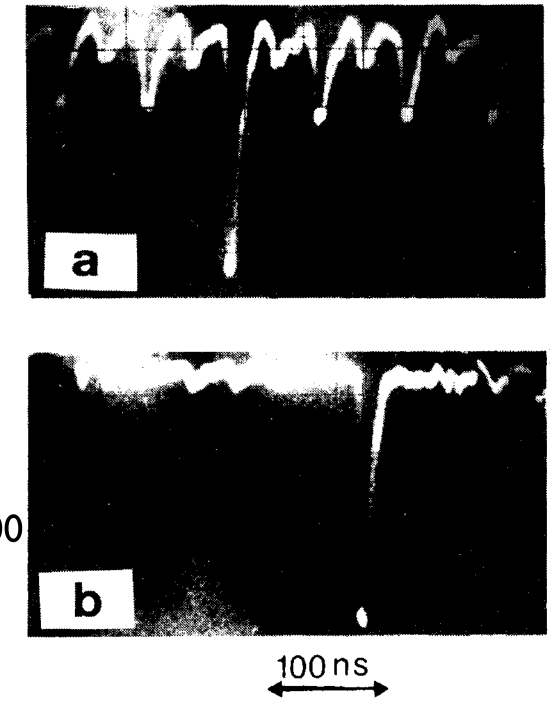

Linewidth sharpening

ACO (Orsay, France), 220 MeV

Nd-Yag at 1.06 µm (36 MW) /2 = 532 nm, => CHG at 177 and 106.4 nm

Coherent Harmonic Generation in the Vacuum Ultra Violet Spectral Range on the Storage Ring ACO, R. Prazeres, J.M. Ortéga, M. Billardon, C. Bazin, M. Bergher, M.E. Couprie, H. Fang, M. Velghe Y. Petroff, Nuclear Inst.and Methods in Physics Reasearch A272 (1988), 68-72

Experimental results on ACO (1987)

Observed harmonic	3	5
Corresponding wavelength [Å]	1773	1064
Integrated ratio R_n^{int}	350	3–4
monochromator bandwidth [Å]	2	2
monochromator angular aperture [mrad^2]	1.4	3
Spectral ratio $R_n(\lambda, \Omega)$	6000	100
Number of coherent photons/pulse	1.5×10^7	10^5
in spectral width [Å]	0.1	0.07
in angular aperture [mrad]	0 2	0.1

First coherent harmonic generation results

Super-ACO (Orsay, France), 700 MeV

Nd-Yag at 1.06 µm / 2 : 100 mJ, 300 ps, 300 MW, 10 Hz=> CHG at 177 nm and 106 nm

Coherent Harmonic Generation in VUV with the optical klystron on the storage ring Super-ACO, R. Prazeres, P. Guyot-Sionnest, D. Jaroszynski, J.M. Ortéga, M. Billardon, M. E. Couprie, M.Velghe Nucl.Inst. Meth.A 304 (1991) 72-76

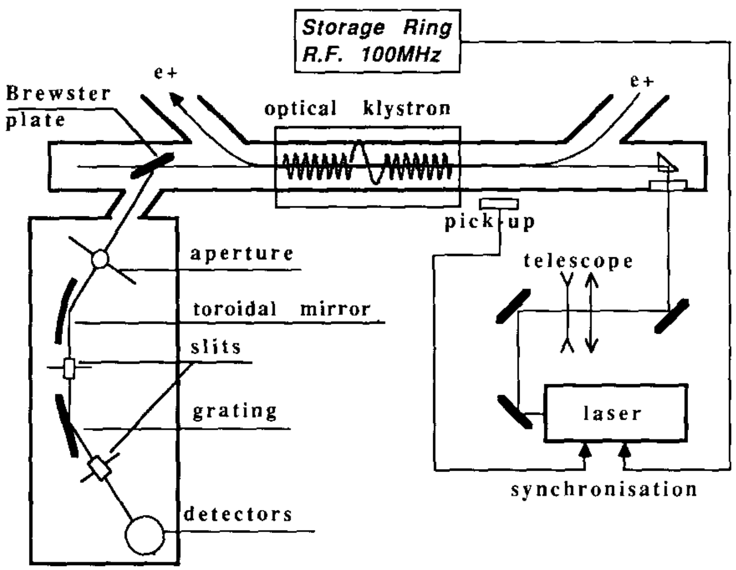

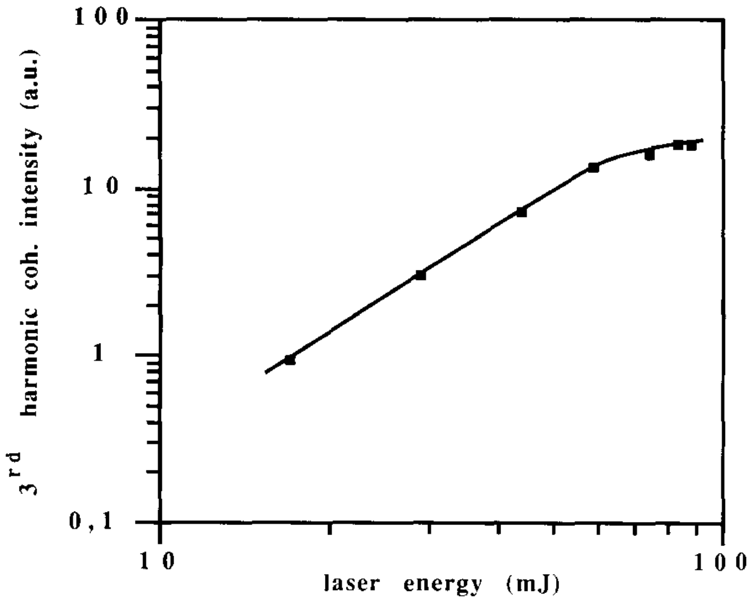

Positron beam			
Current per bunch, i [mA]	6.7	6.7	22
Energy spread, σ_γ/γ	5.6×10^{-4}	5.6×10^{-4}	9.5×10^{-4}
Bunch length, σ_z [ps]	100	100	160
Monochromator			
Resolution, $\delta\lambda$ [Å]	12	2	4
Angular aperture, $\delta\theta$ [mrad]	0.3	0.3	1
Integrated ratio			
Measured, R_n^{int}	270	1400	25
Theoretical, R_n^{int}	3200	20000	260
Spectral ratio, $R_n^{spe}(\lambda,\theta)$	5×10^5	5×10^5	1200
Coherent photons, N_{coh}	4×10^8	4×10^8	4×10^7

Coherent harmonic generation : ex of use of circular polarisation

UVSOR-II, helical optical klystron, change of the laser polarisation

H2 intensity ratio

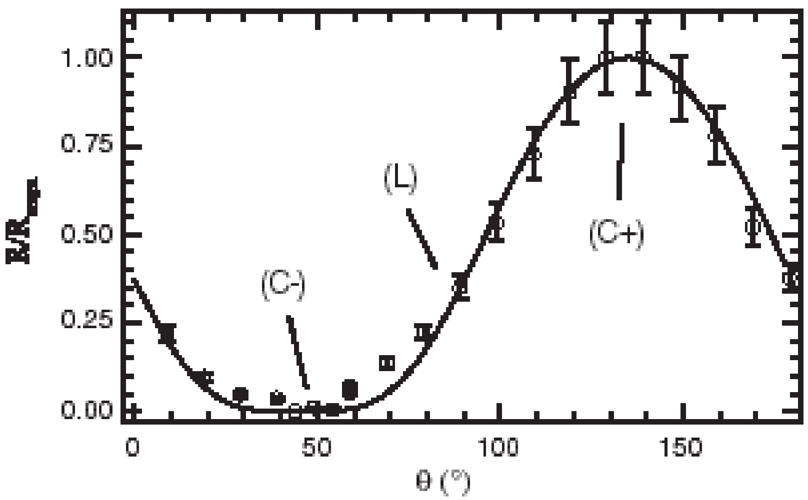

laser helicity

enhancement of laser power (focusing, intensity)
=> broadening due to overmodulation

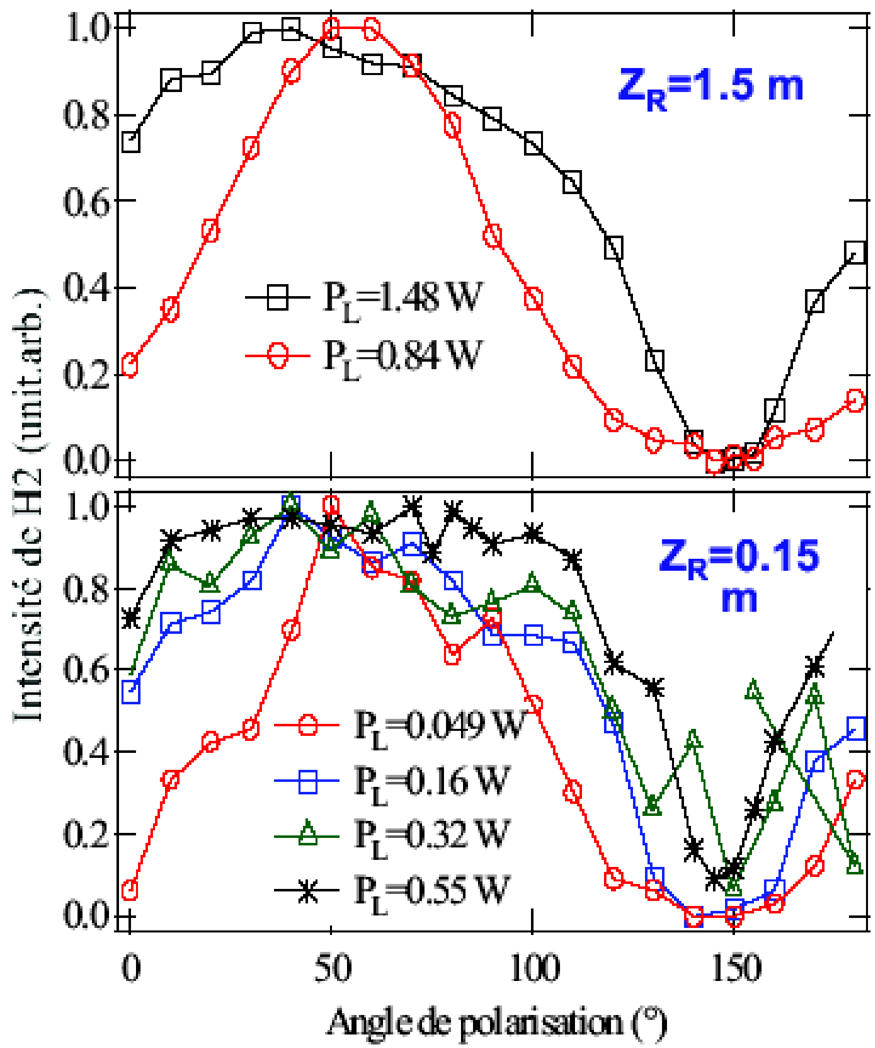

M. Labat, M. Hosaka, M. Shimada, M. Katoh, M.E. Couprie, "Optimization of a seeded Free-Electron Laser with helical undulators", Phys. Rev. Lett. 101, 164803 (2008).

HGHG at BNL

L. H.Yu et al, Science 289, 2000, 932 *L. H.Yu et al, PRL91 2003, 074801*

- Temporal Coherence properties given by the seed (external laser) => High degree of temporal coherence

Stability (reduction of intensity fluctuations and jitter) for user applications (pump probe)

Quicker Saturation => Compactness and cost

DUVFEL (210 MeV, 30 mJ- 800 nm Ti:Sa laser)

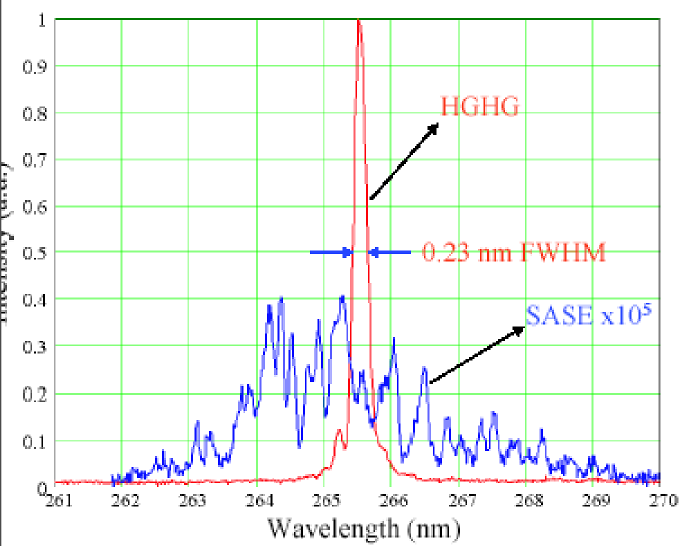

Spectral narrowing

Non Linear Harmonics

Shot to Shot Intensity Fluctuation

Shows High Stability of HGHG output

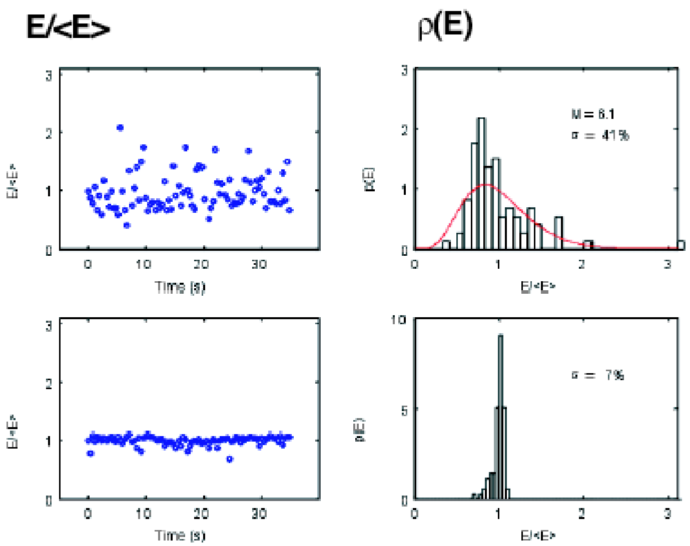

Courtesy L. H. Yu

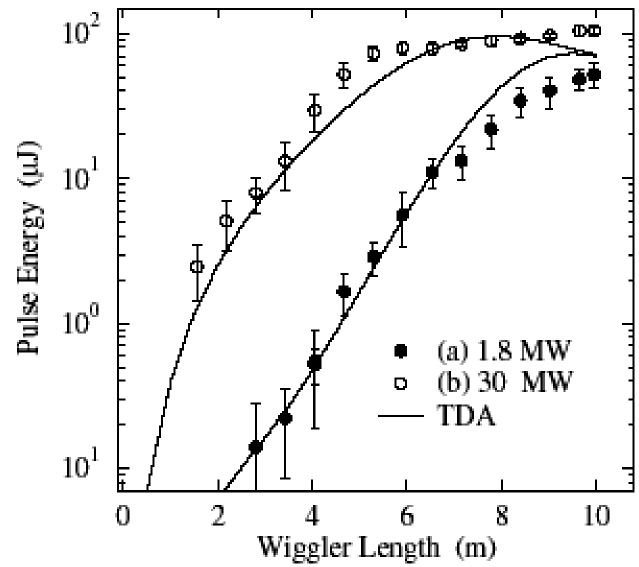

... 2. Pulse energy versus distance in the radiator for two values of the seed laser input power: (a) 1.8 MWand (b) 30 MW. The solid curves are simulation results by the TDA code.

Regimes for seeding

Super-radiant mode

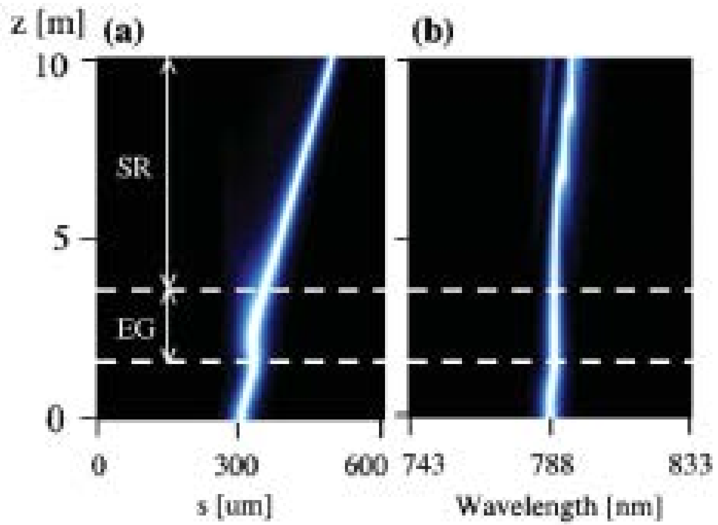

L. Giannessi et al, Appl. Optics 2005, slippage length/potential depth

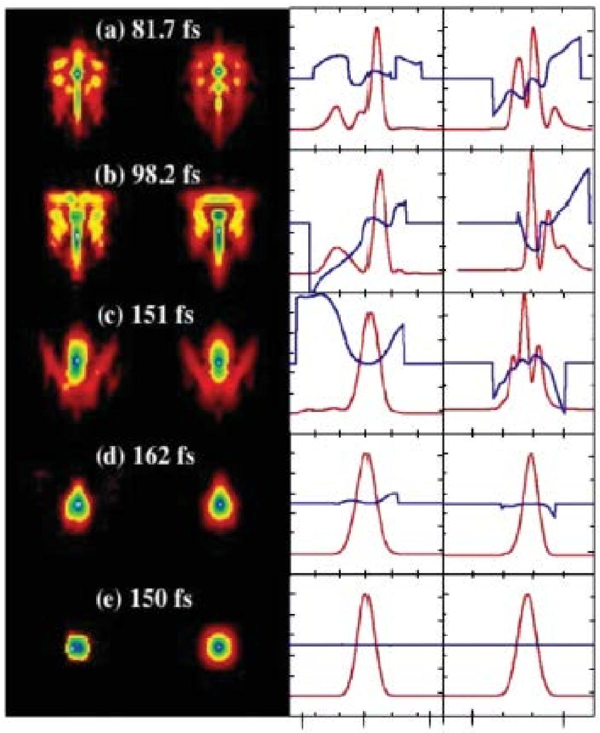

T. Watanabe et al. PRL 98, 034802 (2007)

pulse splitting

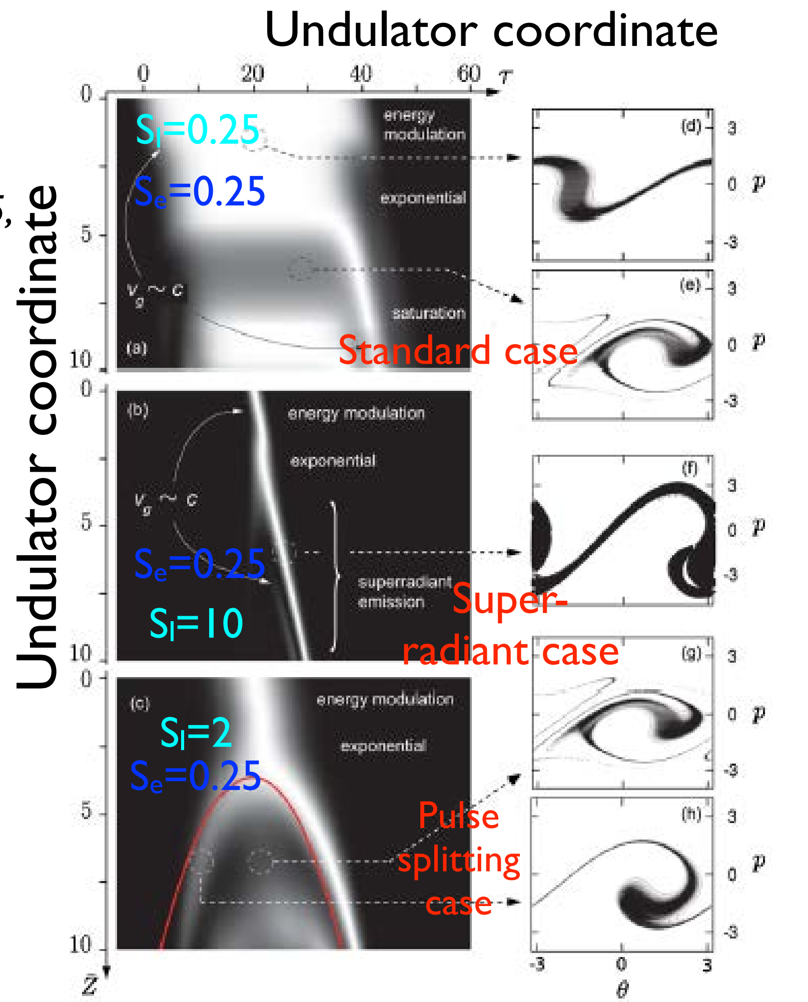

$$S_e = \frac{4\pi\rho N}{L_{..}}$$

$$S_{seed} = \frac{4\pi\rho N}{L_{seed}}$$

M. Labat, N. Joly, S. Bielawski, C. Szwaj, C. Bruni, M.E. Couprie, Pulse splitting in short wavelength seeded FEL, Phys. Rev. Lett. 103, 264801 (2009)

Making use of chirp for tuneability

• Tuneability of the seed

• Combinaison of the chirp on the electron beam and the laser

T. Shaftan, BNL workshop, 04

S. Biedron et al., NIM A475, 401;T. Shaftan, PRE 71, 2005, 046501

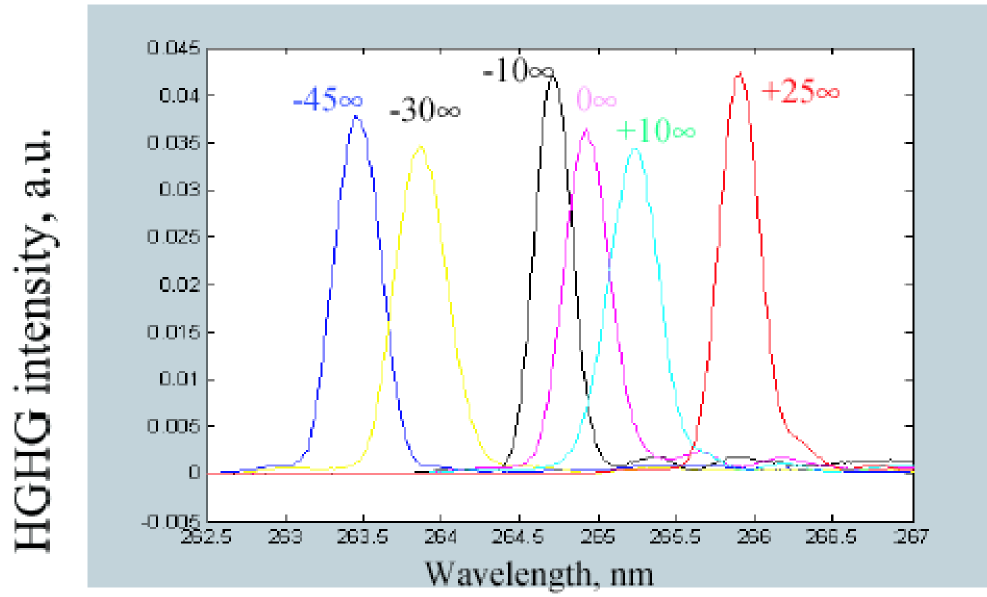

High Harmonic in Gas source

Mc Pherson et al., JOSA B 4, 595 (1987) (Chicago)

M. Ferray et al., J. Phys. B 21, L31 (1988) (Saclay)

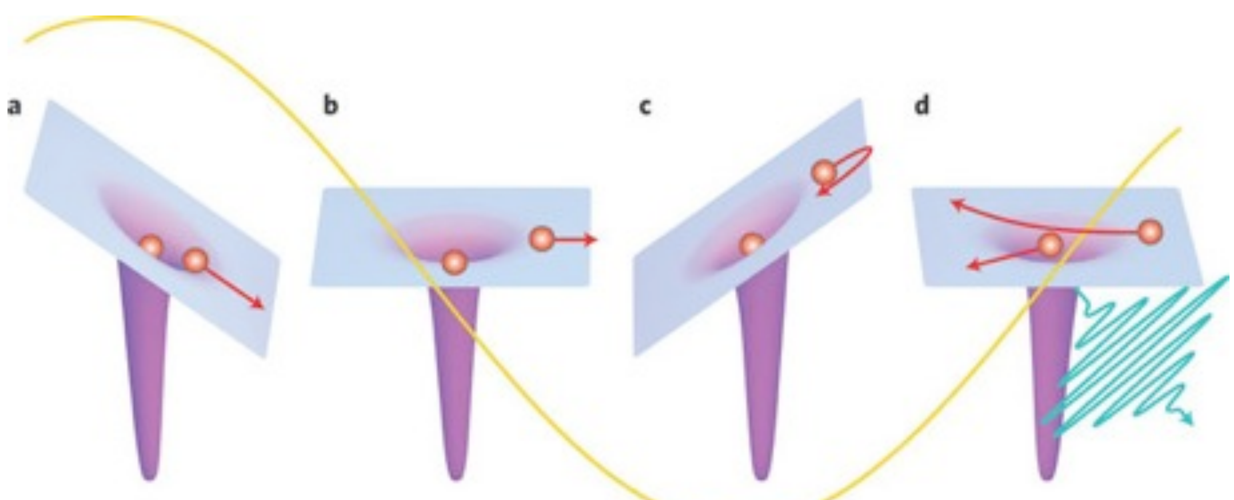

Tunnel ionization   Acceleration and diffusion   Recombination

K. Midorikawa, Ultrafast dynamic imaging, Nature Photonics 5, 640–641 (2011)

High Harmonic in Gas source

Mc Pherson et al., JOSA B 4, 595 (1987) (Chicago)

M. Ferray et al., J. Phys. B 21, L31 (1988) (Saclay)

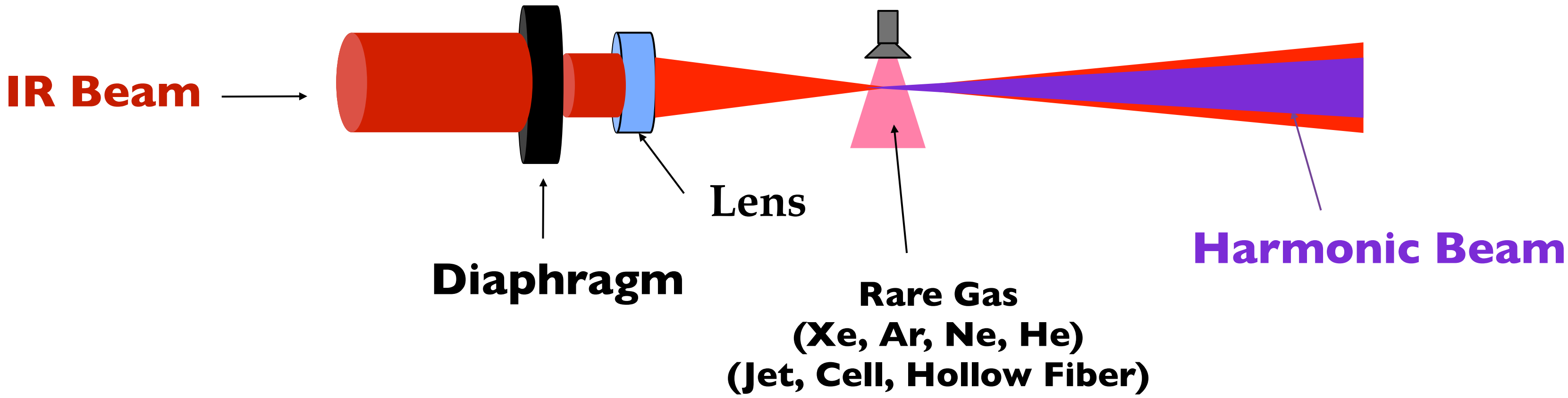

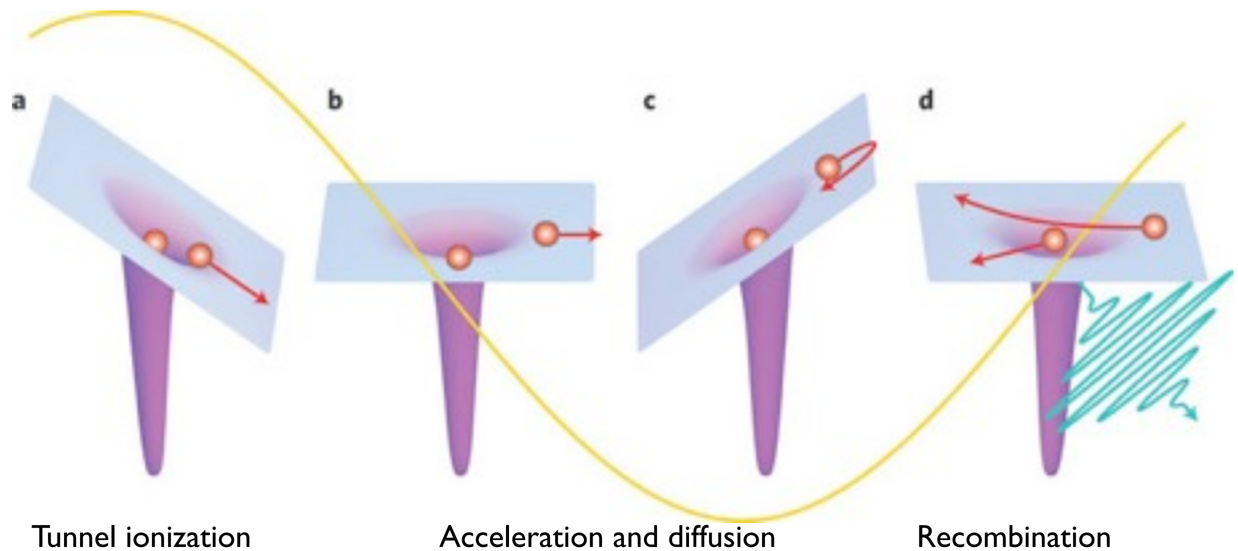

K. Midorikawa, Ultrafast dynamic imaging, Nature Photonics 5, 640–641 (2011)

High Harmonic in Gas source

Mc Pherson et al., JOSA B 4, 595 (1987) (Chicago)

M. Ferray et al., J. Phys. B 21, L31 (1988) (Saclay)

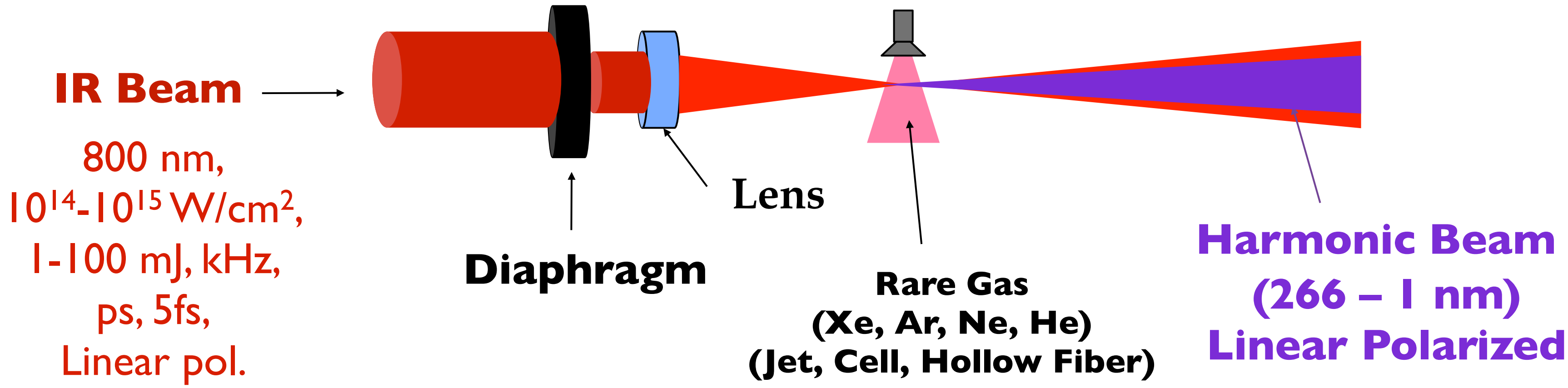

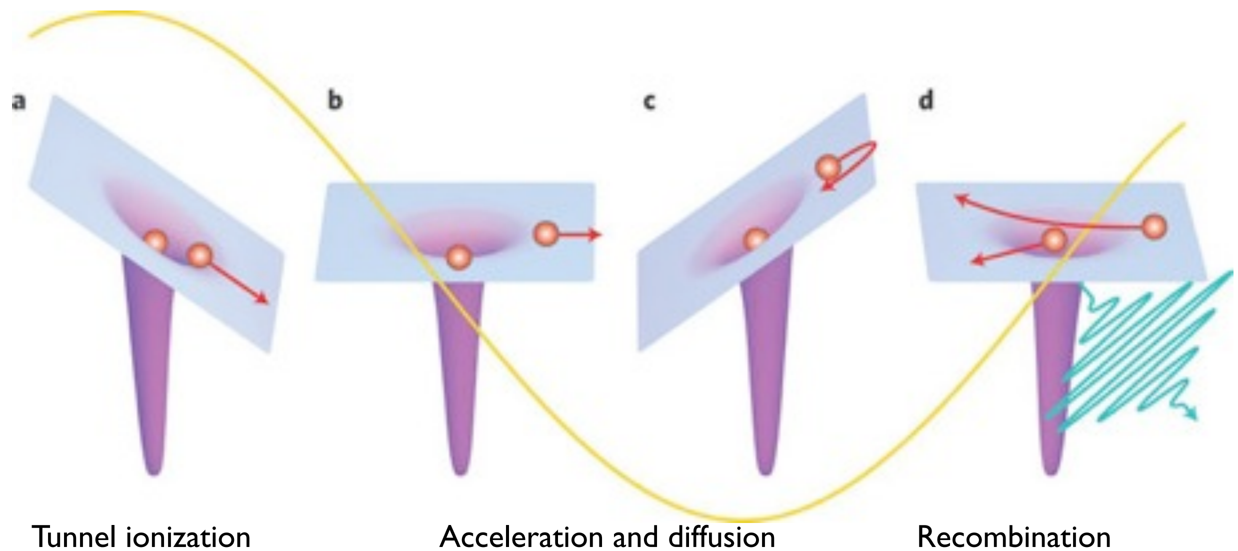

K. Midorikawa, Ultrafast dynamic imaging, Nature Photonics 5, 640–641 (2011)

III-Short wavelength with HHG

High Harmonic in Gas source

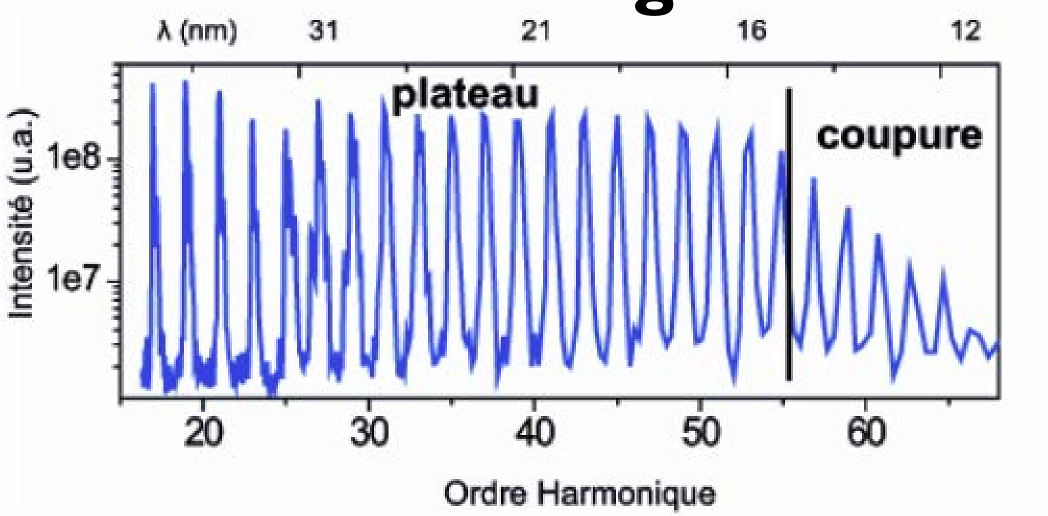

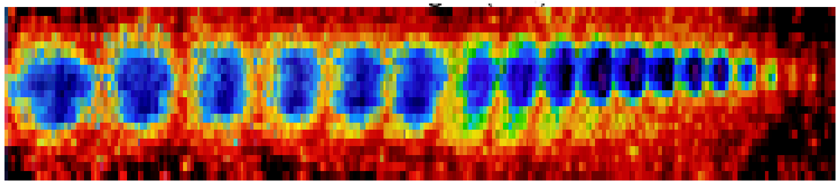

Water window (Ti:Sa 26 fs, 2.7 nm (460 eV) He, 5.2 nm (239 eV) Ne)

longer wavelength

atoms (Ne I_p=21.6 eV, He I_p=24.6 eV), ions

$$h\nu_{\text{cutoff}} = I_p + \frac{0.5 I_p^{3+a}\lambda^2}{\left[\ln \frac{0.86\Delta t)^{2n^*-1} G_{lm} C_{n^* l^*}^2 I_p}{-\ln(1-p)}\right]^2}$$

short pulses (5-7 fs: approching the one cycle limit)

Tuneability of the HHG seed:

- by the laser tuneability
- by frequency mixing ~70% tunability from 180 to 18 nm

with Ti:Sa + OPG *Gaarde et al., J. Phys B 29, L163 (1996)*

- by ajustment of the laser energy, chirp

•*Kim et al., PRA 67 (2003)*

Full tunability from 220 nm to 8 nm with 1.1 to 1.6 µm pump (Ti:Sa + OPA) *Chang et al..Phys. Rev. A 65 (2001)*

Reduction of the cut-off wavelength:

-Ionisation potential: atoms (Ne I_p=21.6 eV, He I_p=24.6 eV), => ions *Milosevic et al. PRA63 (2000)*

- laser of long wavelength *Chang et al., PRA 65 (2001)*
- short pulses

Z. Chang et al, PRL 79, 1997, 2967

Gibson, Science, 2003. Seres et al, Nature 2005

B. Shang et al, PRA 65, 2001, 011804

> 10 nJ/ pulse @ 4.37 nm

M. Zepf et al, PRL 99, (2007), 143901

High Harmonic in Gas source

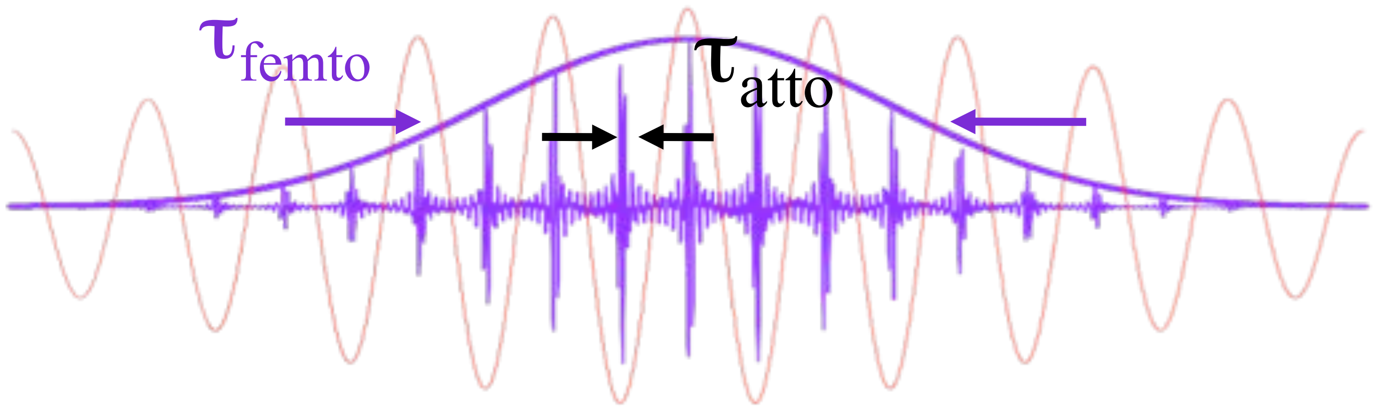

Time domain

High Harmonic in Gas source

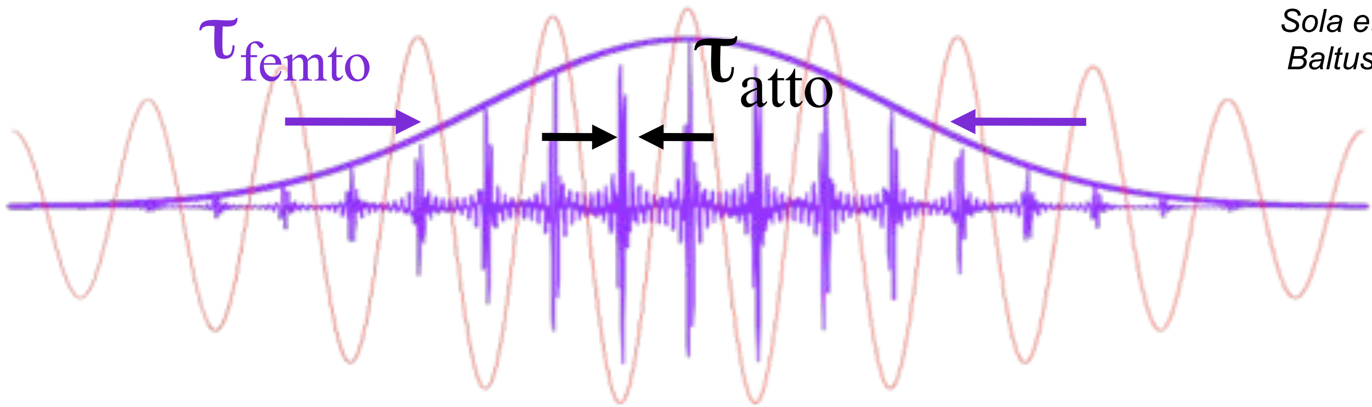

Isolated atto pulse :

« Amplitude » or « Polarization » gating

Sola et al., Nature Physics (2006)
Baltuska et al. Nature 421 (2003)

Time domain

High Harmonic in Gas source

Isolated atto pulse :

« Amplitude » or « Polarization » gating

Sola et al., Nature Physics (2006)
Baltuska et al. Nature 421 (2003)

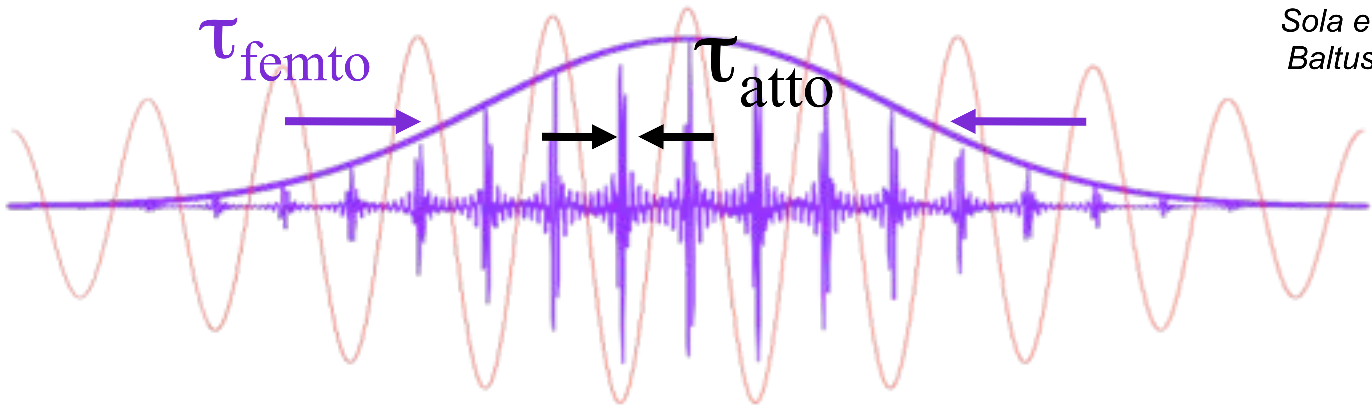

Time domain

$\Delta\nu_{atto} \sim 1/\tau_{atto}$

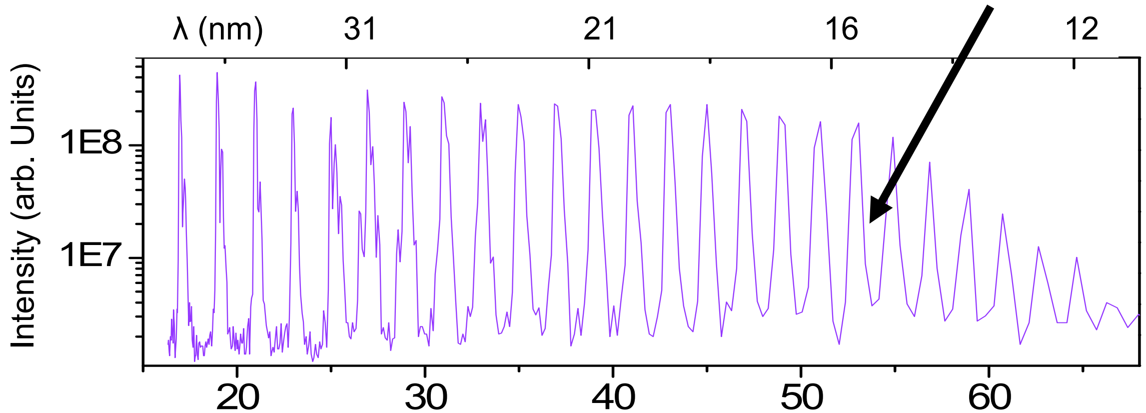

Spectral domain

High Harmonic in Gas source

Isolated atto pulse :

« Amplitude » or « Polarization » gating

Sola et al., Nature Physics (2006)
Baltuska et al. Nature 421 (2003)

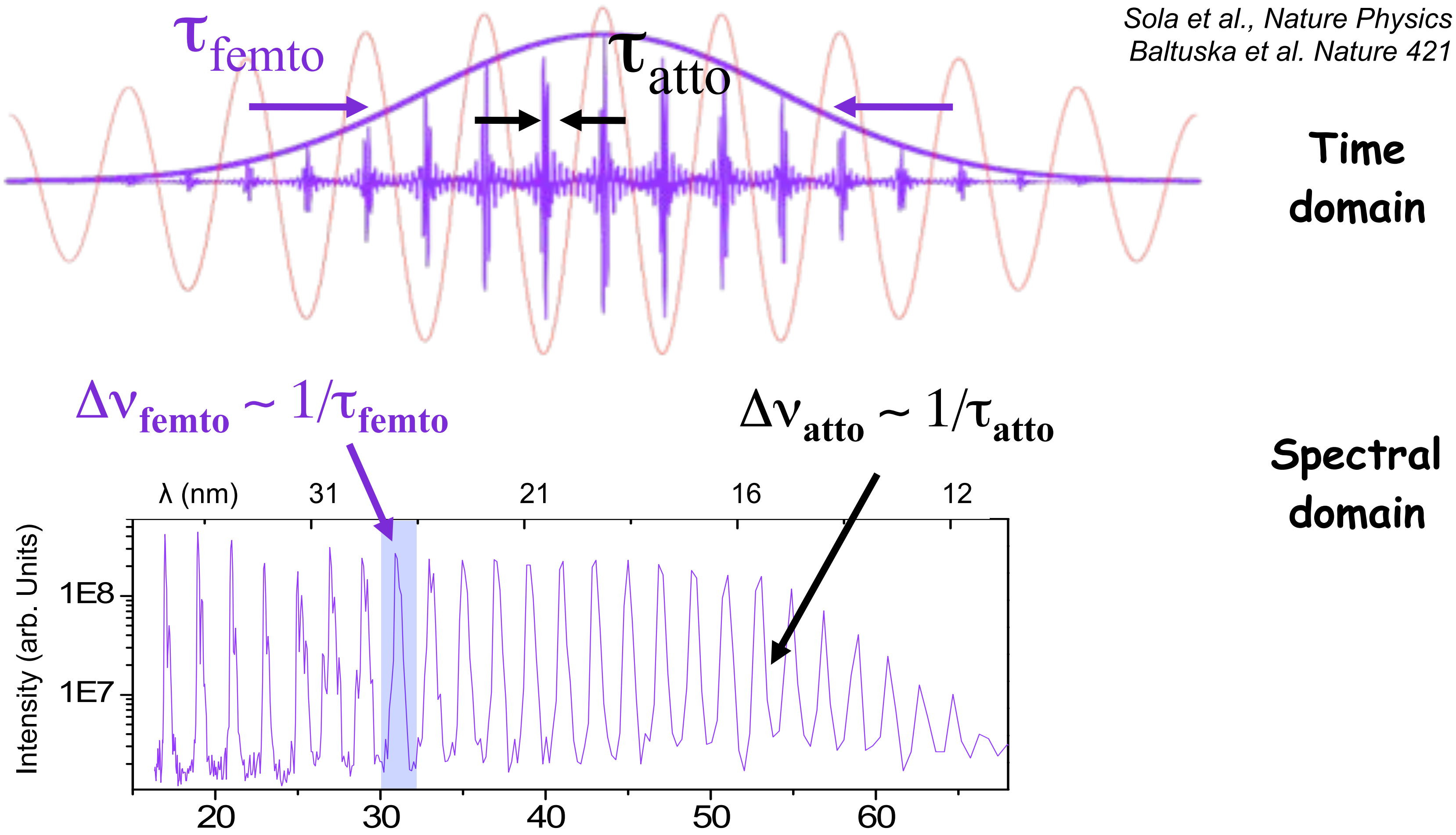

III-Short wavelength with HHG

High Harmonic in Gas source

Isolated atto pulse :

« Amplitude » or « Polarization » gating

Sola et al., Nature Physics (2006)
Baltuska et al. Nature 421 (2003)

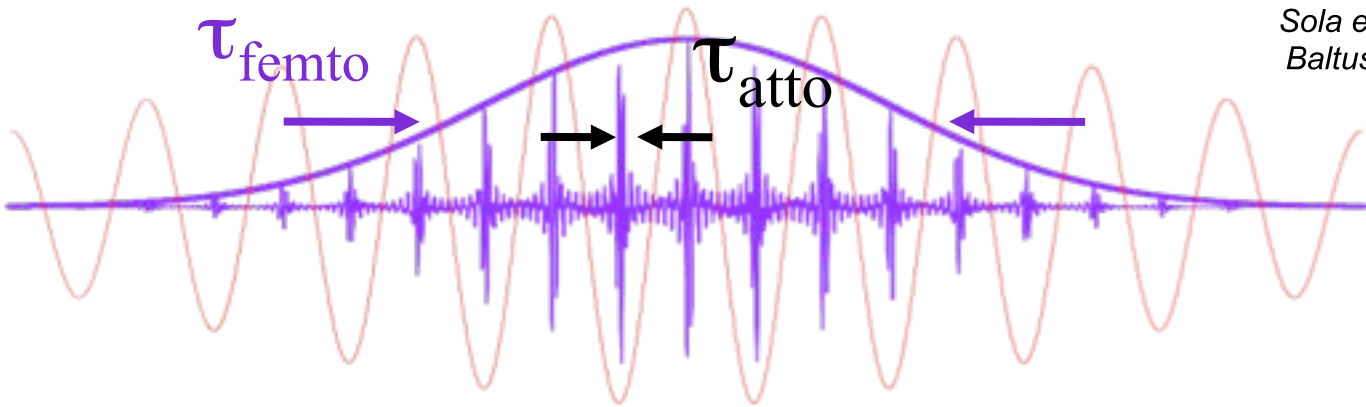

Time domain

$\Delta\nu_{femto} \sim 1/\tau_{femto}$

$\Delta\nu_{atto} \sim 1/\tau_{atto}$

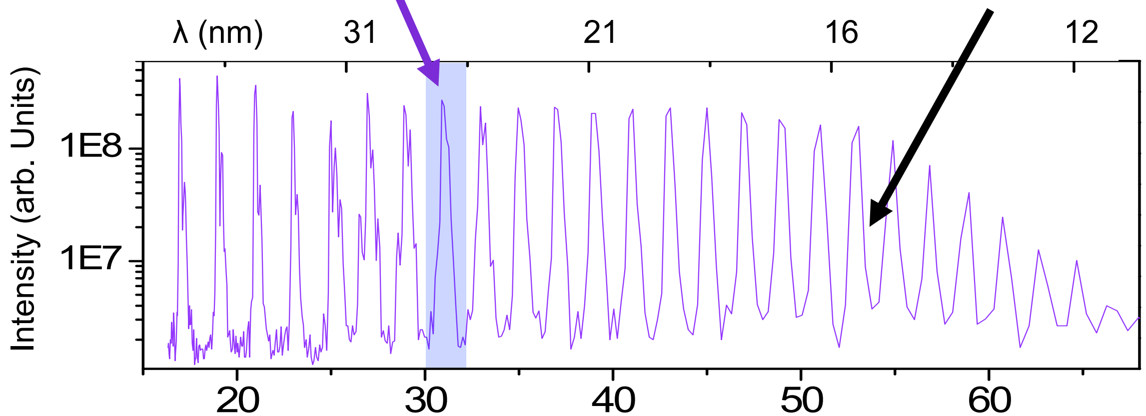

Spectral domain

Harmonic train (atto pulse): linear phase

III-Short wavelength with HHG

High Harmonic in Gas source

Isolated atto pulse :

« Amplitude » or « Polarization » gating

Sola et al., Nature Physics (2006)
Baltuska et al. Nature 421 (2003)

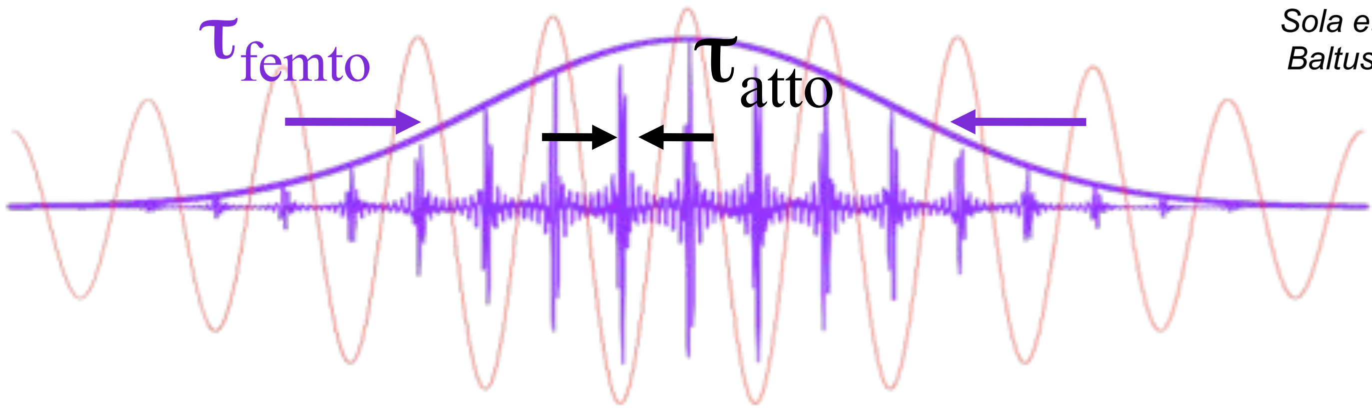

Time domain

$\Delta\nu_{femto} \sim 1/\tau_{femto}$

$\Delta\nu_{atto} \sim 1/\tau_{atto}$

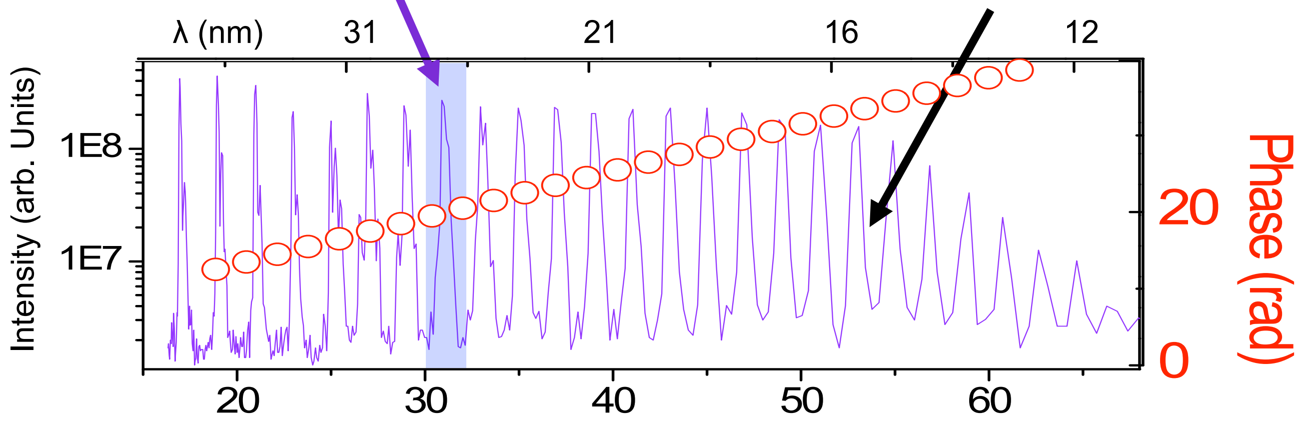

Spectral domain

Harmonic train (atto pulse): linear phase

High Harmonic in Gas source

Isolated atto pulse :

« Amplitude » or « Polarization » gating

Sola et al., Nature Physics (2006)
Baltuska et al. Nature 421 (2003)

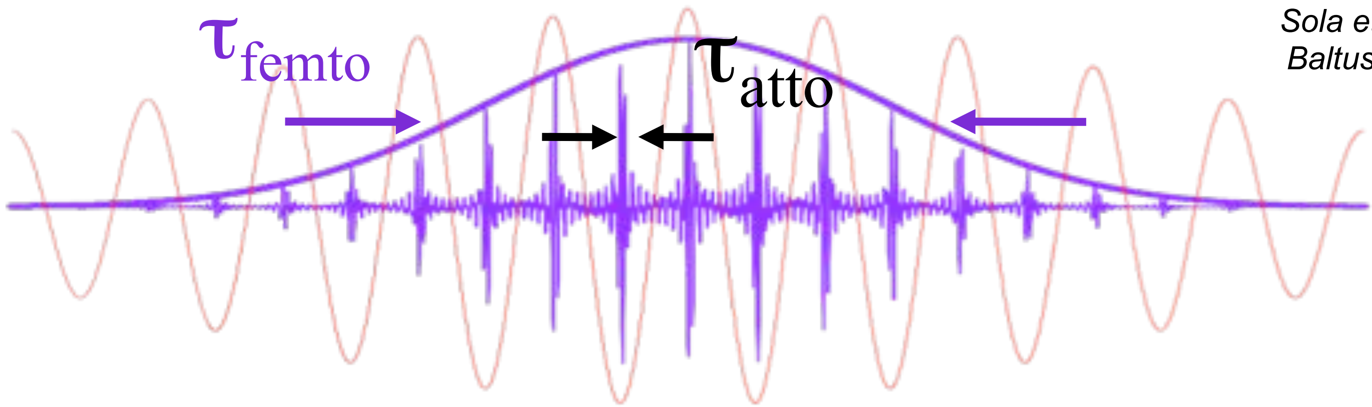

Time domain

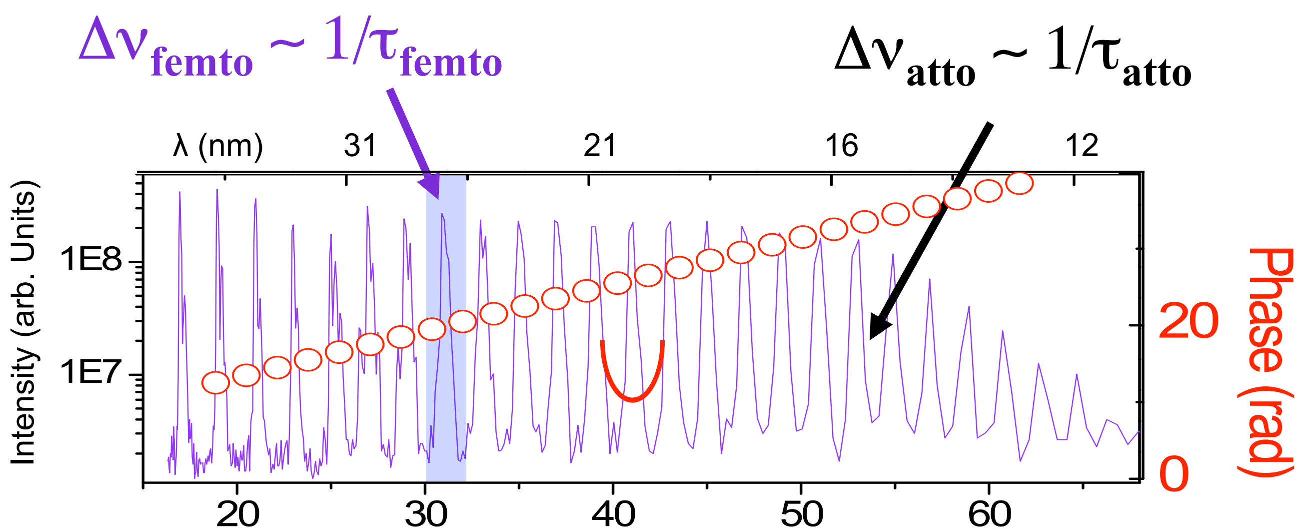

Spectral domain

Harmonic train (atto pulse): linear phase

Single harmonic (fs pulse): ~ quadratic phase (can be compensated)

III-Short wavelength with HHG

High Harmonic in Gas source

Fresnel bi interferometer

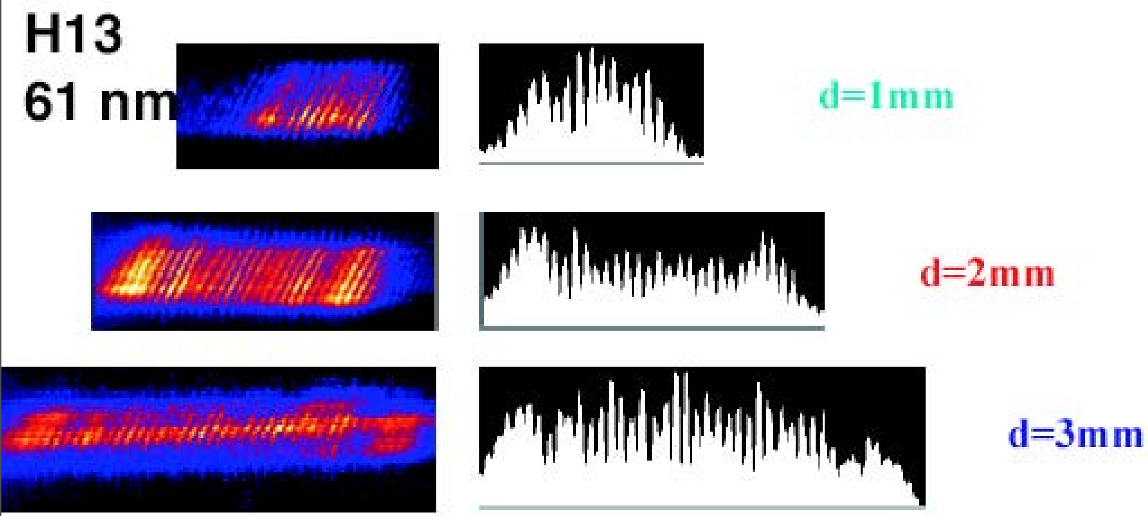

Le Déroff et al., PRA61 (2000) 043802

Ne, 13.5 nm, 25 nJ, DV=0.35 mrad
He, 8.9 nm, 1 nJ, DV=0.3 mrad

E.J.Takahashi et al., Apply. Phys. Lett 84, 4 (2004)
Opt. Lett. 27, 2000, 1920
Phys. Rev A 68, 2003, 023808
Y.Tamaki et al, JJAP 40, 2001, L1154
Y. Mairesse et al, Science 302, 1540
Sola et al., Nature Physics (2006)
Baltuska et al. Nature 421 (2003)

Young pineholes

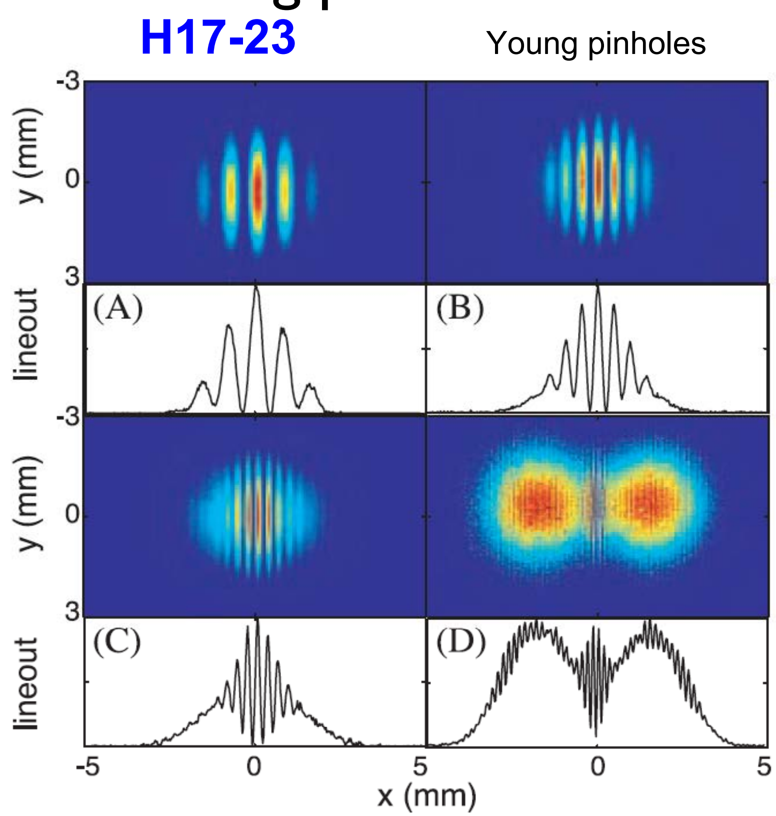

Bartels et al., Science 297,376 (2002)

$1.2<M^2<4$

Le Déroff et al., Optics Lett. 23 (1998)

Issues for alignment and synchronisation

Monitoring the UV -VUV radiation of simply the generating laser?

Spatial overlap

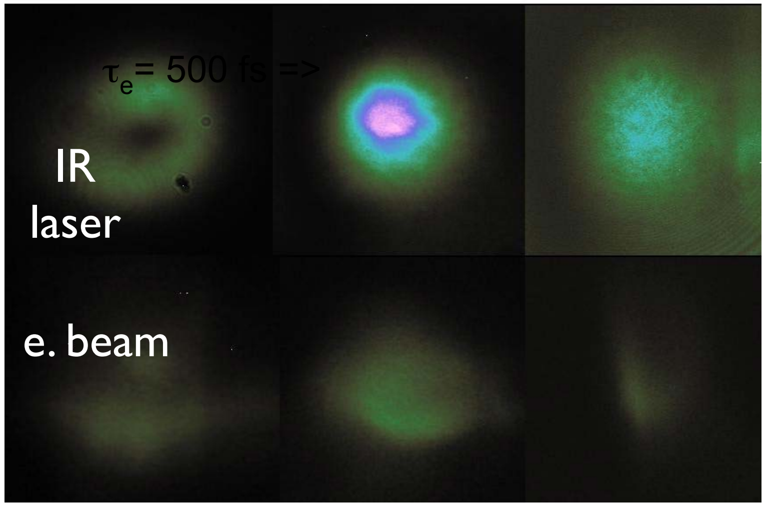

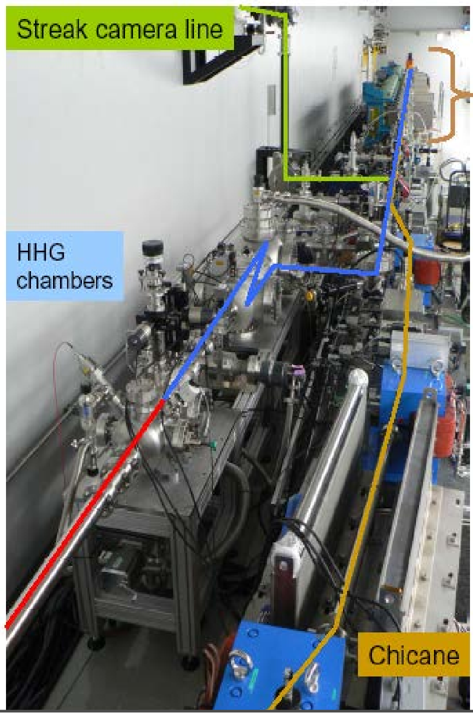

SCSS Test Accelerator

Synchronisation

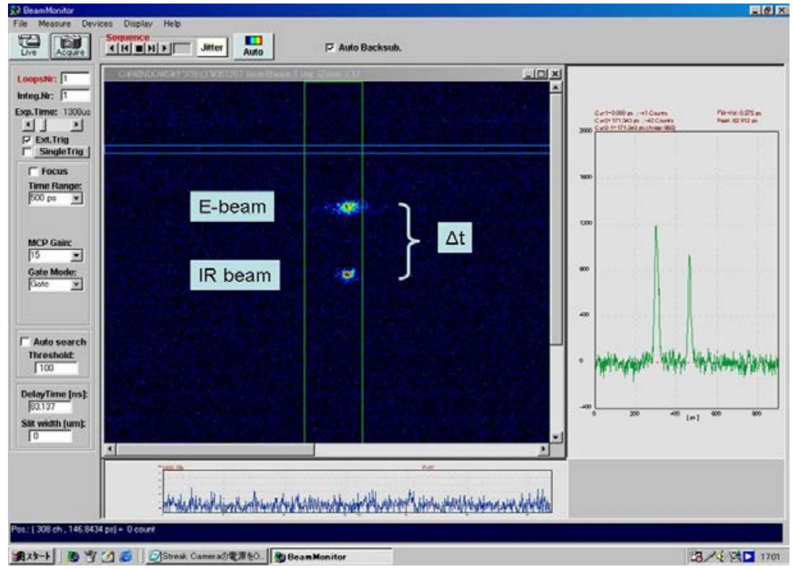

SCSS Test Accelerator

Spectral tuning

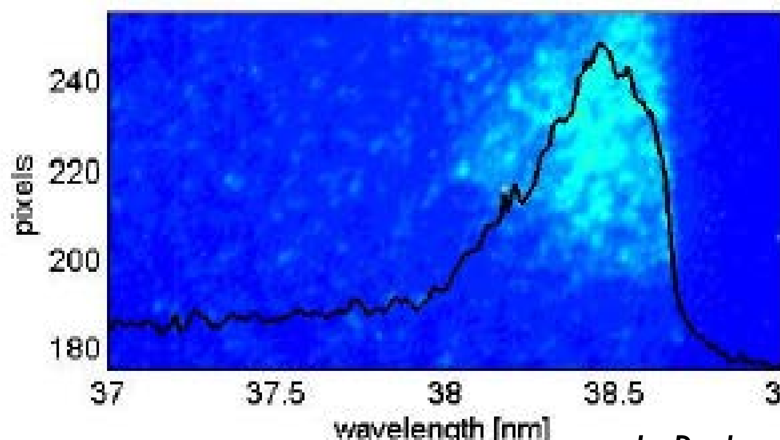

S-FLASH

J. Bodewadt FEL 2010 Malmö

First demonstration of HHG seeding on the SCSS Test Accelerator (Japan)

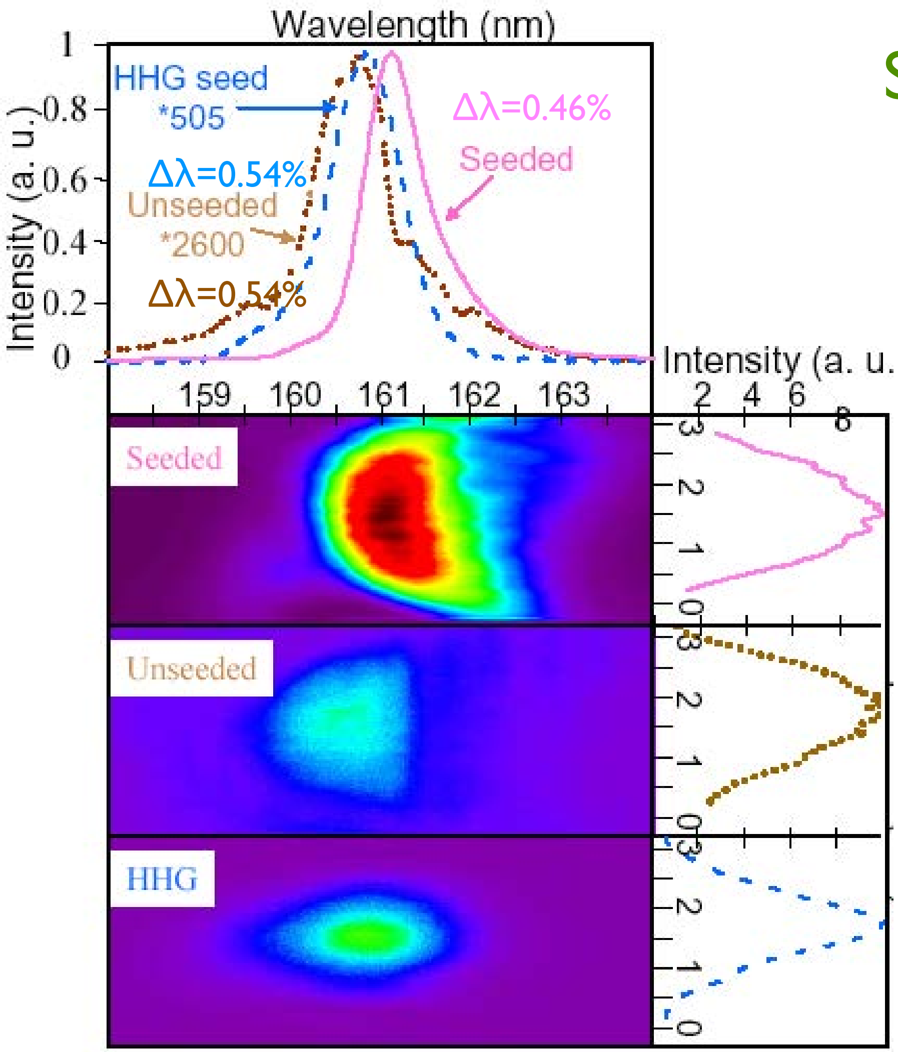

Seed : 160 nm, 1 4.5 m long section of undulator, 150 MeV

Rather good alignement and spectral tuning, 0.3 nJ seed

- Larger amplification
- Spectral narrowing => Improvement of the longitudinal coherence

G. Lambert et al., Nature Physics Highlight, (2008) 296-300

First demonstration of HHG seeding on the SCSS Test Accelerator (Japan)

Seed : 160 nm, 2 sections of 4.5 m long undulator, 150 MeV

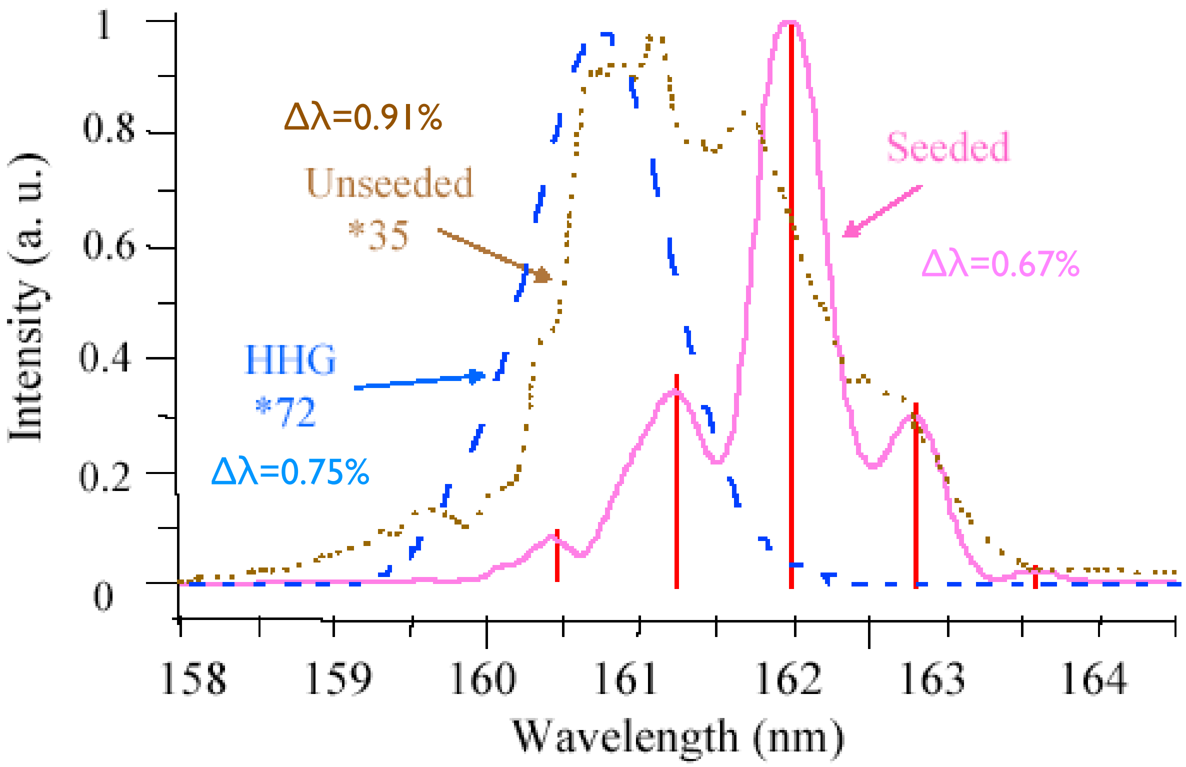

Imperfect alignement, seed 3 nJ

- saturation for the HHG seeded FEL (sidebands)
- larger redshift
- smaller spectral narrowing
- limited amplification with respect to SASE

G. Lambert et al., Nature Physics 889 (2008) 296-300

First demonstration of HHG seeding on the SCSS Test Accelerator (Japan) : wavelength stability

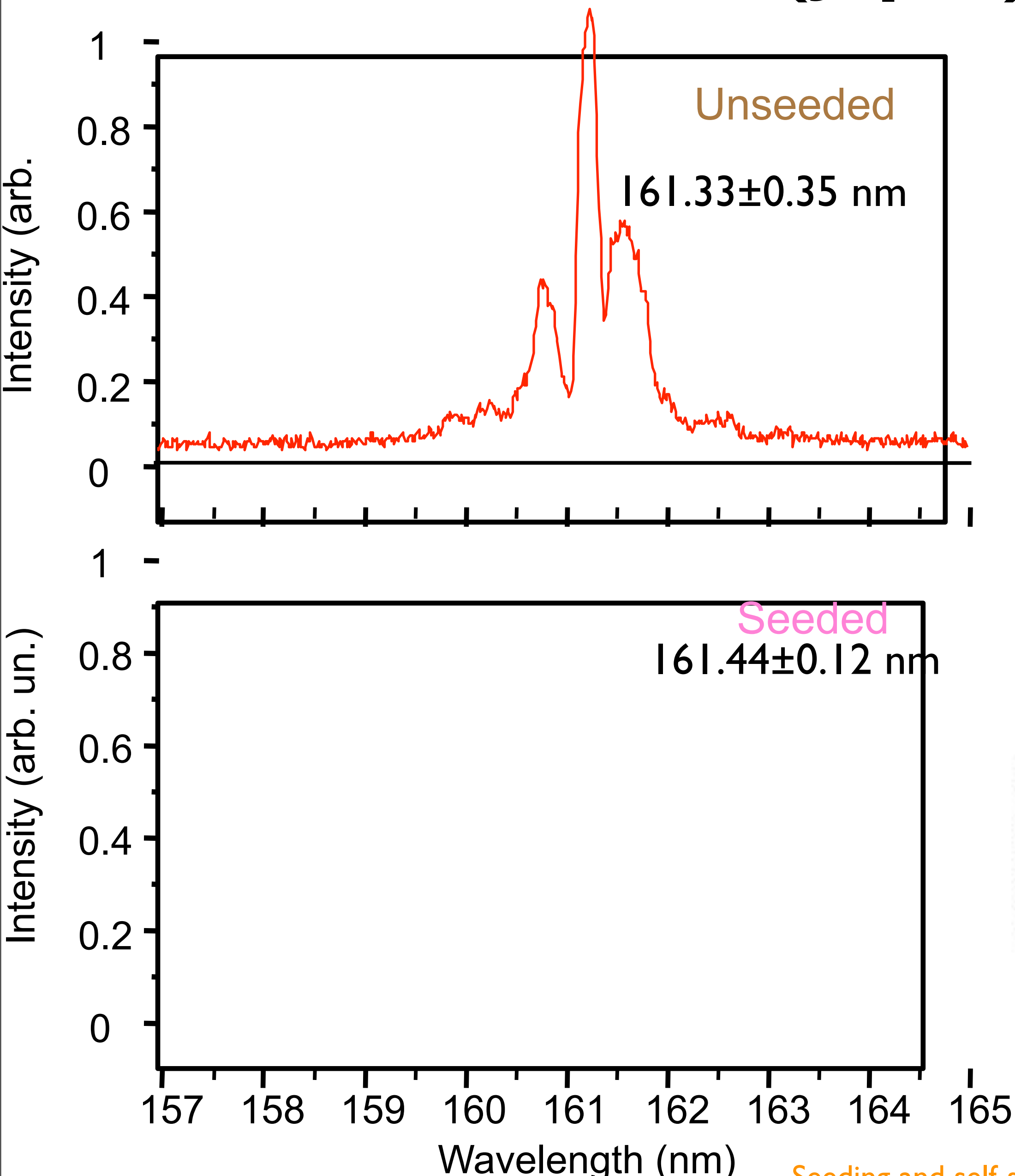

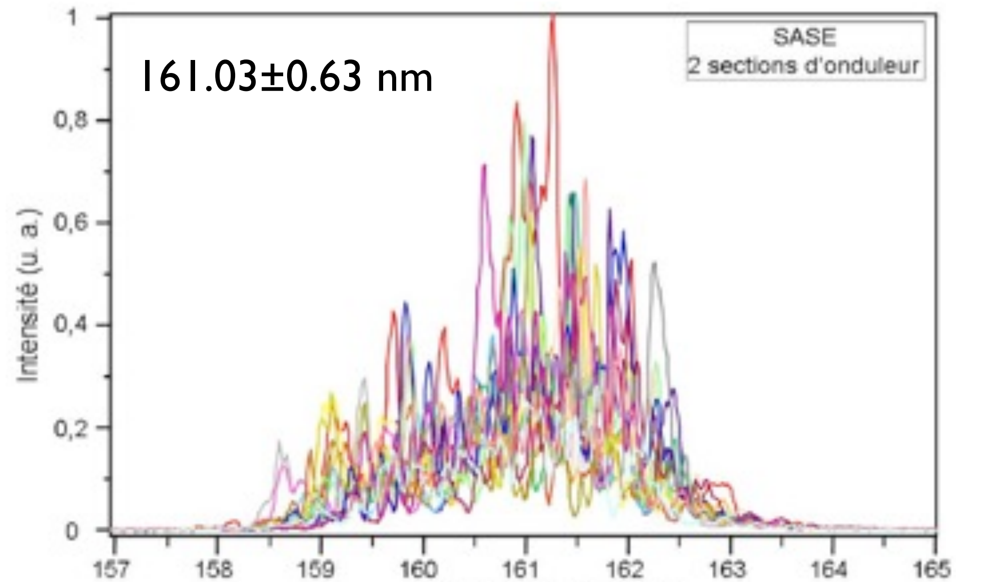

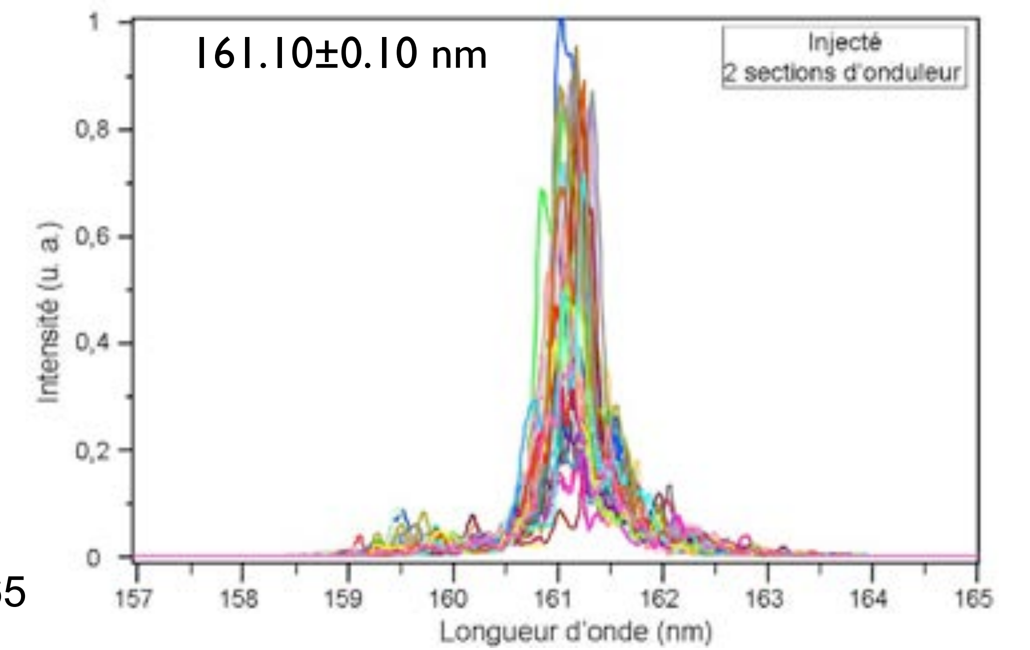

III-Short wavelength seeding with HHG

First demonstration of HHG seeding on the SCSS Test Accelerator (Japan) : wavelength stability

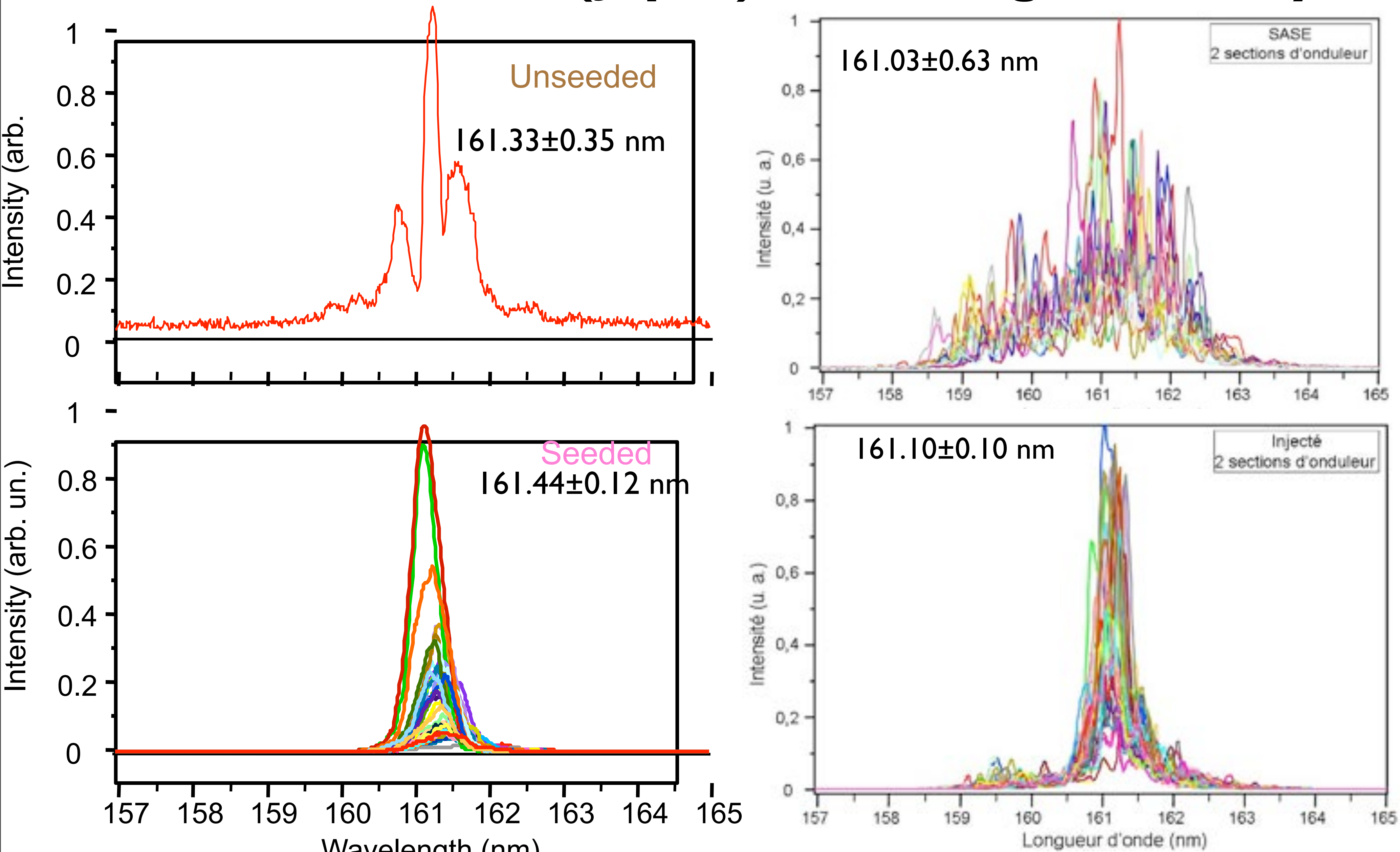

Seeding and self-seeding at New Fel sources, ICTP, Trieste, italy, 10-12 Dec. 2012

First demonstration of HHG seeding on the SCSS Test Accelerator (Japan) : wavelength stability

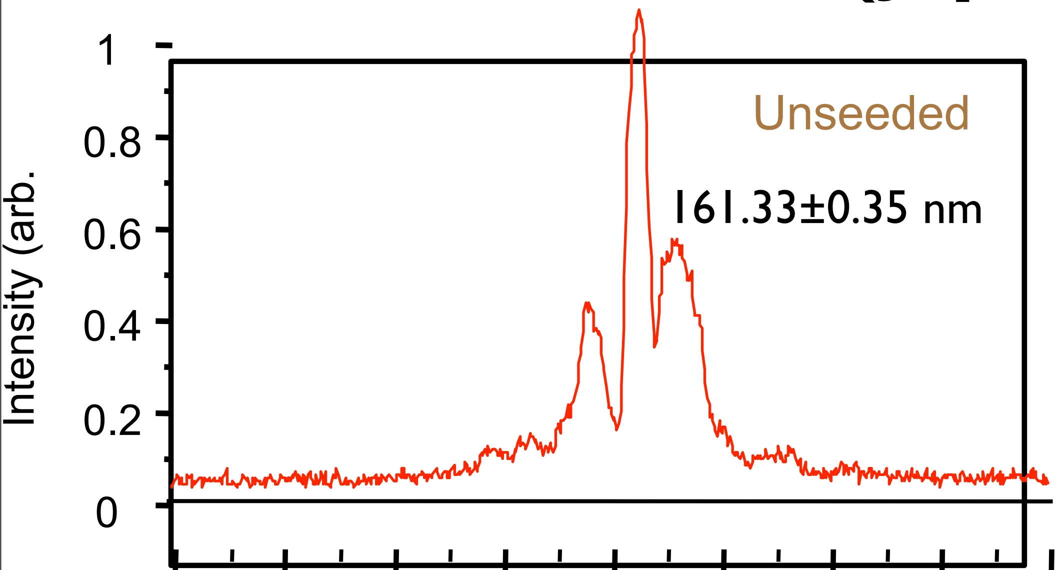

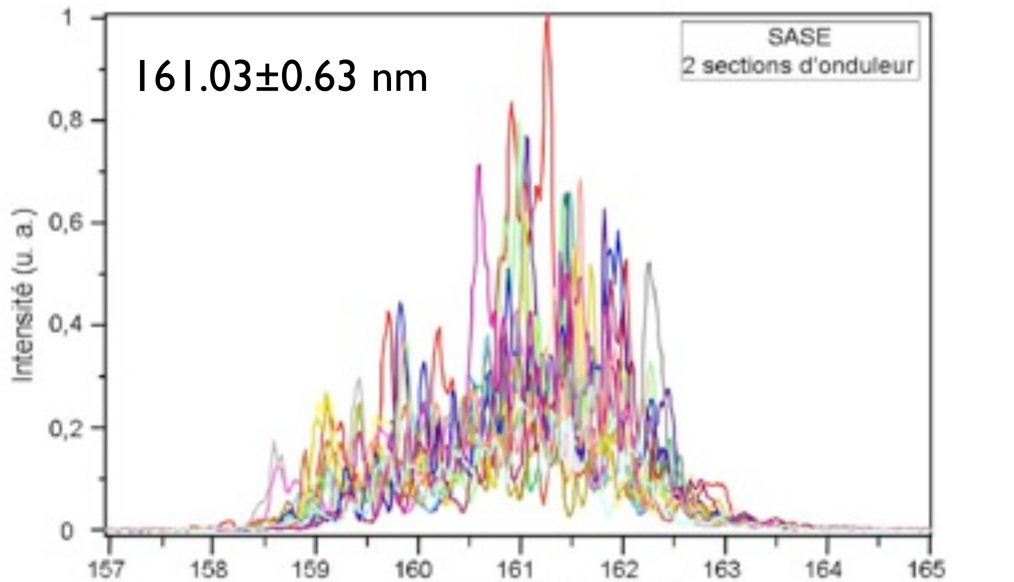

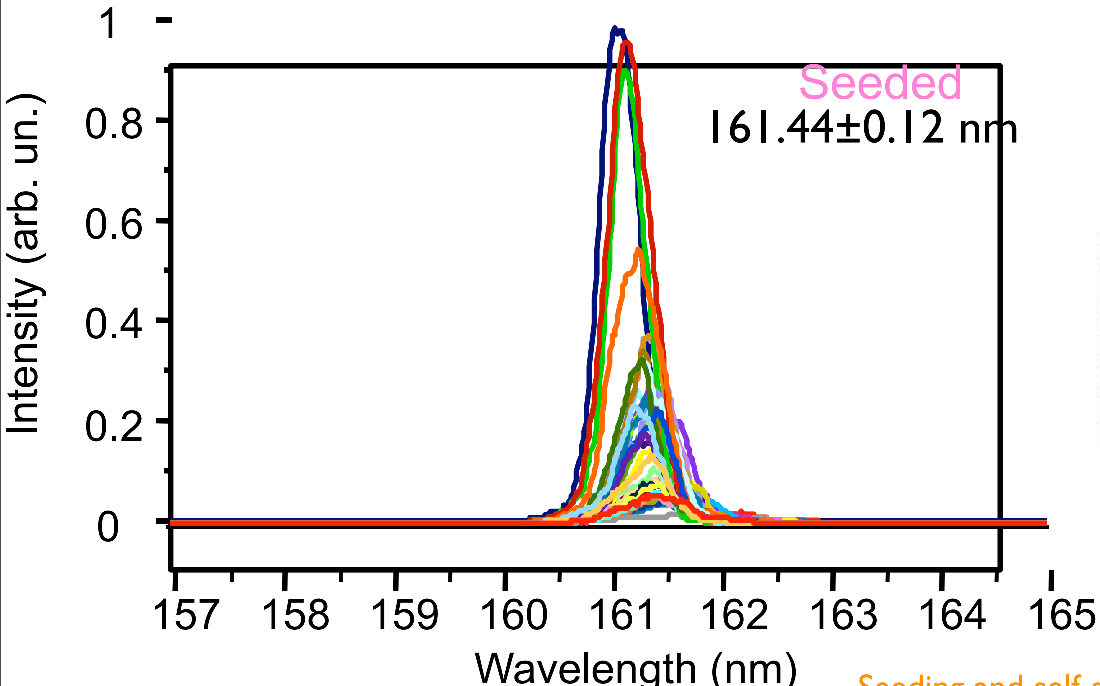

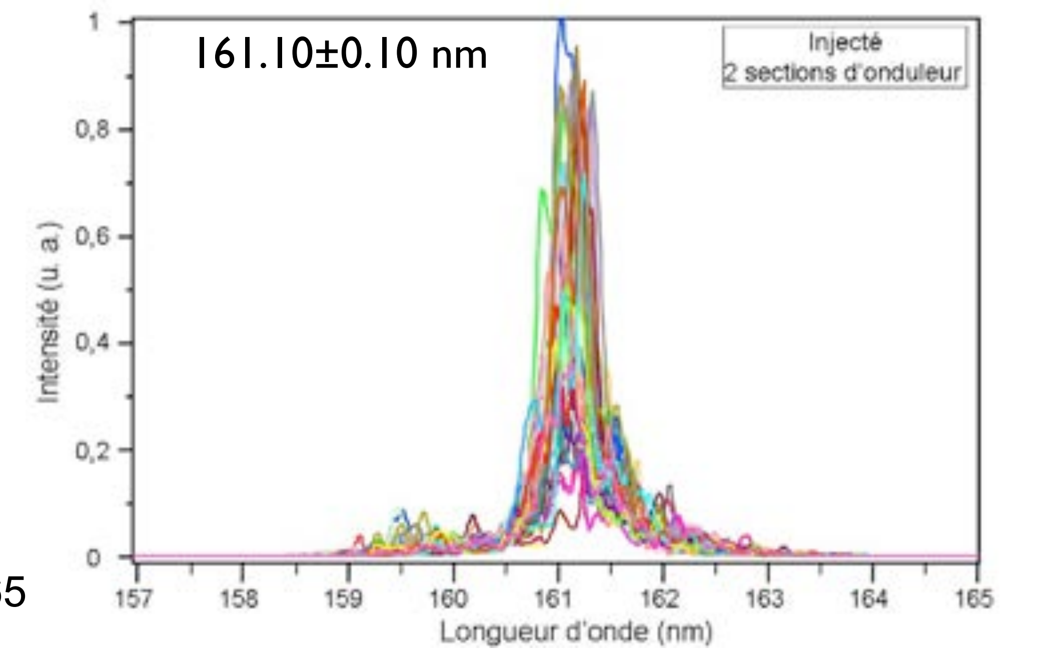

Seeding and self-seeding at New Fel sources, ICTP, Trieste, italy, 10-12 Dec. 2012

First demonstration of HHG seeding on the SCSS Test Accelerator (Japan) : wavelength stability

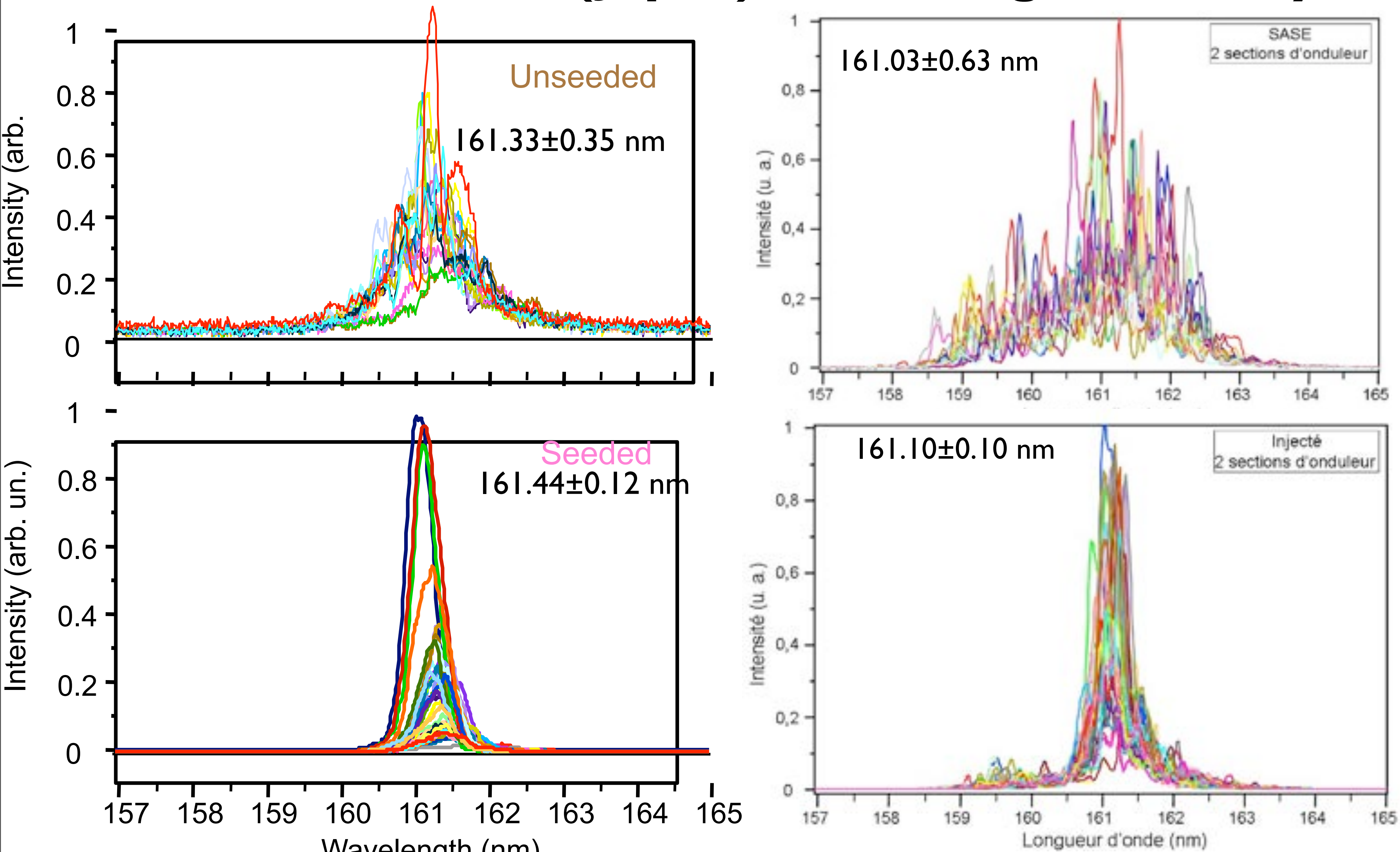

Seed level study

Rather low HHG seed intensity required:

Debunched mode (3 ps, 1 undulator)

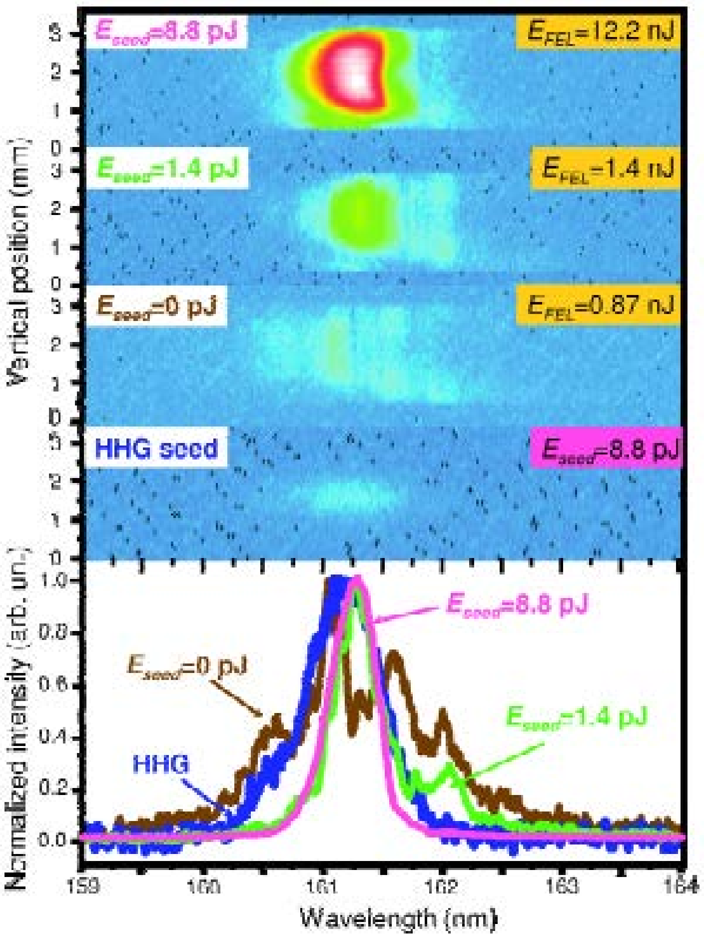

Two thresholds

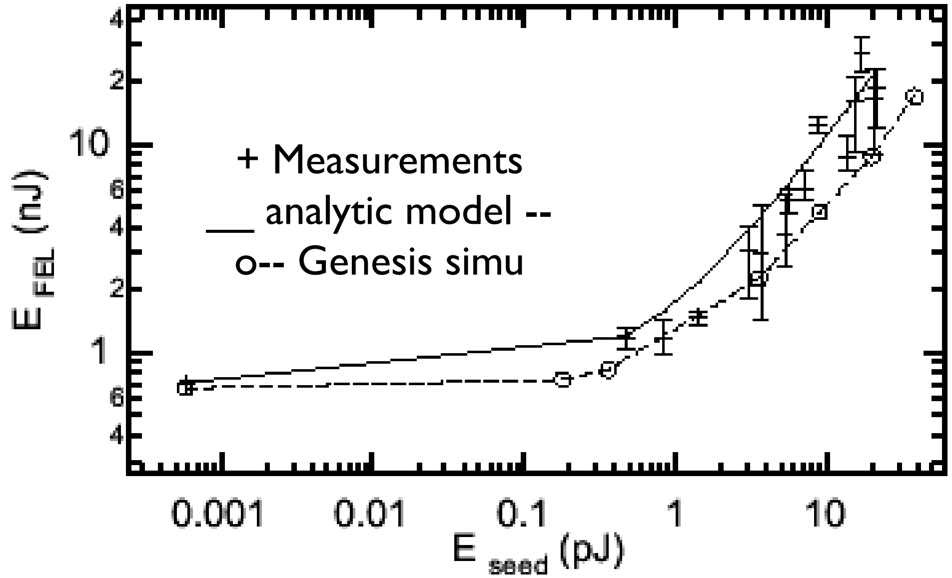

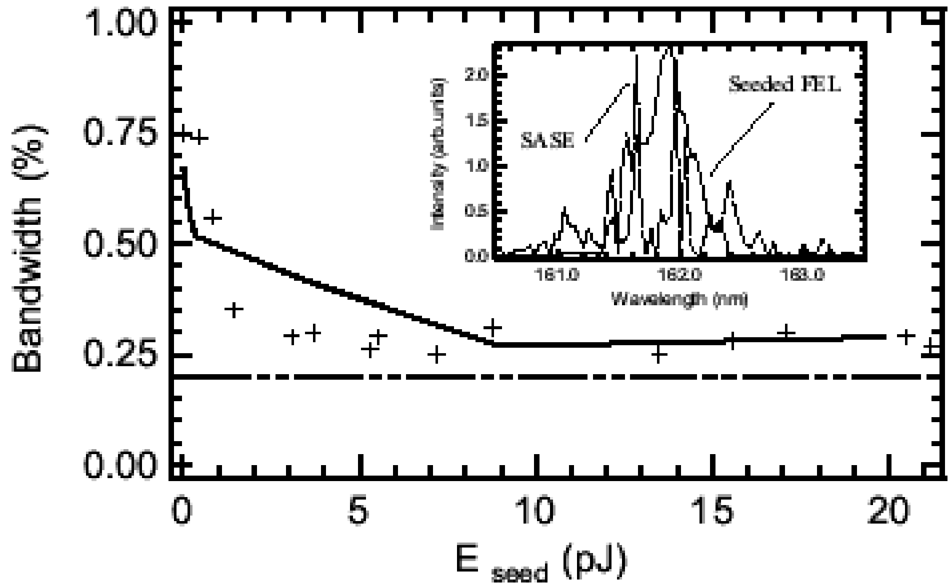

G. Lambert, T. Hara, M. Labat, T. Tanikawa, Y. Tanaka, Y. Yabashi, D. Garzella, B. Carre, M. E. Couprie, Seed level requirement for improving temporal coherence of a FEL, EPL 88-5-54002, 2009

III-Short wavelength seeding with HHG

Seeded FEL with plateau HHG @ 60 nm

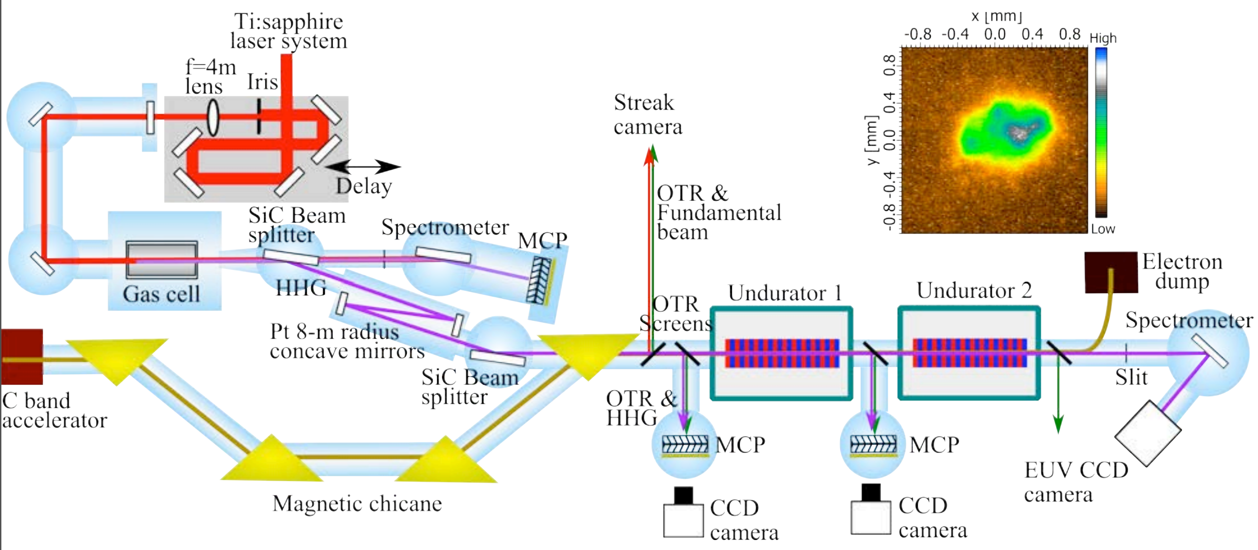

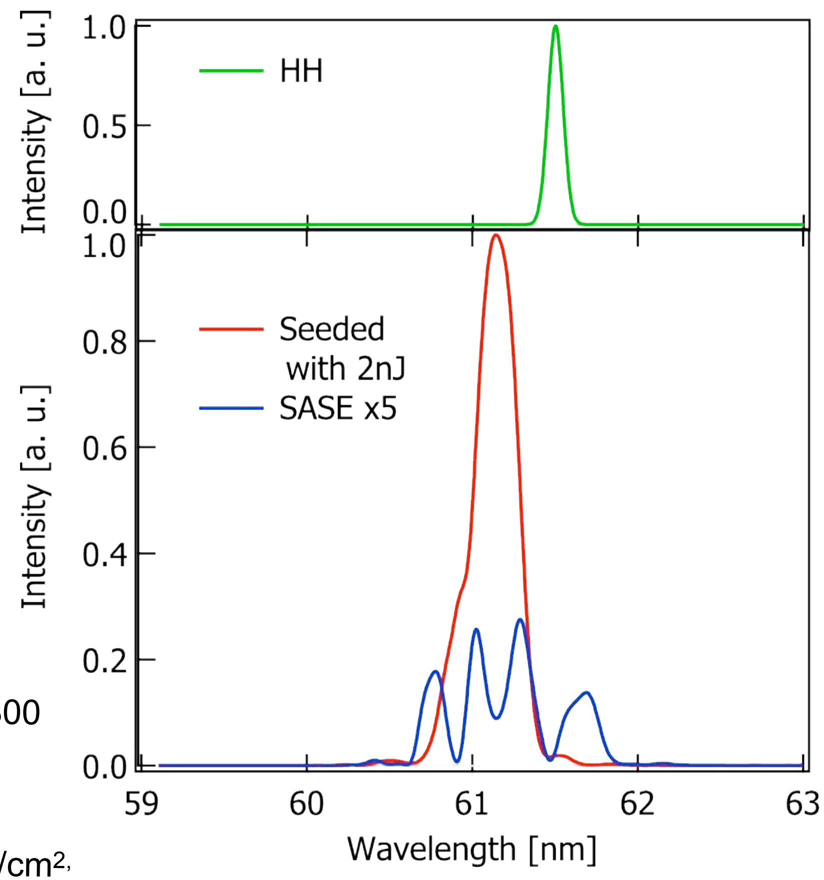

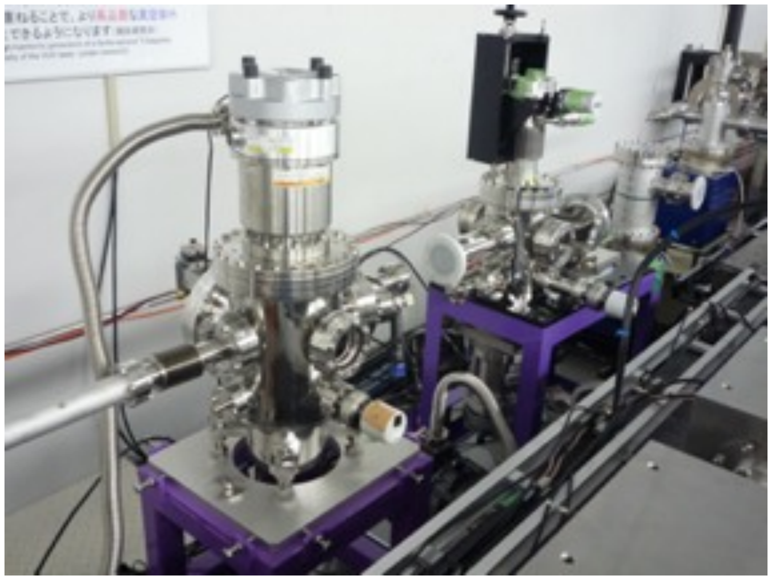

Laser upgrade : ~200 mJ, 800 nm, 200 fs, ϕ50mm, M^2:~ 1.4Jitter:<200fs

HHG : 70 ~ 50 nm, > 5 MW/cm², ~ 200 fs, ϕ 1mm, > 10 nJ, 30 Hz

Extreme ultraviolet free electron laser seeded with high-order harmonic of Ti:sapphire laser T. Togashi, E. J. Takahashi, K. Midorikawa, M. Aoyama, K. Yamakawa, T. Sato, A. Iwasaki, S. Owada, T. Okino, K. Yamanouchi, F. Kannari, A. Yagishita, H. Nakano, M.E. Couprie, Kenji Fukami, T. Hatsui, I T. Hara, T. Kameshima, H. Kitamura, N. Kumagai, I S. Matsubara, M. Nagasono, I H. Ohashi, T. Ohshima, Y. Otake, T. Shintake, K. Tamasaku, H. Tanaka, T. Tanaka, K. Togawa, H. Tomizawa, T. Watanabe, M. Yabashi, T. Ishikawa Optics Express, 1, 2011, 317-324

Non linear harmonics

Seed : 160 nm, 2 sections of 4.5 m long undulator, 150 MeV, bunched beam 400 fs, 0.3 nJ

- Large redshift
- spectral narrowing

Debunched beam 400 fs, 2 und. sections

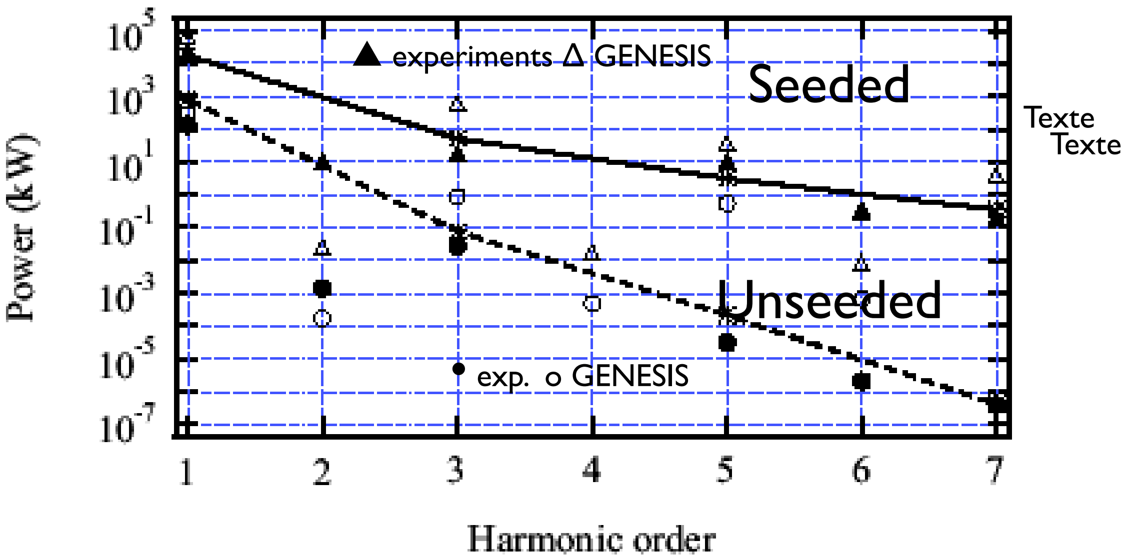

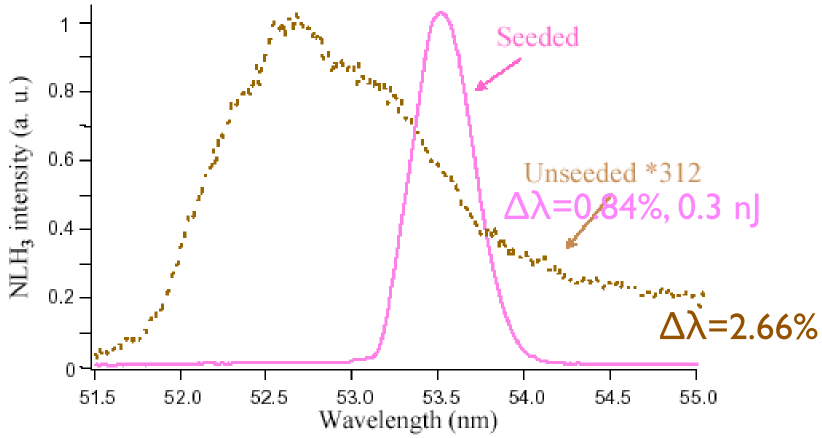

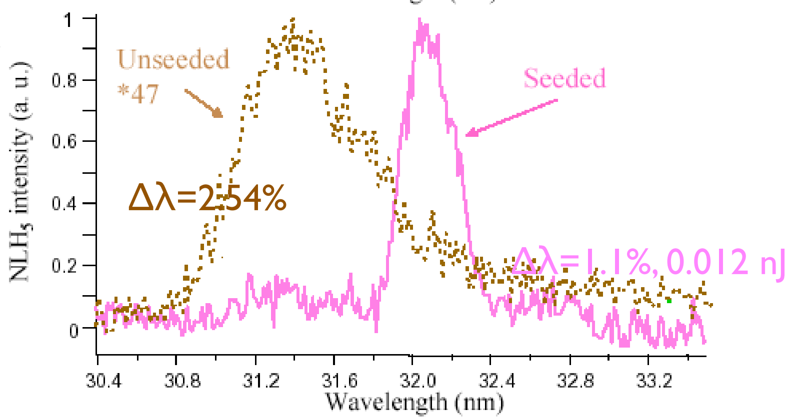

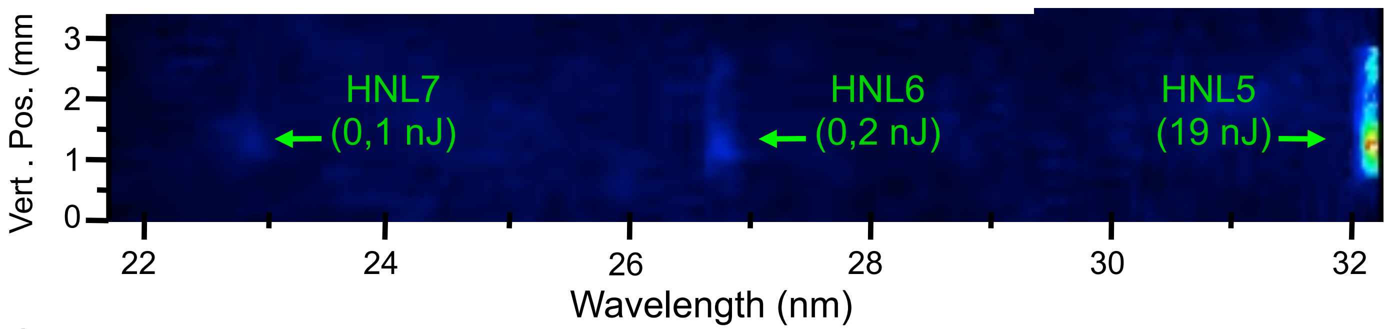

Nonlinear harmonic generation in a free-electron laser seeded with high harmonic from gas T. Tanikawa, G. Lambert, T. Hara, M. Labat, Y. Tanaka, M. Yabashi, O. Chubar, M.E. Couprie, EPL. 2010

HHG seeding + cascaded configuration

SPARC
266 nm
133 nm

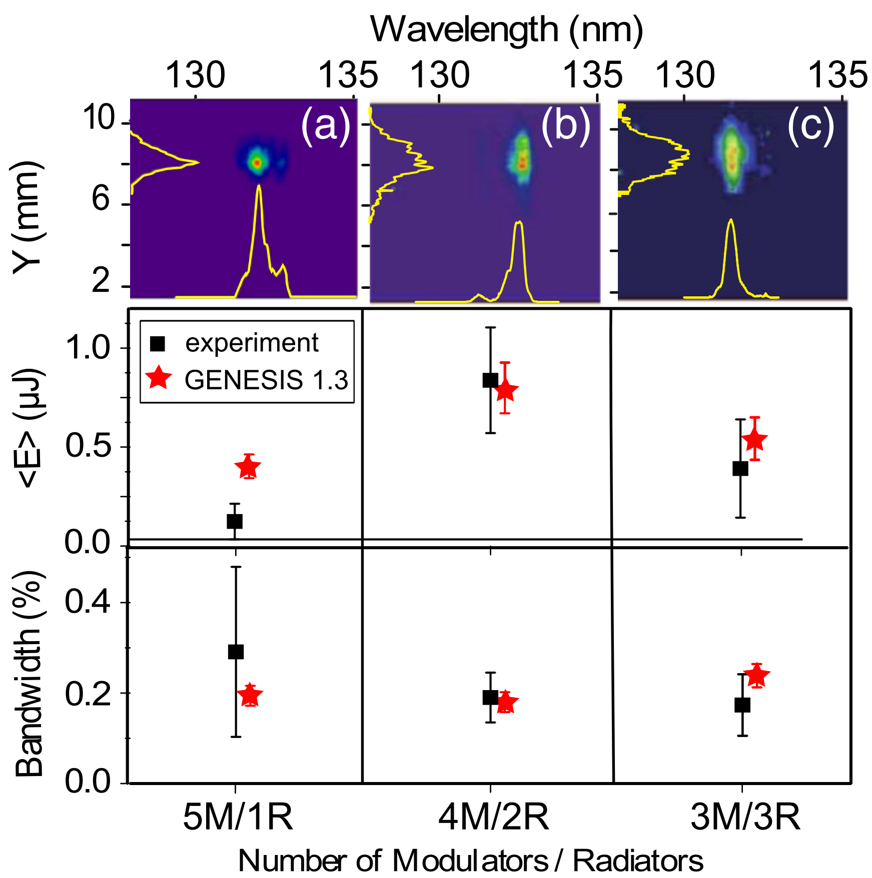

M. Labat et al. , Phys. Rev. Lett. 107, 224801 (2011)

Further prospects opened now by HHG in atomic/ molecular gas

Major evolutions 2008-2012:

1. HHG driven in IR (800 nm) by a few-cycle pulse

Generation of Quasi-continuum (near single atto pulse) → tunability

2. HHG driven by mid-IR OPA/OPCPA lasers sources (1-4 µm)

- Cutoff : $h\nu_{max} = I_P + 3.17U_p; U_p \propto I_L\lambda_L^2$ → extension to keV range with good efficiency
- Generation of Quasi-continuum (near single atto pulse) → tunability

3. HHG in aligned molecules

- Generation of elliptical polarization

HHG driven in IR (800 nm) by a few-cycle pulse

Single-cycle nonlinear optics

E. Goulielmakis, M. Schultze, M. Hofstetter, V. S. Yakovlev, J. Gagnon, M. Uiberacker, A. L. Aquila, E. M. Gullikson, D. T. Attwood, R. Kienberger, F. Krausz, U. Kleineberg, Science 320, 1614-1617 (2008).

- Generation of Quasi-continuum (near single atto pulse) → tunability

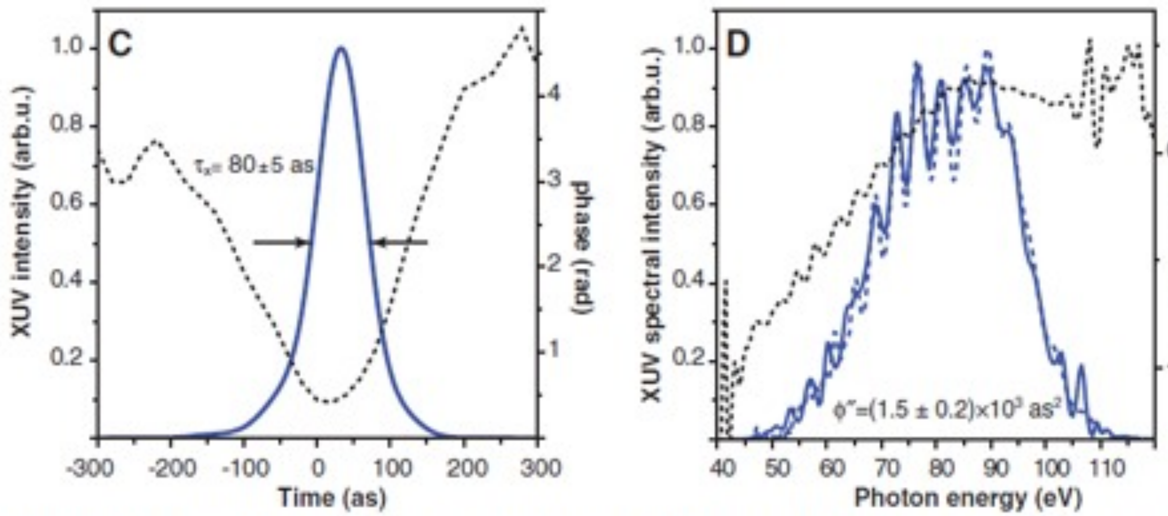

Fig. 3. Sub-100-as XUV pulse retrieval. (**A**) Measured ATR spectrogram compiled from 126 energy spectra of photoelectrons launched by an XUV pulse with a bandwidth of ~28 eV (FWHM) and recorded at delay settings increased in steps of 80 as. Here, a positive delay corresponds to the XUV pulse arriving before the NIR pulse. The high flux of the XUV source allows this spectrogram to be recorded within ~30 min. (**B**) ATR spectrogram reconstructed after ~10^3 iterations of the FROG algorithm (17). (**C**) Retrieved temporal intensity profile and spectral phase of the XUV pulse. The intrinsic chirp of the XUV emission (Fig. 4B) is almost fully compensated by a 300-nm-thick Zr foil introduced into the XUV beam between the attosecond source and the ATR measurement. Arrows indicate the temporal FWHM of the XUV pulse. (**D**) XUV spectra evaluated from the measurement of the XUV-generated photoelectron spectrum in the absence of the NIR streaking field (blue dashed line) and from the ATR retrieval (blue solid line). The black dotted line indicates the retrieved spectral phase.

ATR : atomic transient recorder

HHG driven by mid-IR laser

- Cutoff extension : $h\nu_{max} = I_P + 3.17U_p;\ U_p \propto I_L\lambda_L^2$
- Generation of Quasi-continuum (near single atto pulse) → tunability

High harmonic generation with long-wavelength few-cycle laser pulses
B. E. Schmidt, A. D. Shiner, M. Giguère, P. Lassonde, C. a Trallero-Herrero, J.-C. Kieffer, P. B. Corkum, D. M. Villeneuve, and F. Légaré, J. Phys. B 45, 074008 (2012)

Multi-electron recombination

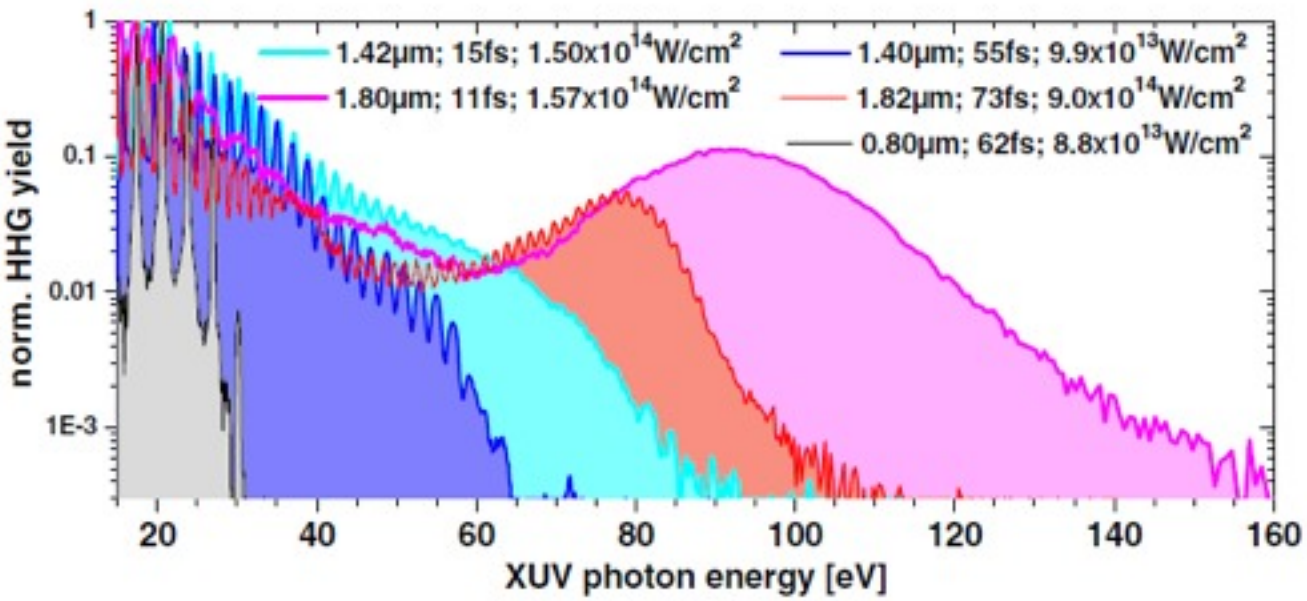

Figure 5. Semi-log plot of high harmonic yield in xenon at different driving laser wavelengths (grey: 0.8 μm; bluish: 1.4 μm; reddish: 1.8 μm). Each measurement was performed at intensity close to the corresponding saturation intensity and shows the benefit of increased driving wavelength and decreased pulse duration, respectively. Pulse durations and intensities are given in the legend. The striking enhancement around 95 eV originates from the giant resonance in xenon, an effect due to multi-electron correlation upon the recombination step in HHG.

HHG driven by mid-IR laser

Bright Coherent Ultrahigh Harmonics in the keV X-ray Regime from Mid-Infrared Femtosecond Lasers
Popmintchev, T; Chen, MC; Popmintchev, D; Arpin, P; Brown, S; Alisauskas, S; Andriukaitis, G; Balciunas, T; Mucke, OD; Pugzlys,; Baltuska, A; Shim, B; Schrauth, SE; Gaeta, A; Hernandez-Garcia, C; Plaja, L; Becker, A; Jaron-Becker, A; Murnane, MM; Kapteyn, HC, Science 336, 1287-1291 (2012)

- HHG driven in (high pressure) He by mid-IR laser at 3.7 µm : cutoff at 1.6 keV
- Quasi continuum → near single atto pulse

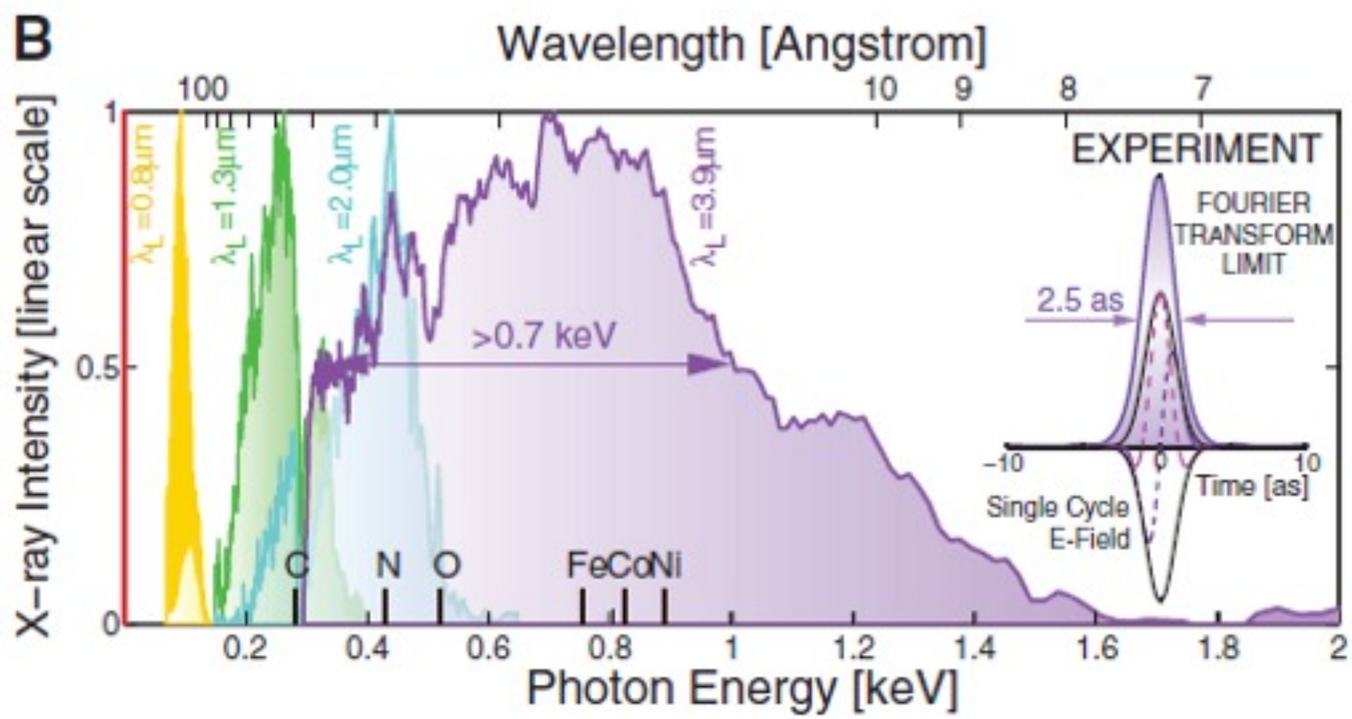

HHG driven by mid-IR laser

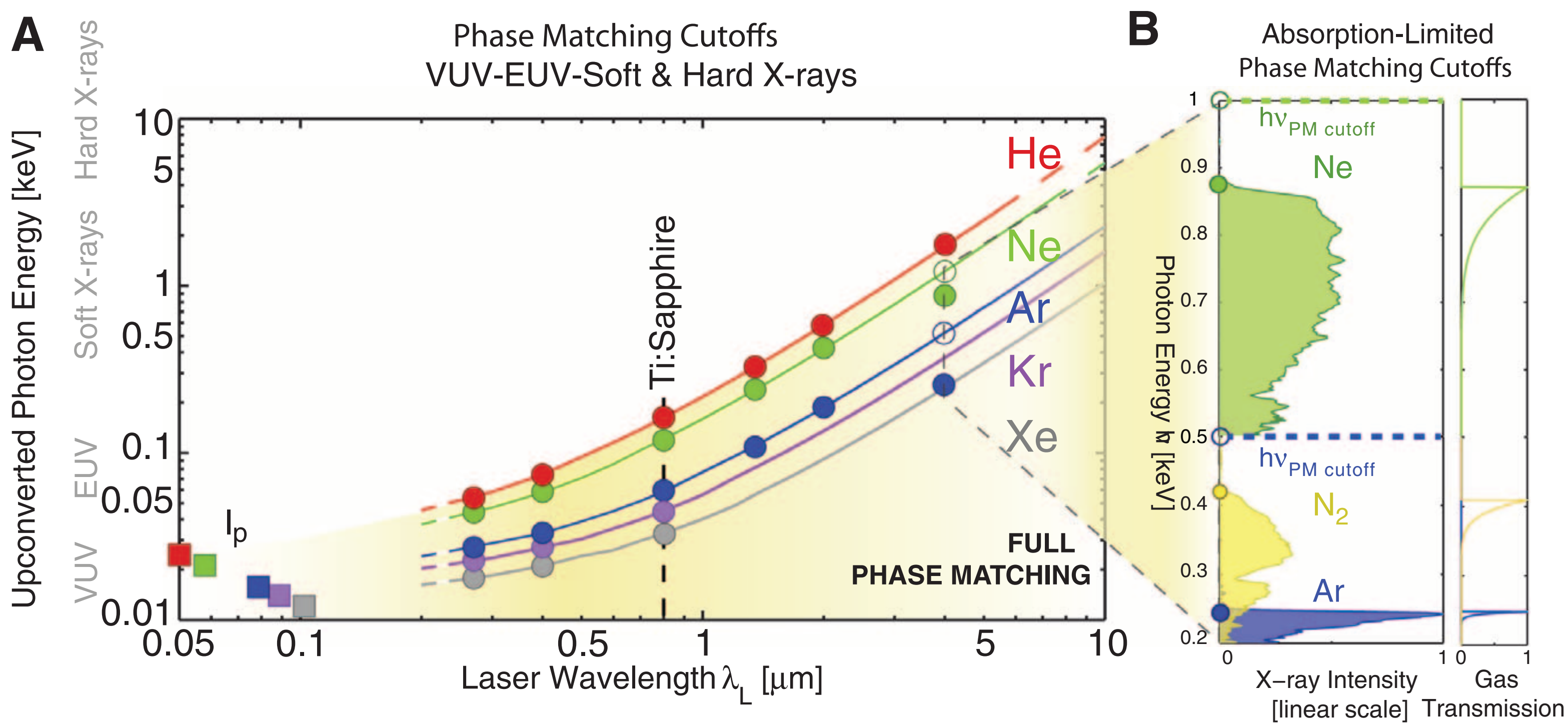

Fig. 2. (**A**) Predicted and observed HHG phase-matching cutoffs as a function of laser wavelength from the UV to the mid-IR. Solid circles show the observed cutoffs; open circles show the predicted cutoffs for Ar and Ne [which cannot be reached due to inner-shell absorption, as shown in (**B**)]. Solid squares on the left show the ionization potentials (I_p) of the different atoms. (**C**) Unified picture of optimal phase-matched high-harmonic upconversion, including microscopic and macroscopic effects.

HHG driven by mid-IR laser

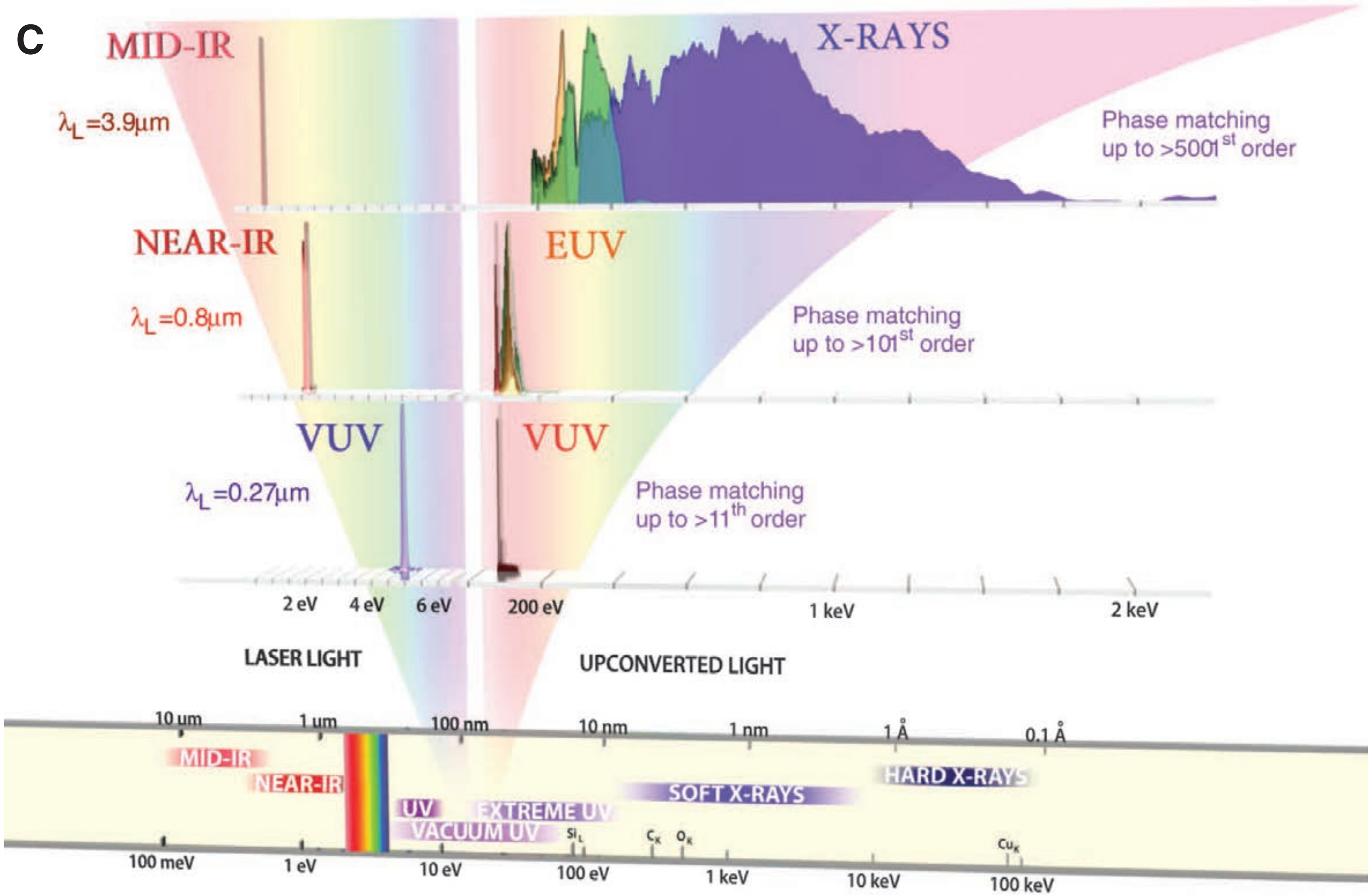

Flux : orders of magnitude

Laser (10 kHz reprate) wavelength / energy per pulse

0.8 µm / 2 mJ

1.6 µm / 1 mJ

3.0 µm / 1 mJ (extrapolation)

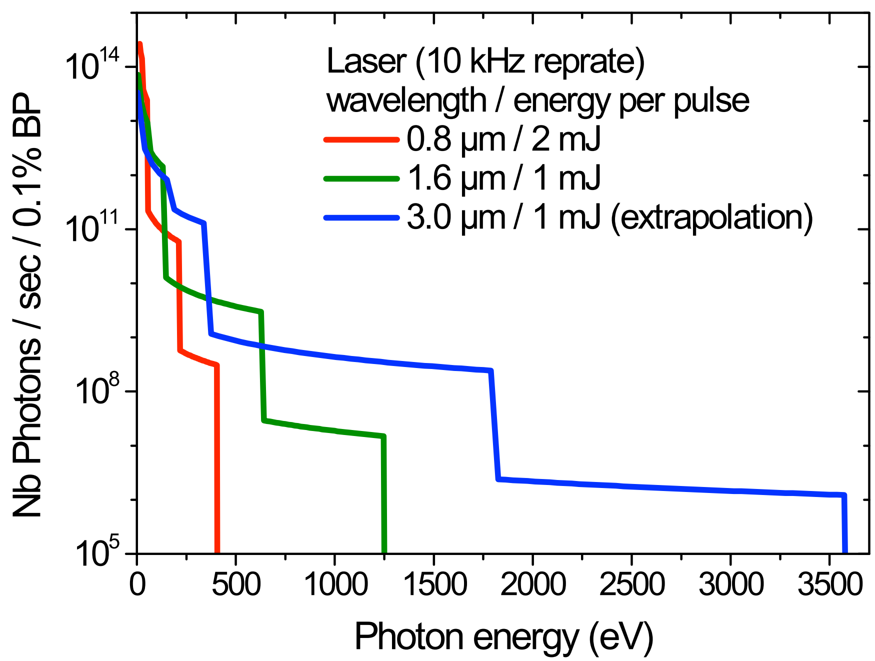

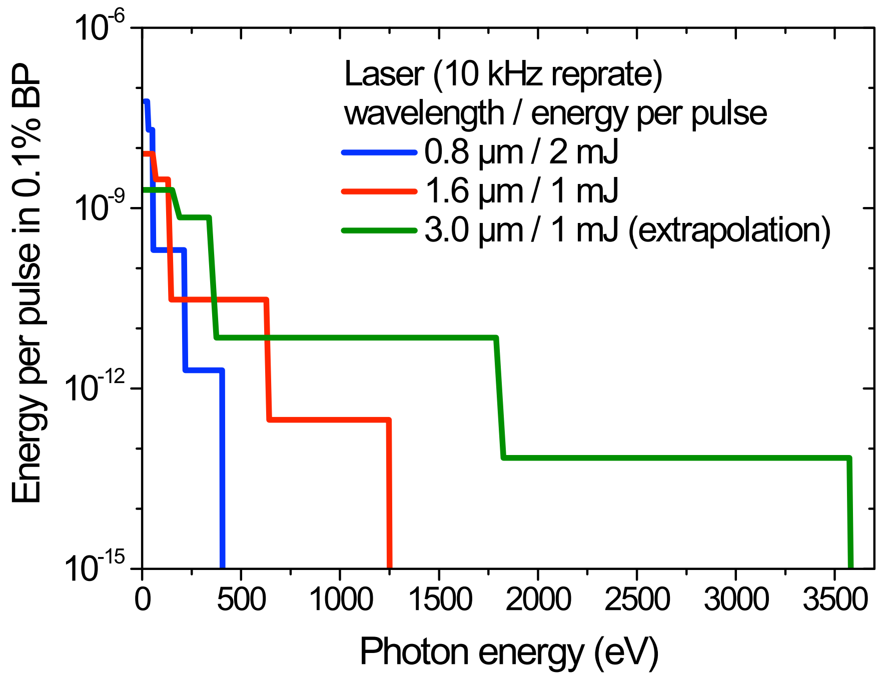

(origin graphs by BC)

Flux : orders of magnitude

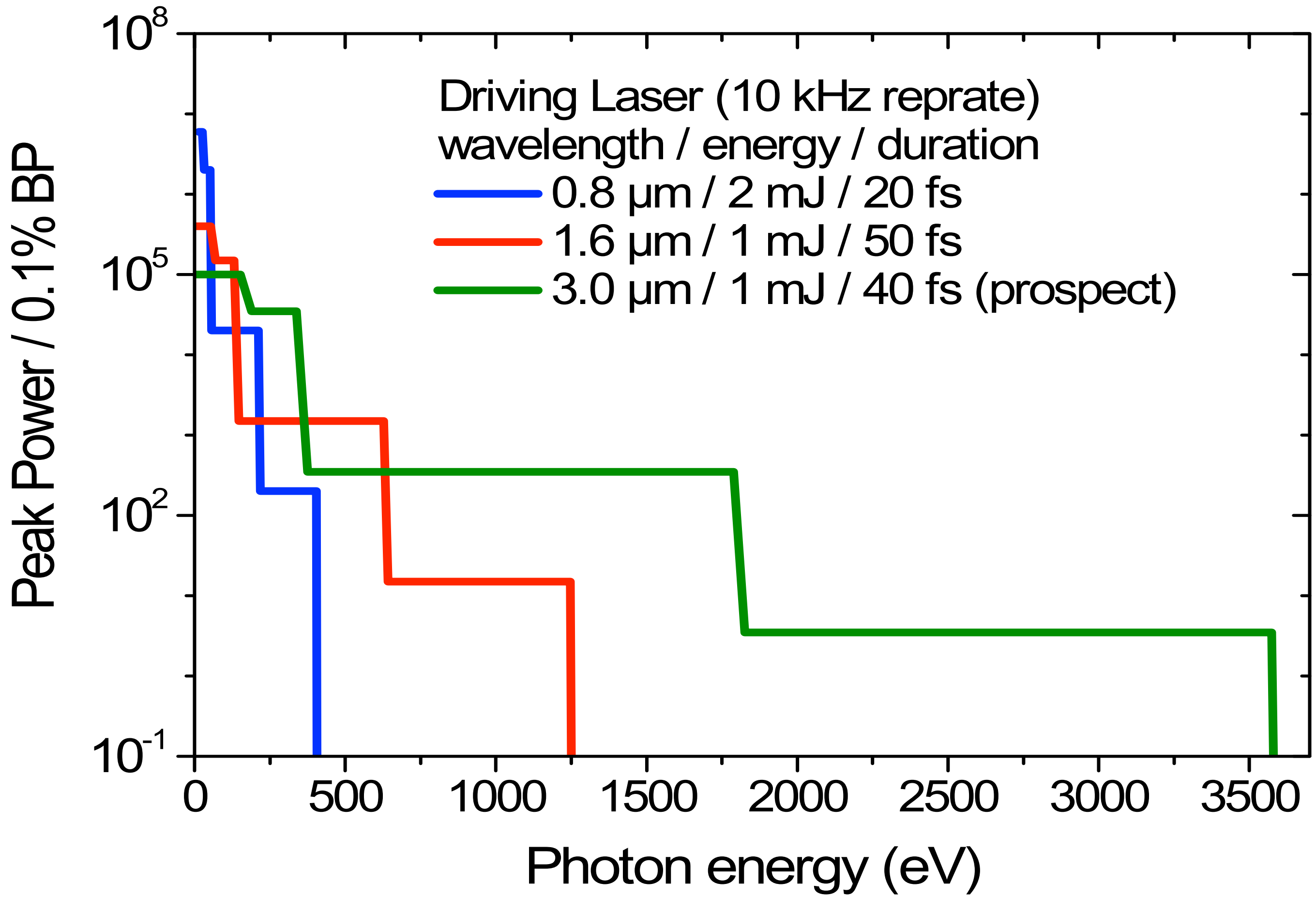

(origin graphs by BC)

Polarization

Elliptical polarization can be produced in HHG from aligned molecules
Origin : Phase difference between $d_{\parallel}$ and $d_{\perp}$ components of the dipole
(due to non isotropic Coulomb potential, recolliding electronic wave ≠ plane wave, multiple orbital dynamics)

Elliptically Polarized High-Order Harmonic Emission from Molecules in Linearly Polarized Laser Fields
X. Zhou, R. Lock, N. Wagner, W. Li, H. C. Kapteyn, and M. M. Murnane, PRL 102, 073902 (2009)

Ellipticity close to 0.4 in N_2

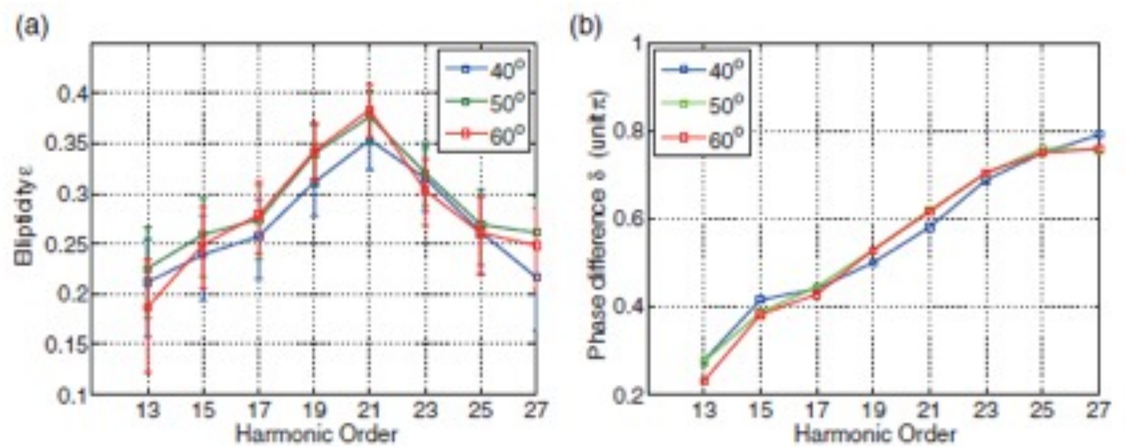

FIG. 4 (color online). (a) Ellipticity ε for relative angles between the pump and probe of $\theta = 40°$, $50°$, and $60°$, as a function of harmonic order for N_2. (b) Calculated phase difference δ between the parallel and perpendicular components of HHG emission in N_2.

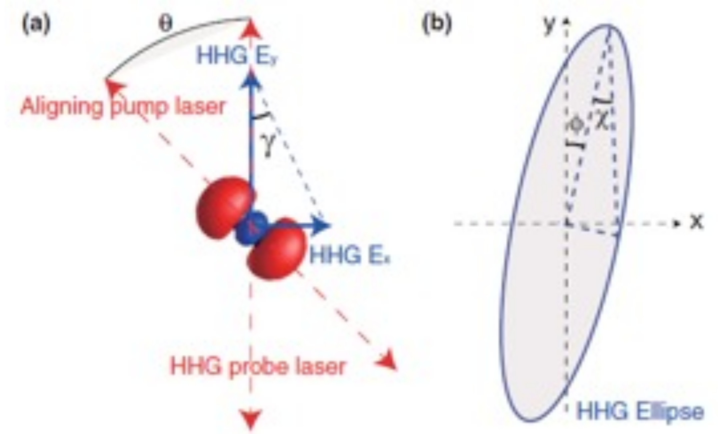

FIG. 1 (color online). High harmonic generation from aligned N_2. (a) HHG components parallel and perpendicular to the probe laser polarization can be generated. The angle γ is defined by $\tan(\gamma) = |E_x|/|E_y|$, where x and y are the lab frame axes. (b) The orientation angle ϕ of the HHG ellipse is defined as the angle between the major axis of the ellipse (max. transmission direction through polarizer) and the y axis. The angle χ is defined by $\tan(\chi) = \varepsilon$, where ε is the ellipticity. ϕ and θ are positive for clockwise rotation from the y direction and negative for counterclockwise rotation.

cannot be explained with single active electron model and strong field approximation

Polarization

High Harmonic Spectroscopy of Multichannel Dynamics in Strong-Field Ionization

Y. Mairesse, J. Higuet, N. Dudovich, D. Shafir, B. Fabre, E. Mével, E. Constant, S. Patchkovskii, Z. Walters, M.Yu. Ivanov, and O. Smirnova, PRL 104, 213601 (2010)

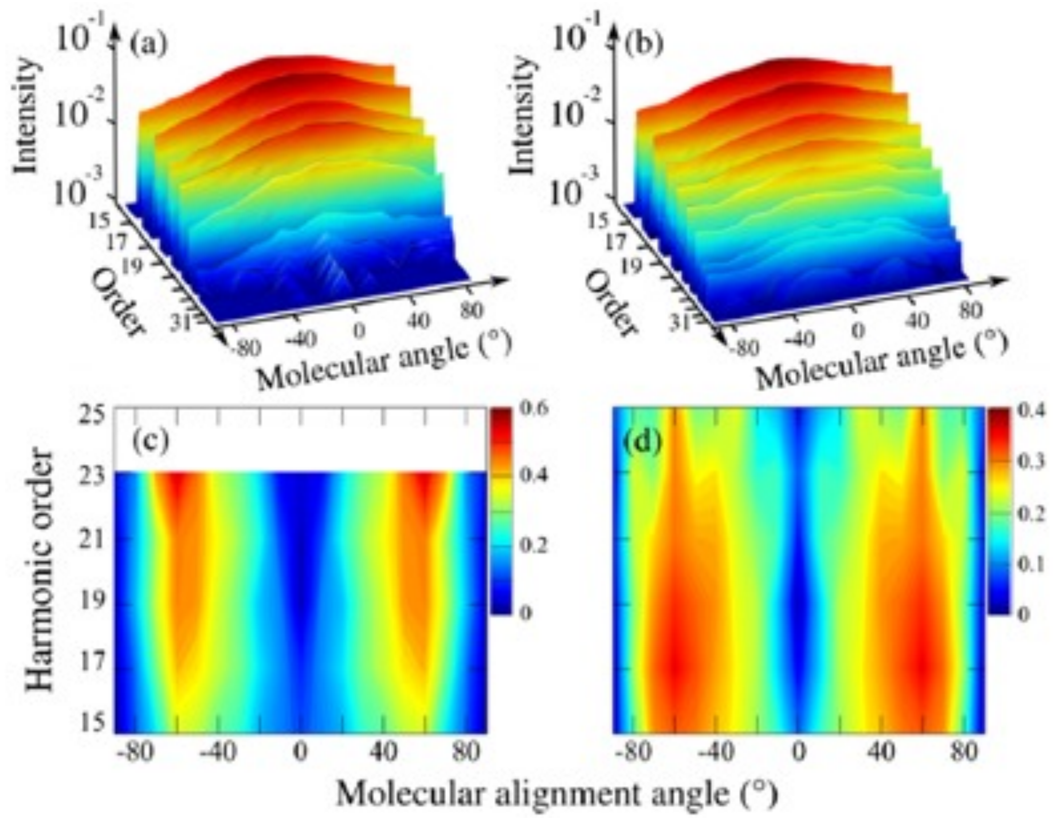

FIG. 2 (color online). Measured harmonic spectra (a),(b) and ellipticity (c),(d) as a function of the molecular alignment angle Θ at $I = 8 \times 10^{13}$ W/cm^2 [(a),(c)] and $I = 1 \times 10^{14}$ W/cm^2 [(b),(d)].

Ellipticity close to 0.4 in N_2

High Harmonic Generation on solid target

Intense laser pulse interacting with a near discontinuous plasma-vacuum boundary
=> the laser electric field can efficiently couple to the plasma surface
=> the electrons oscillate in phase : relativistic mirror oscillating at the laser frequency.
Position of this mirror surface : temporal function of the incident optical laser cycle => the phase of the reflected light wave is modulated => no longer sinusoidal => high order harmonics content

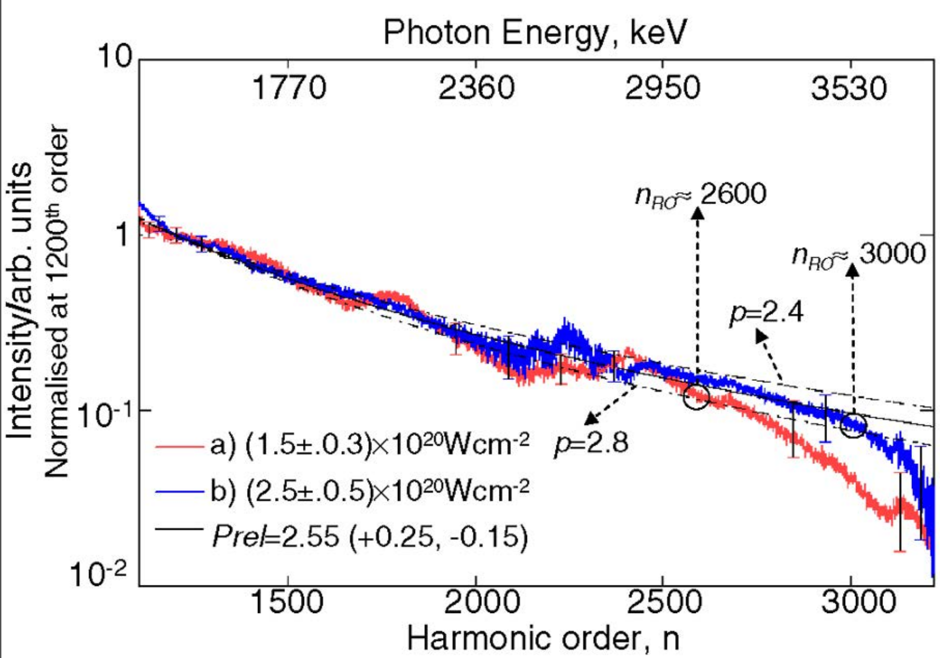

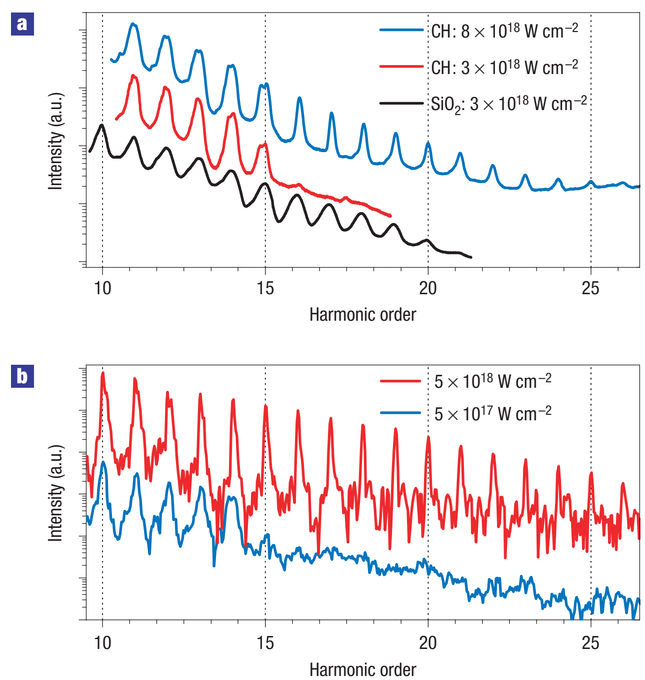

3.3 Å (3.8 keV), Harmonic order > 3200
4 ° cone emission (13° halo)
Vulcan PW laser (600 J, 500 fs)

C.Thaury et al., Nature Physics 3, 2007, 424-429

3 μJ @3 keV, B. Dromey. et al, Phys. Rev. Lett. 99 (2007) 085001
B. Dromey. et al. Nature Physics 2 (2006) 456

Kagome fiber source

Medium : kagome hollow-core photonic crystal fibre filled with noble gas.

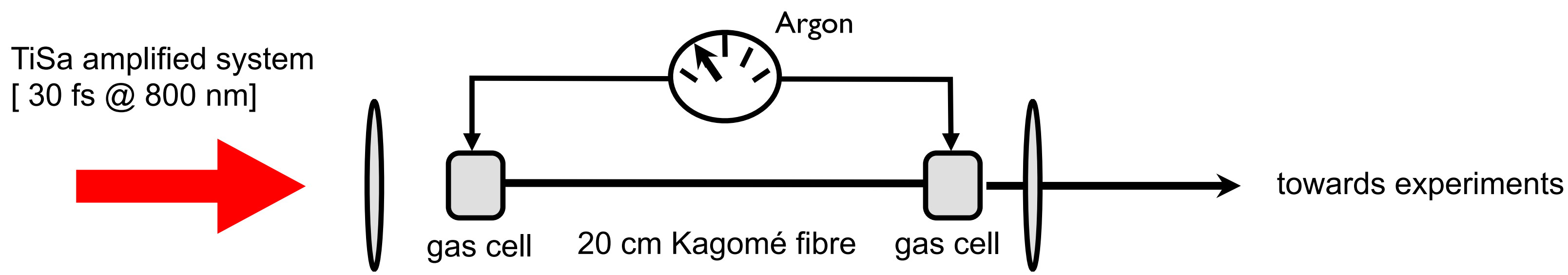

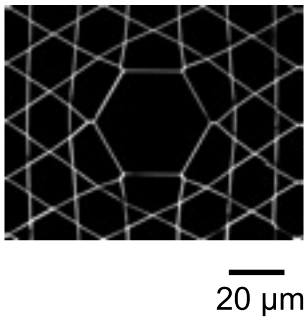

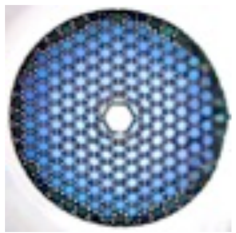

Diffraction-limited DUV pulses of >50 nJ, fs-duration, continuously tunable from below 200 nm to above 300 nm

N.Y. Joly, et al., "Bright spatially coherent wavelength tunable deep UV laser source using an Ar-ˇfilled photonic crystal fibre," PRL 106, 203901 (2011)
P. Hölzer et al., Femtosecond non linear fiber optics in the ionization regime, PRL 107, 203901 (2011)
J.Travers, W. Chang, J. Nold, N.Y. Joly, P. S. J. Russel, Ultrafast nonlinear opitcs in gas-filled hollow-cre photonic crystal fibers, J. Opt. Soc. Am. B 28 (12), A11-A26 (2011)

Hollow core family

bandgap fiber

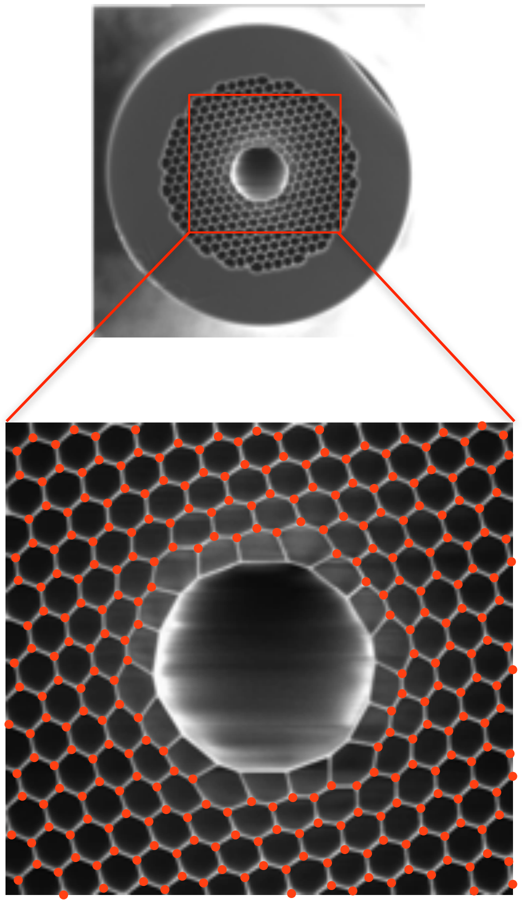

fibre kagomé

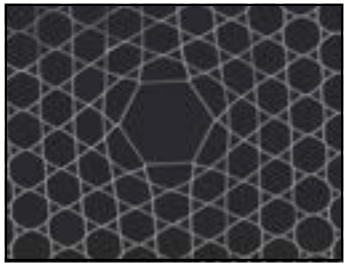

Hollow core family

bandgap fiber

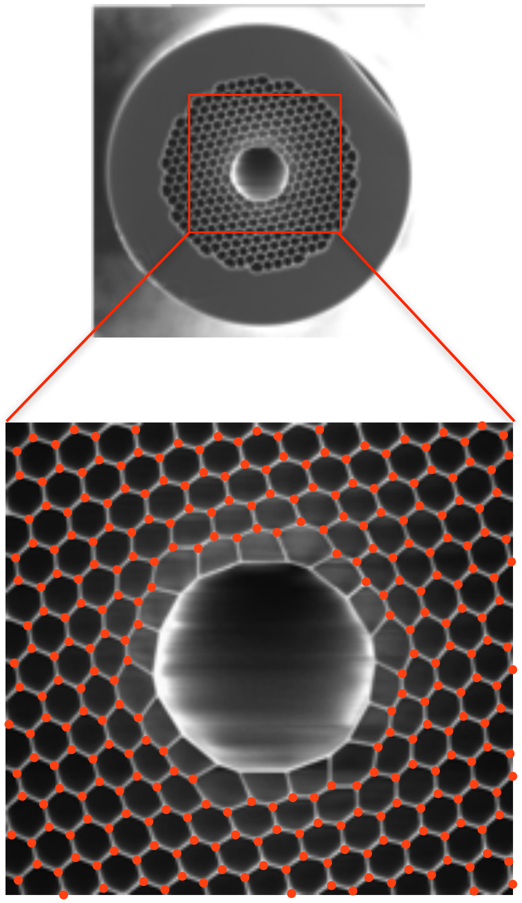

fibre kagomé

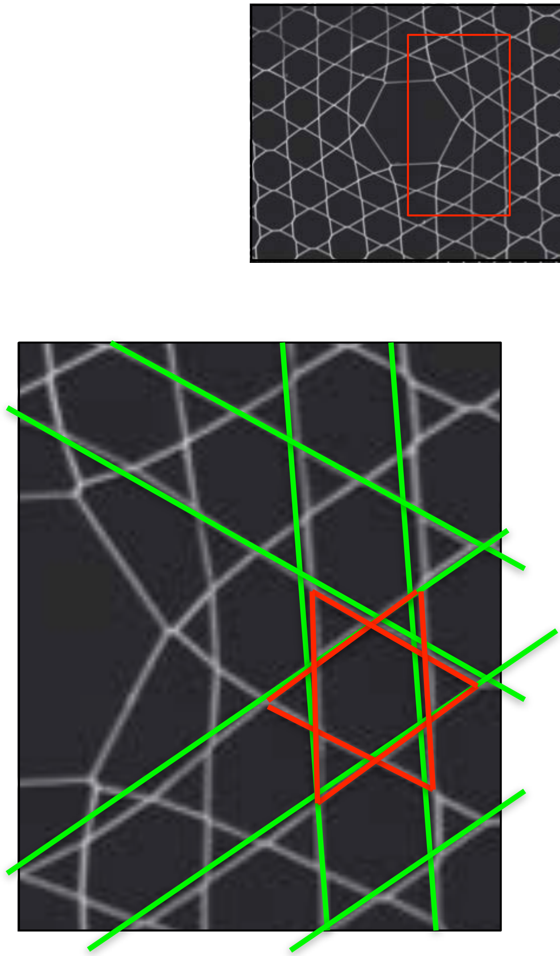

Hollow core family

bandgap fiber

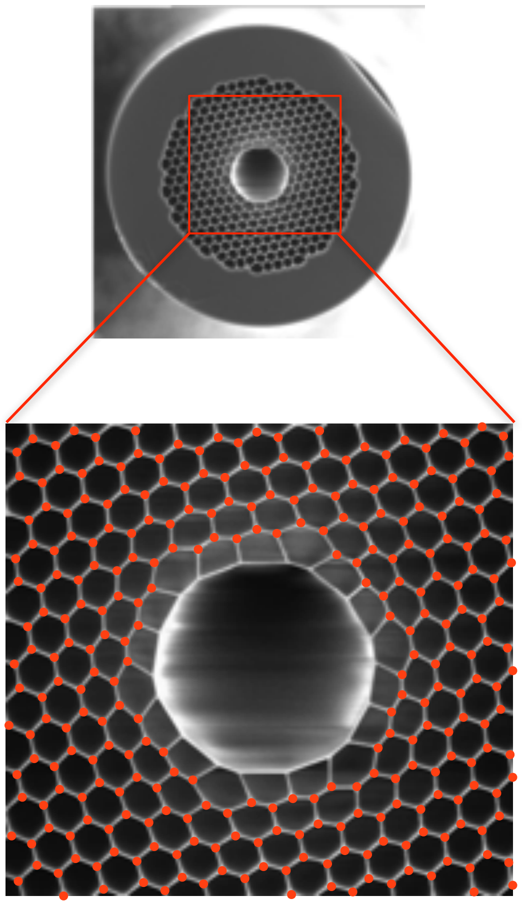

fibre kagomé

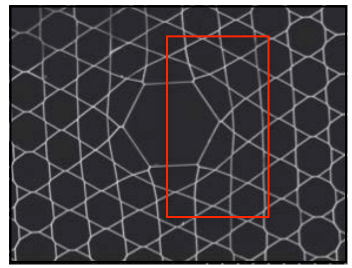

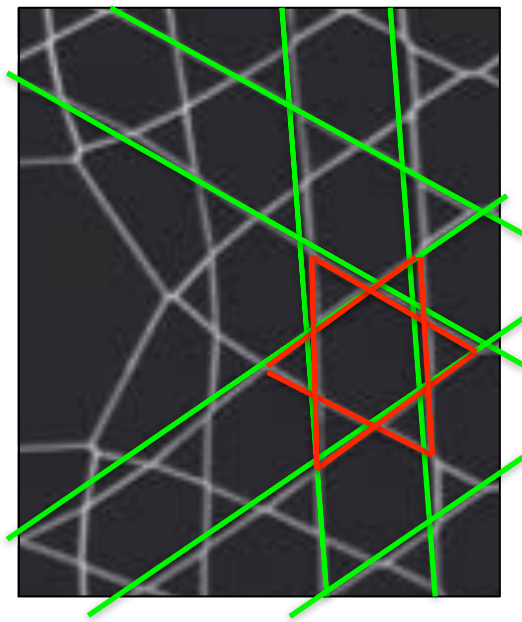

Kagomé basket [かごめ]

Hollow core family

bandgap fiber

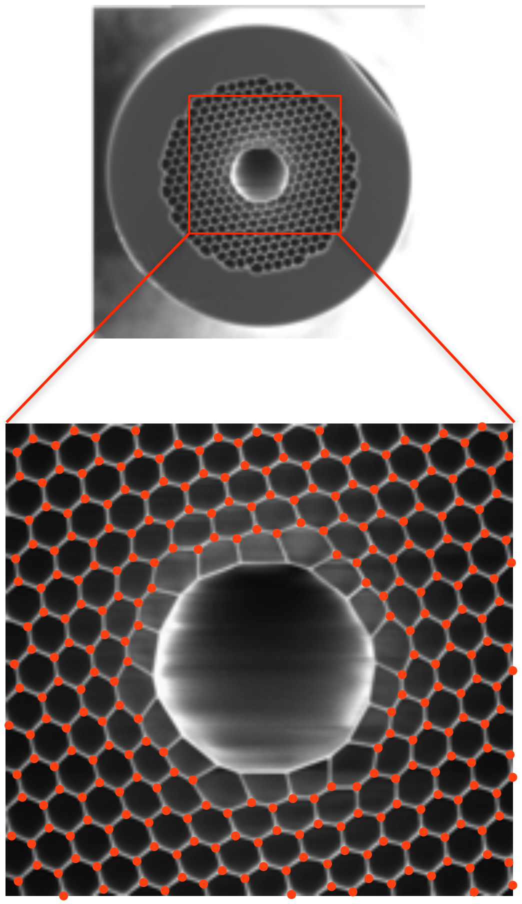

fibre kagomé

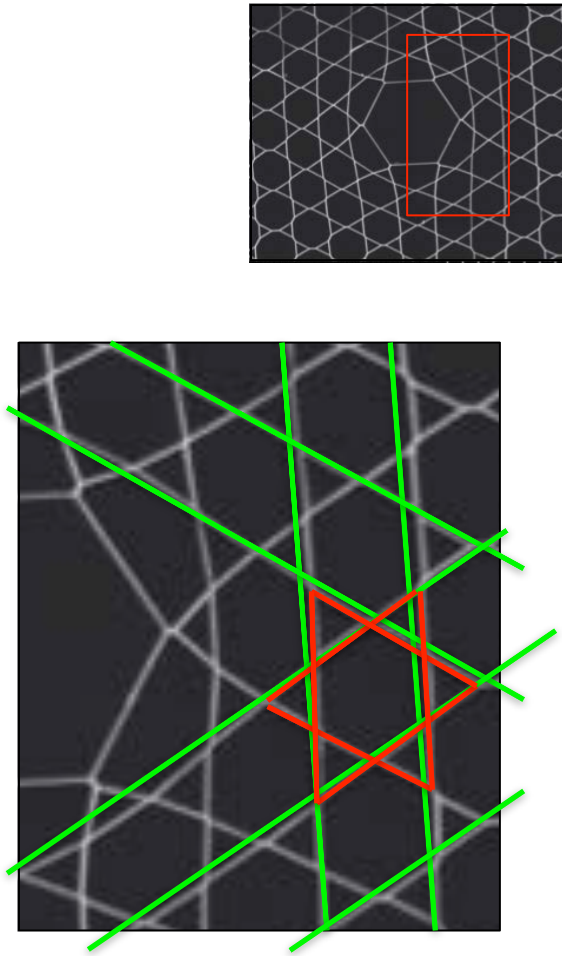

Hollow core family

bandgap fiber

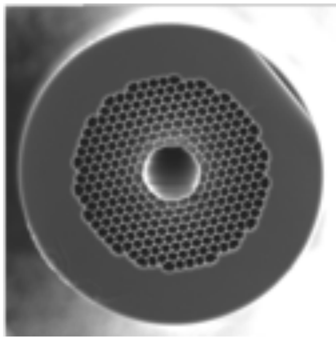

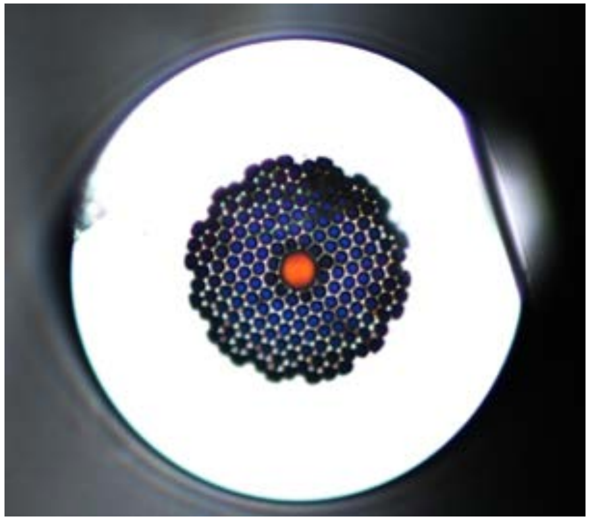

fibre kagomé

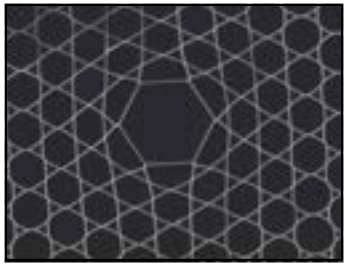

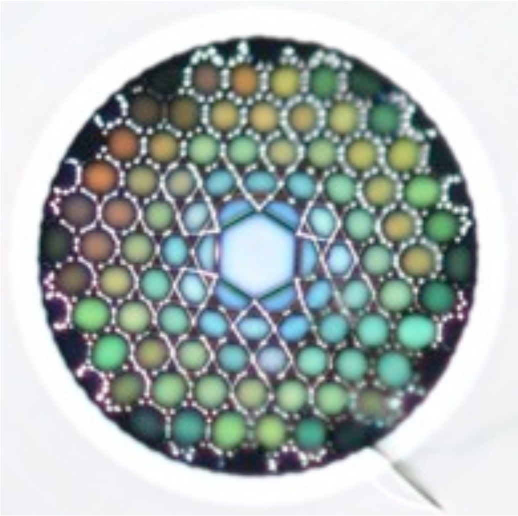

Hollow core family

bandgap fiber

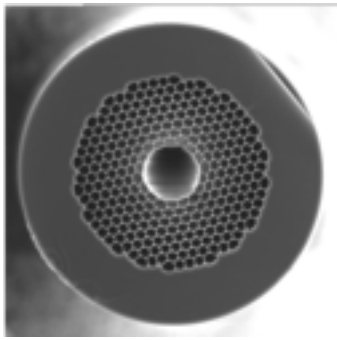

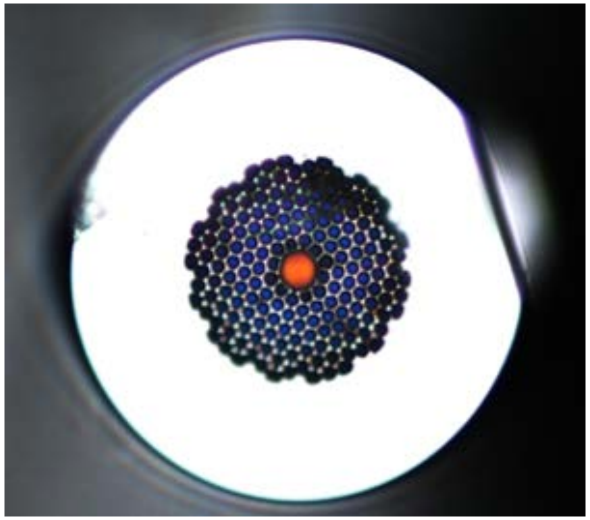

fibre kagomé

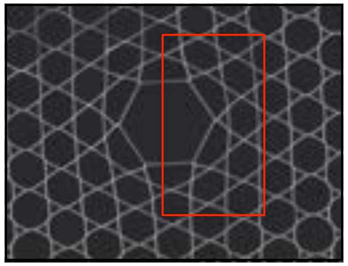

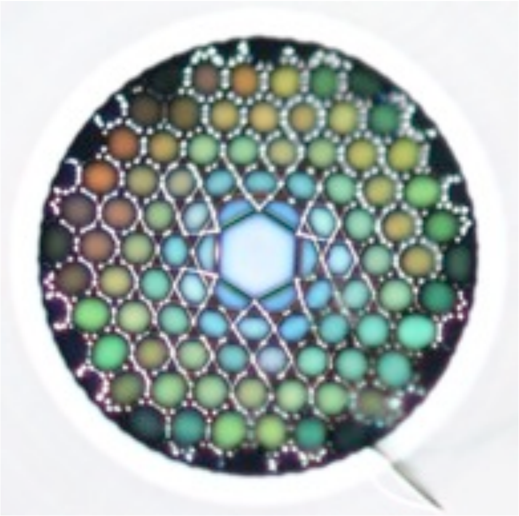

Hollow core family

bandgap fiber

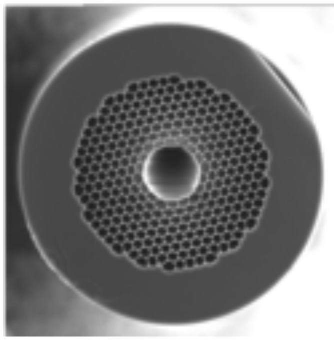

fibre kagomé

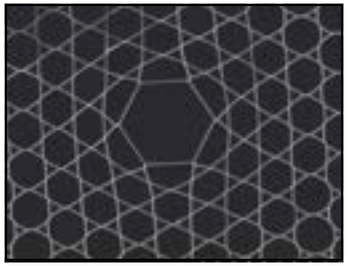

In hollow-core photonic crystal fibres (HC-PCF), light propagates in an effectively diffractionless manner, and can then interact efficiently with any material filling the core region

Hollow core family

bandgap fiber

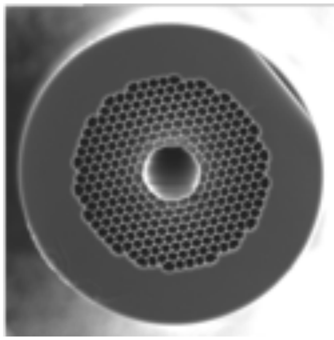

- narrow transmission band
- low loss (dB/km)
- strong variation of dispersion over the transmission band

fibre kagomé

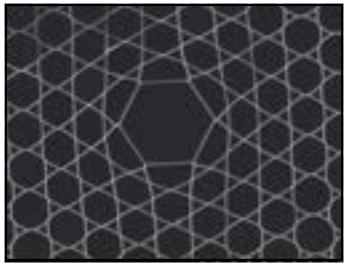

- no bandgap
- large spectral transmission
- high loss (dB/m)
- very low dispersion

In hollow-core photonic crystal fibres (HC-PCF), light propagates in an effectively diffractionless manner, and can then interact efficiently with any material filling the core region

very broad band transmission trasnmission associated to ultra-low dispersion

Analytical form for the dispersion

$$n_{mn}(\lambda, P, T) = \sqrt{n_{\text{gas}}^2(\lambda, P, T) - \frac{u_{mn}^2}{k^2 a^2}}$$

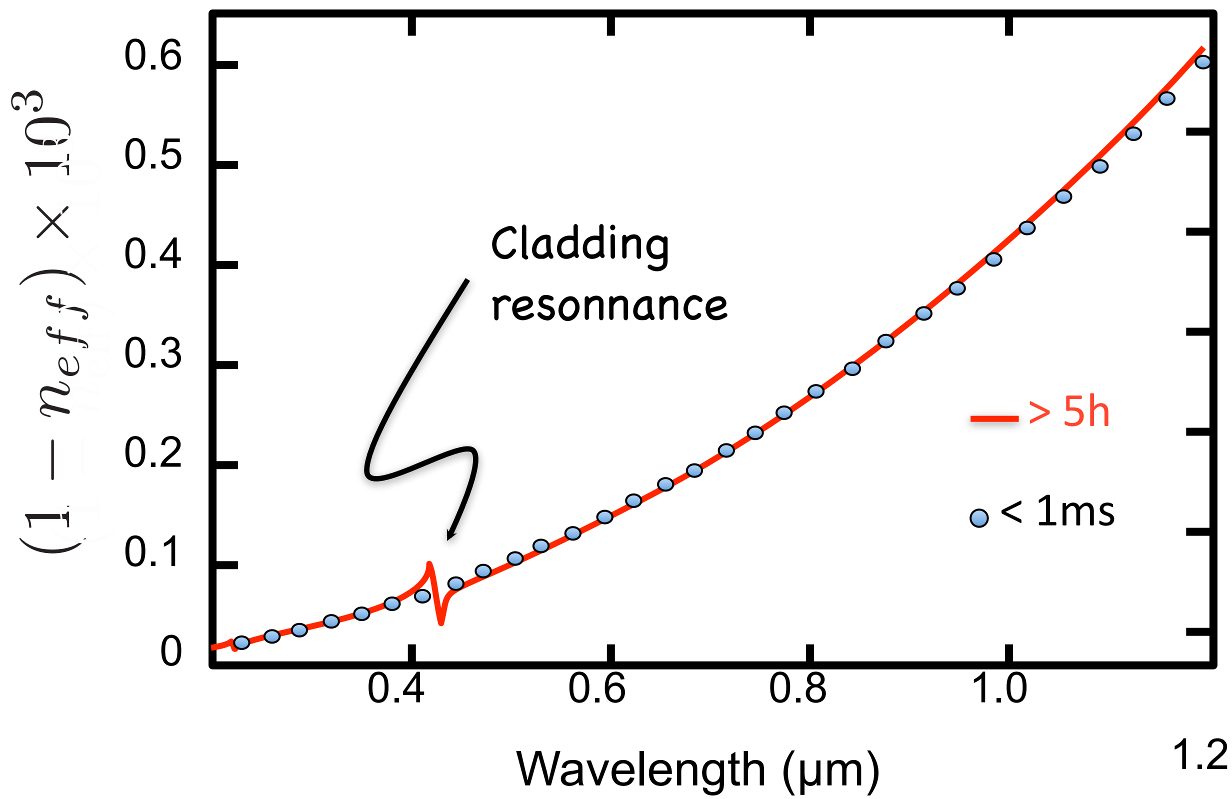

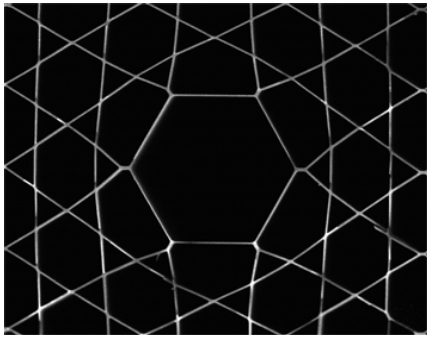

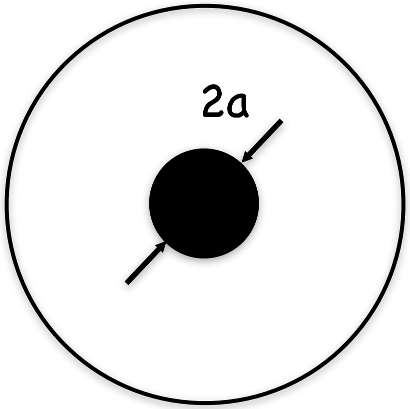

=> nonlinear effects and especially spectral broadening

Modelling : non linear Schrödinger equation including the non linear contribution of the gas (refractive index, effective area of the core)

very broad band transmission trasnmission associated to ultra-low dispersion

Analytical form for the dispersion

$$n_{mn}(\lambda, P, T) = \sqrt{n^2_{\text{gas}}(\lambda, P, T) - \frac{u^2_{mn}}{k^2 a^2}}$$

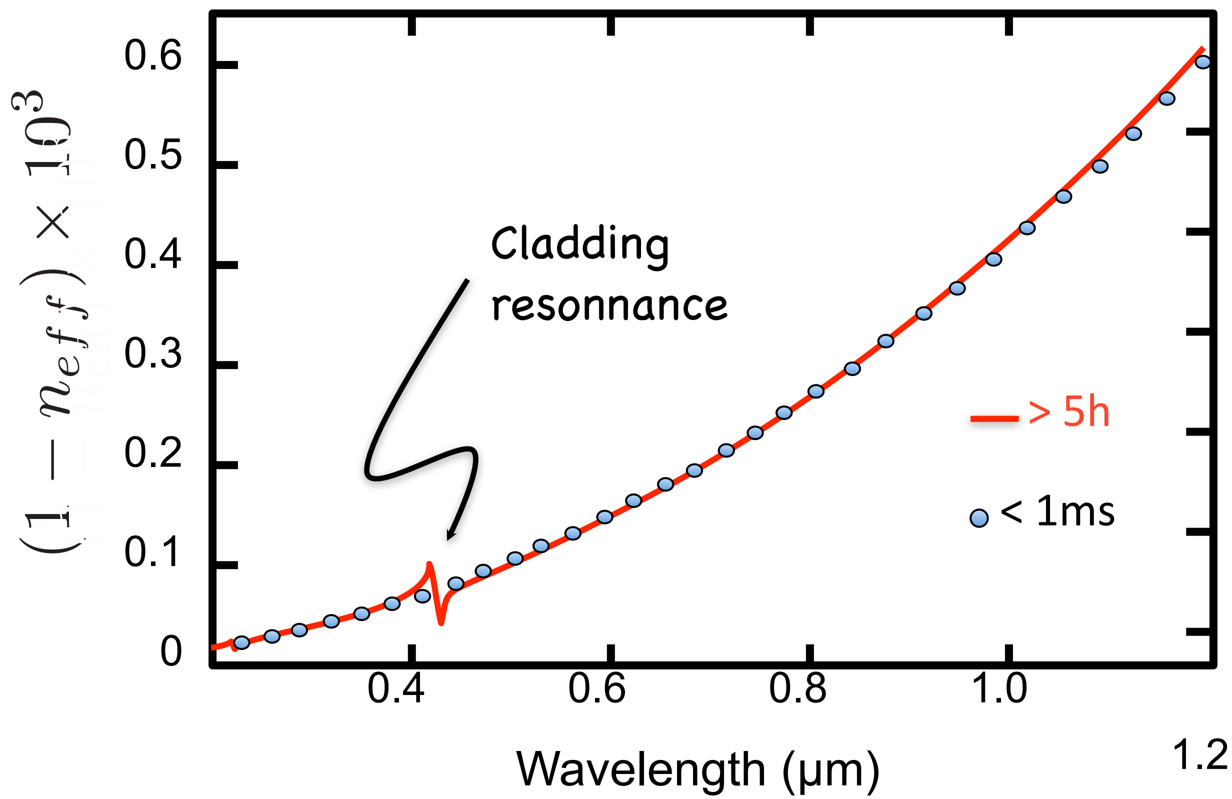

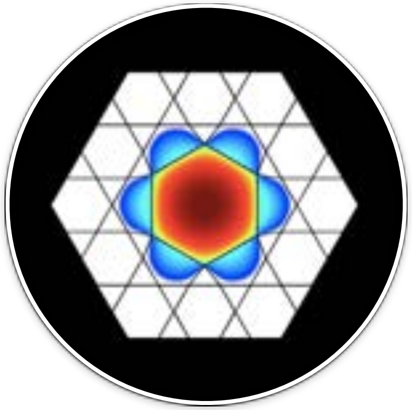

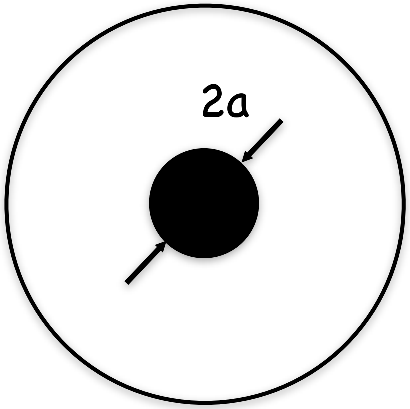

=> nonlinear effects and especially spectral broadening

Modelling : non linear Schrödinger equation including the non linear contribution of the gas (refractive index, effective area of the core)

Soliton effect

In ideal case (only one term of dispersion + Kerr effect) we can have soliton. Its order is N.

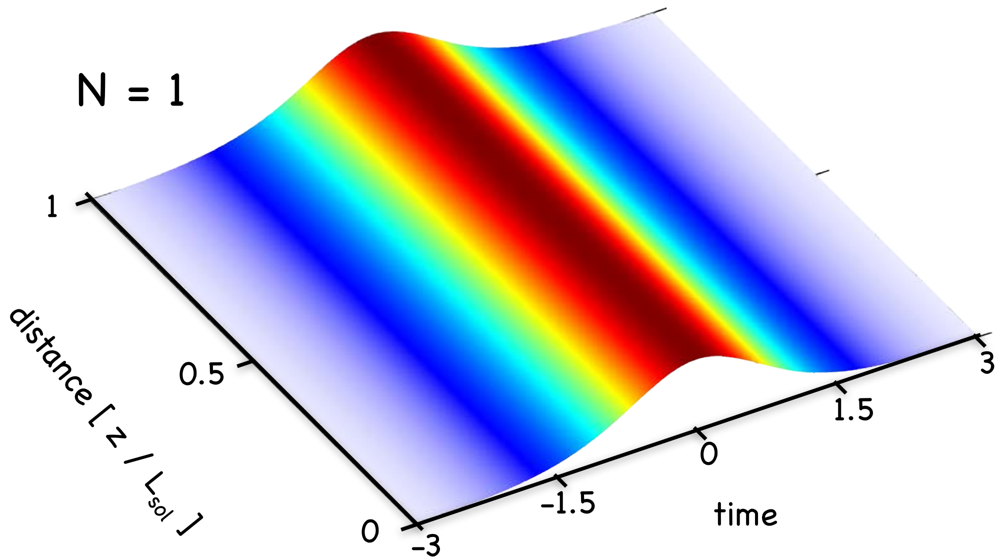

Dispersion length

$$N^2 = \frac{L_D}{L_{NL}} = \frac{\gamma P_0 t_0^2}{|\beta_2|}$$

Nonlinear length

Soliton effect

In ideal case (only one term of dispersion + Kerr effect) we can have soliton. Its order is N.

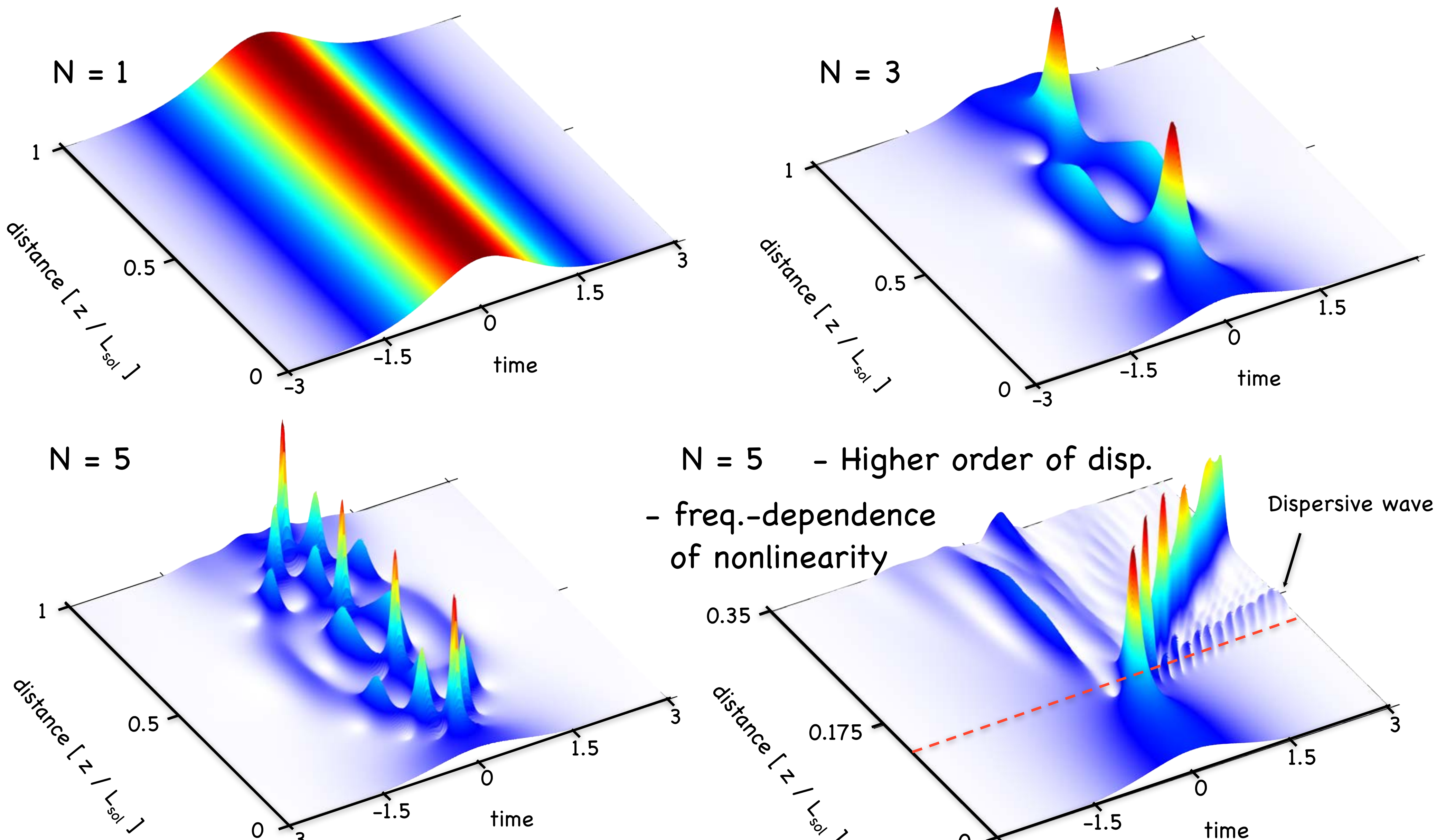

Dispersion wave emission

When the self compression reaches a few cycles (10 fs), it emits resonant dispersive wave at phase-matched wavelength in the UV spectral range

Quality factor of the compression $Q_C \sim \frac{3.7}{N}$ Length to max. compression $L_{\text{fiss.}} = \frac{L_D}{N} = \frac{t_0^2}{N\,|\beta_2|}$

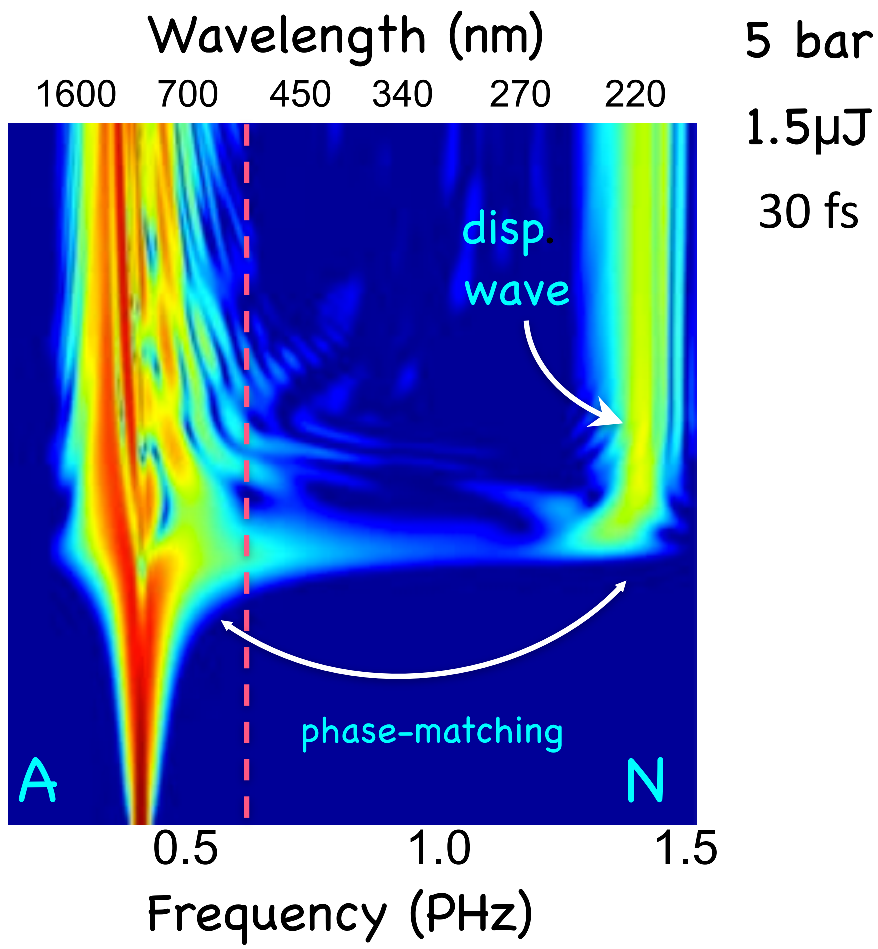

Modelling : non linear Schrödinger equation including the non linear contribution of the gas (refractive index, effective area of the core)

Dispersion wave emission

When the self compression reaches a few cycles (10 fs), it emits resonant dispersive wave at phase-matched wavelength in the UV spectral range

Quality factor of the compression $Q_C \sim \frac{3.7}{N}$ Length to max. compression $L_{\text{fiss.}} = \frac{L_D}{N} = \frac{t_0^2}{N\,|\beta_2|}$

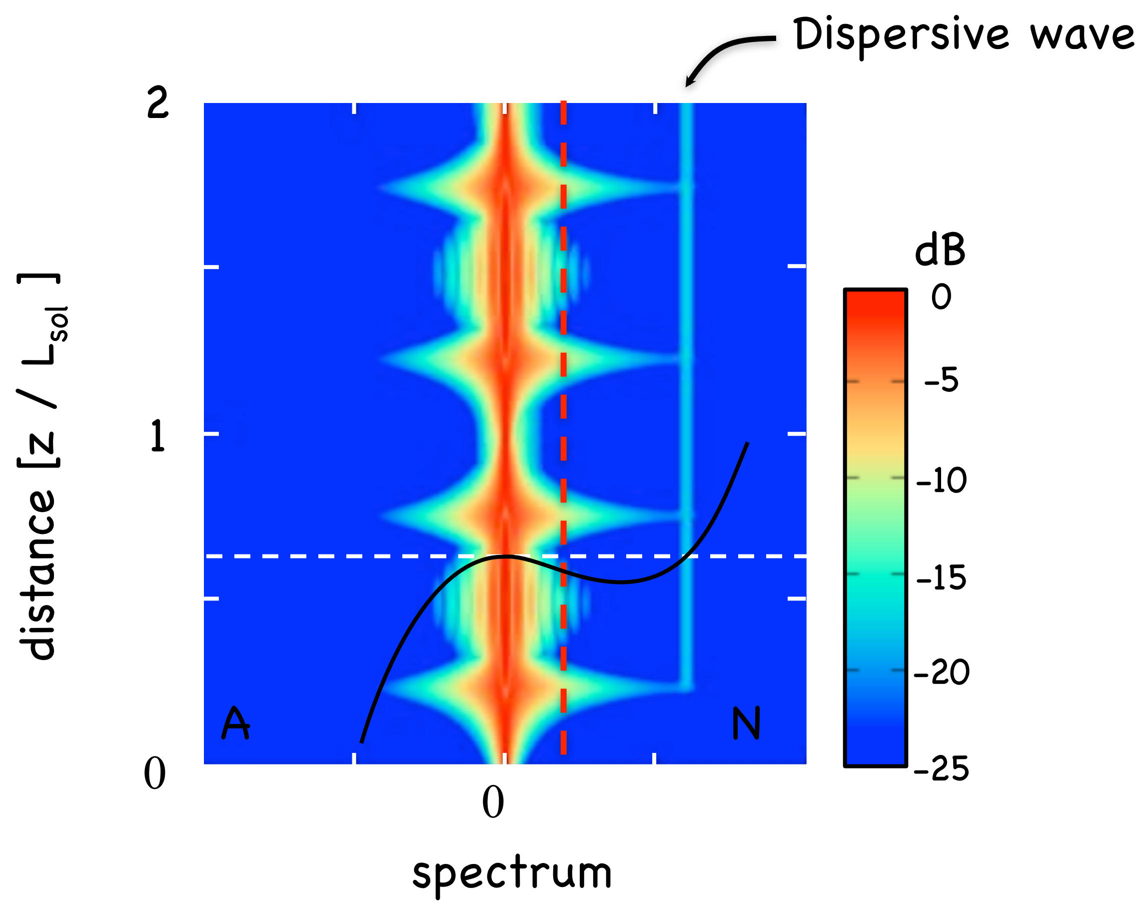

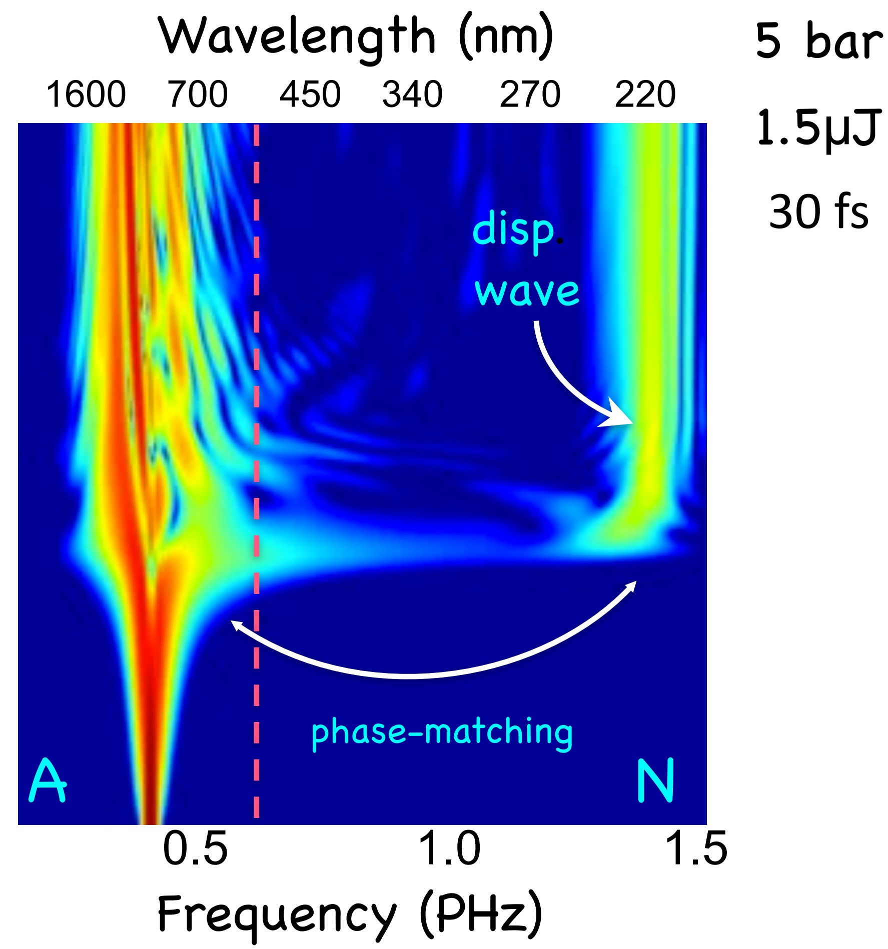

Modelling : non linear Schrödinger equation including the non linear contribution of the gas (refractive index, effective area of the core)

Kagome fiber source properties

Tunability of the UV with the gas pressure

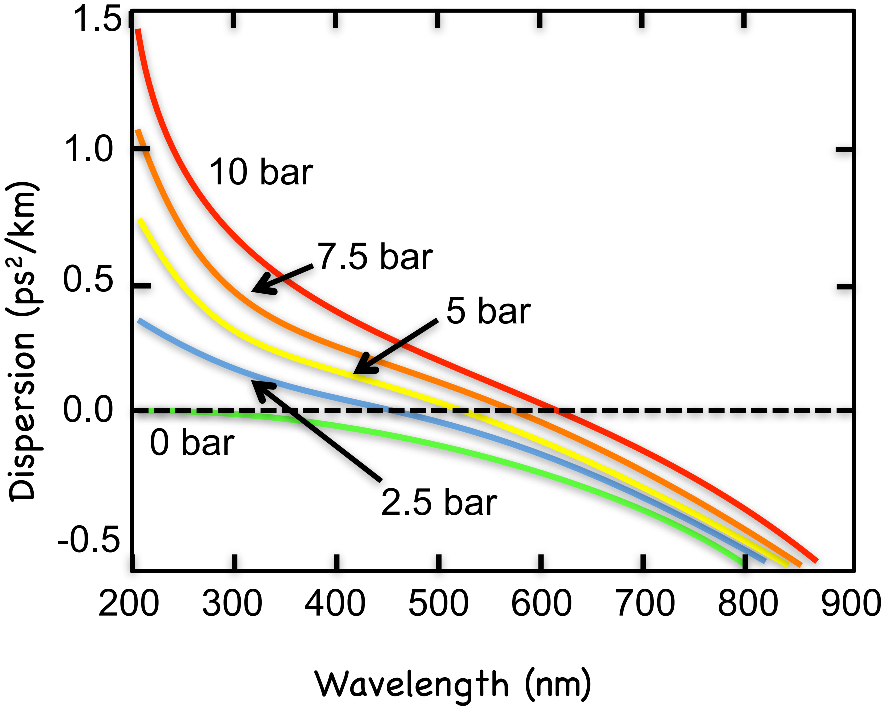

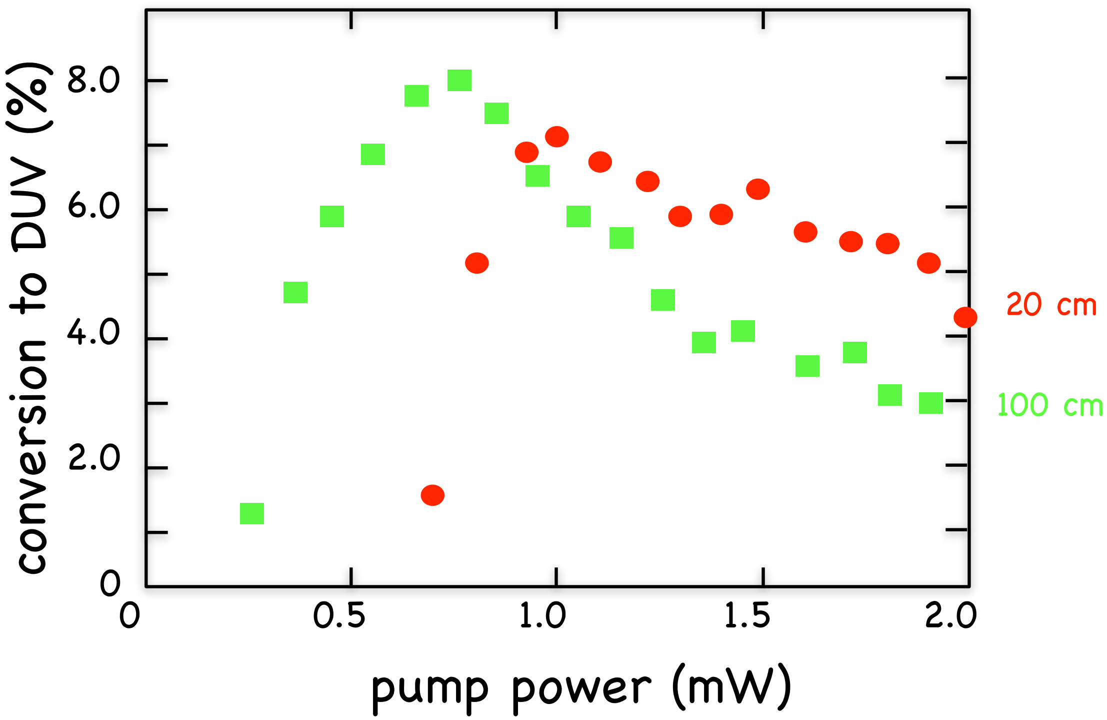

Tunability obtained by controlling both pressure and input power

Influence of the input pulse duration

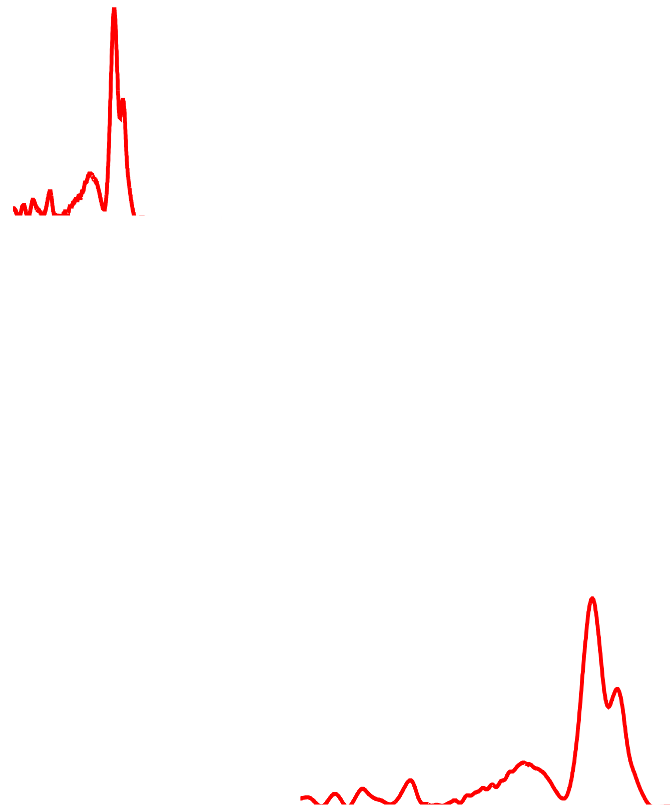

The quality of the compression is inversely proportional to the soliton order
=>, the quality of the generated band is then strongly affected by N

Influence of the input pulse duration

$\delta t = 30 \; fs$

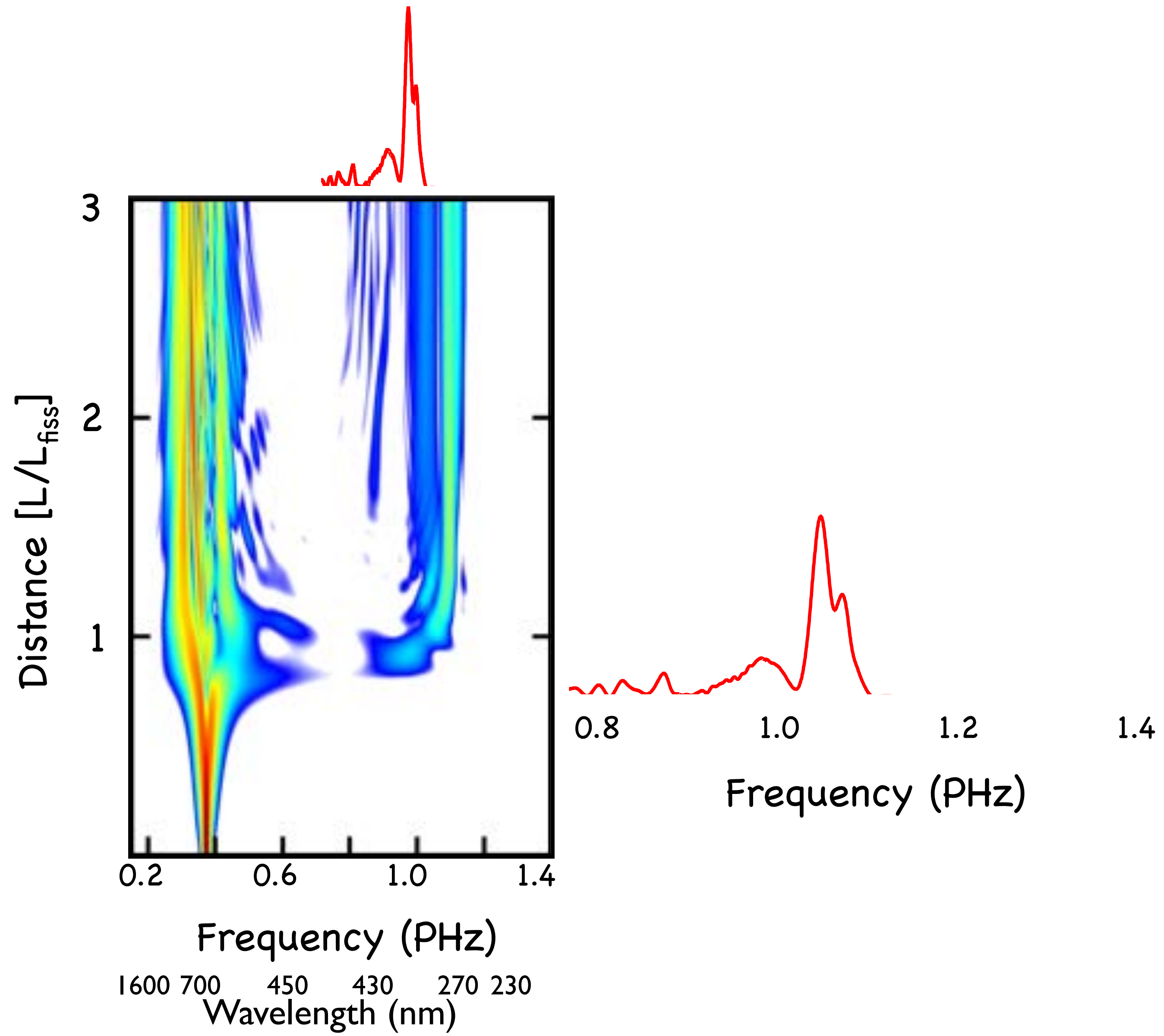

The quality of the compression is inversely proportional to the soliton order
=>, the quality of the generated band is then strongly affected by N

Influence of the input pulse duration

$\delta t = 60\ fs$

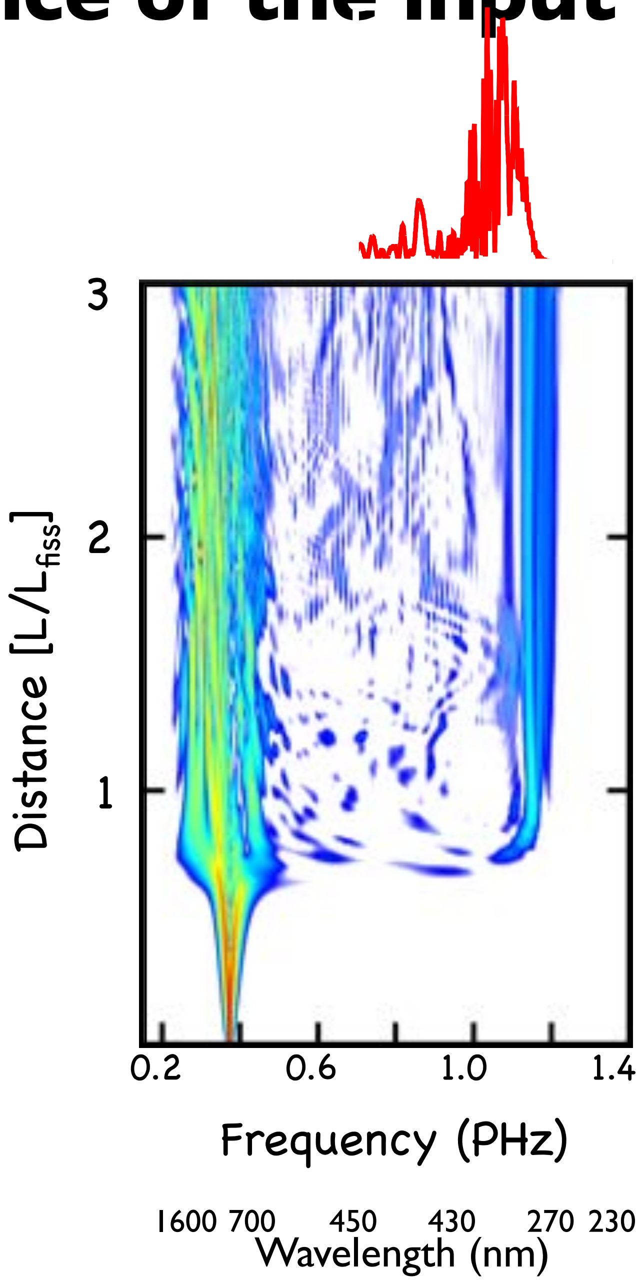

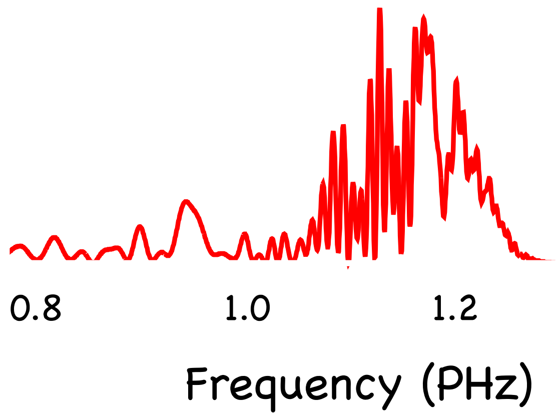

=> the longer the pulse duration, the less clean is the emerging UV band

Influence of the input pulse duration

$\delta t = 120\ fs$

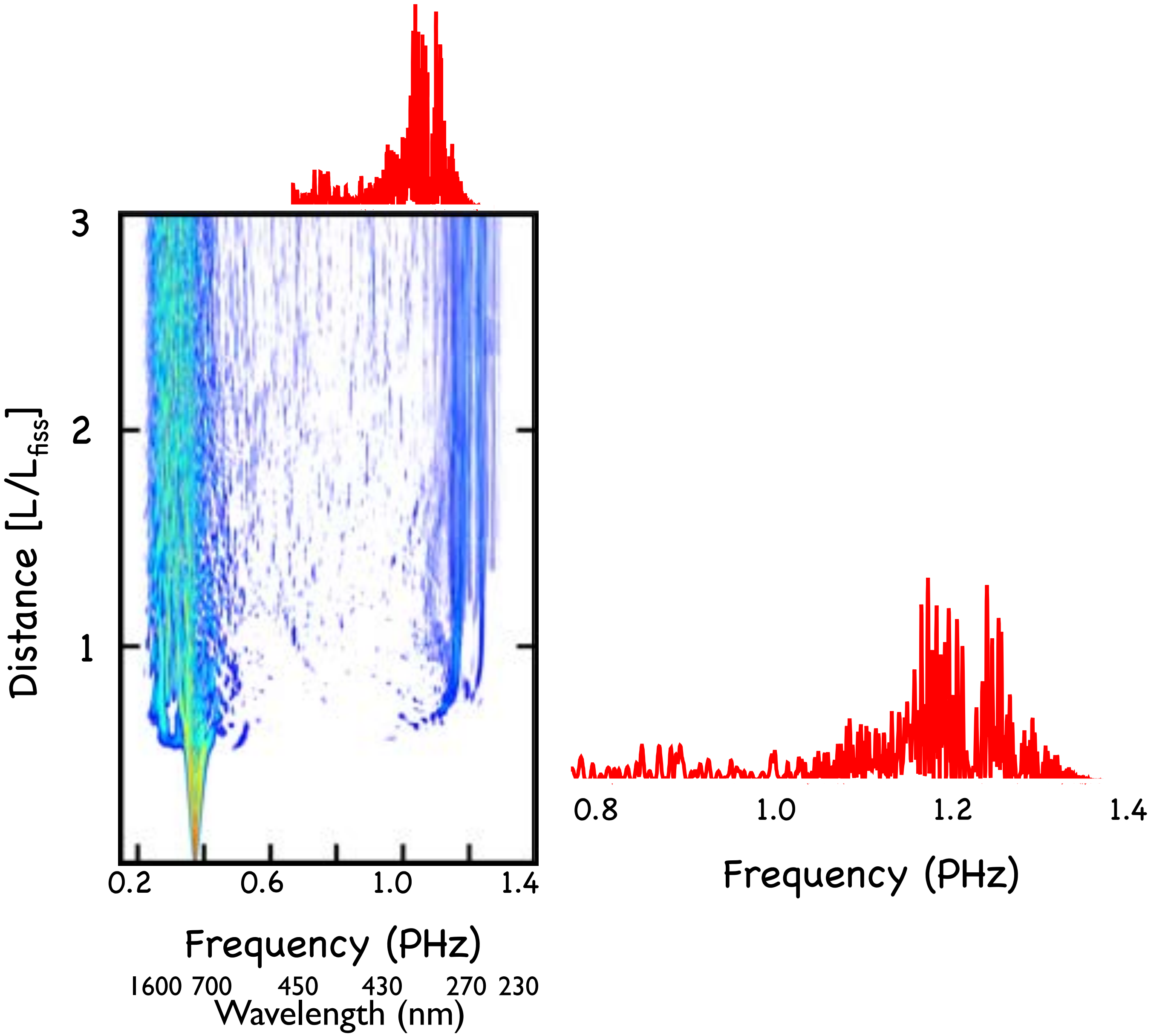

=> the longer the pulse duration, the less clean is the emerging UV band

Influence of the input pulse duration

$\delta t = 15 \ fs$

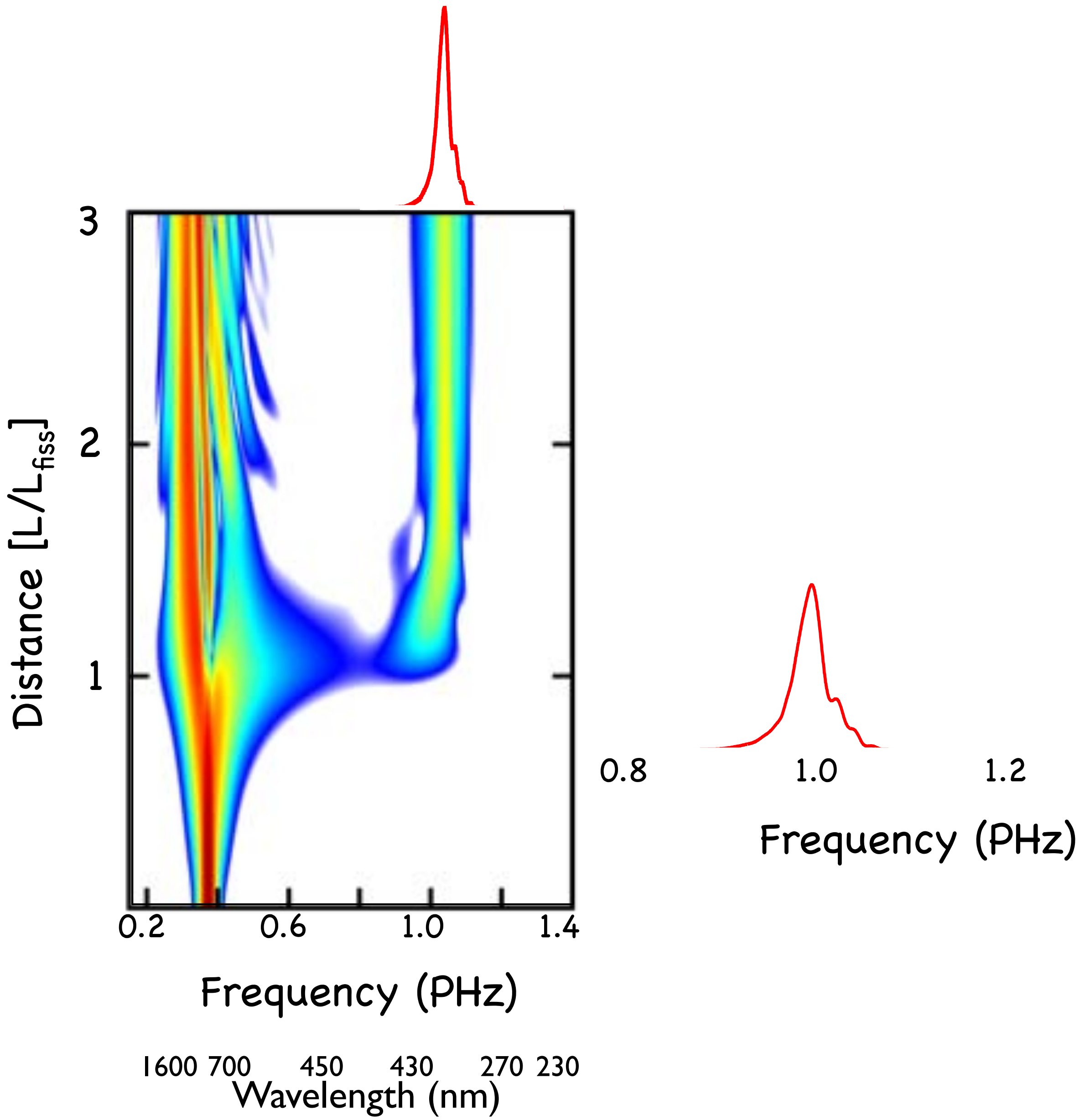

=> Ideally, pulses <60 fs should be used

Proposed experiment at SPARC

SPARC (Frascati, Italy), 176 MeV, 50 A, 1 π mm.mrad, 0.01%

Kagome fiber UV at 275 nm, 10 nJ, 10 fs, 1 MW

=> FEL at 280 nm

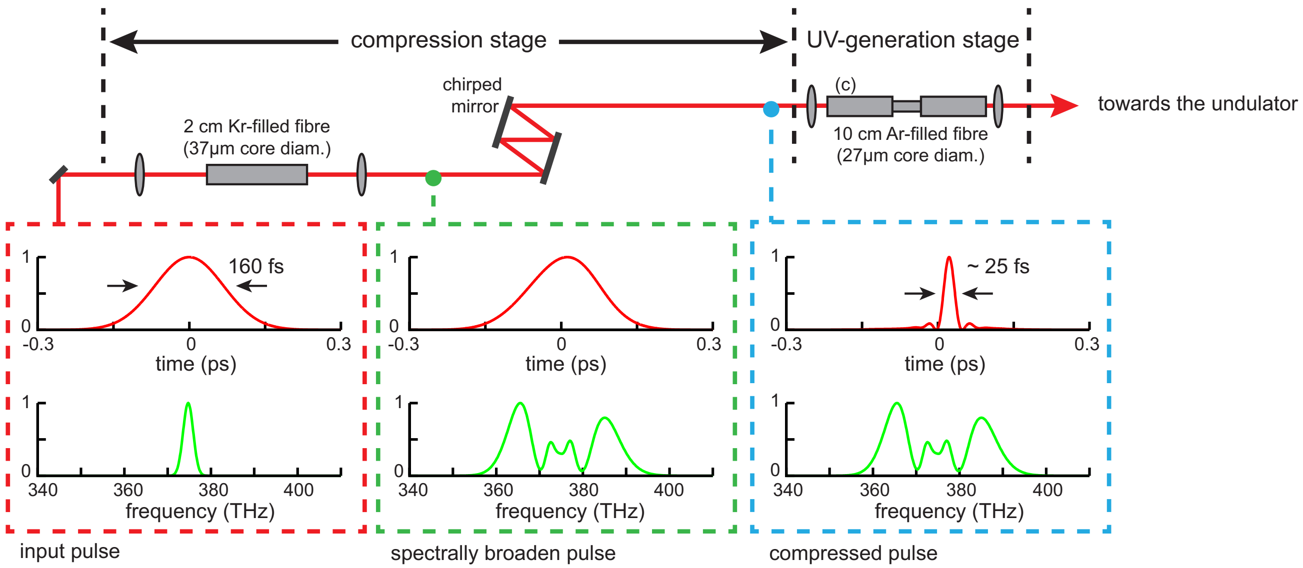

First stage: compress the pulse (10 cm Ar-filled Kagome), second stage : 2 cm Kr filled (37 μm core) for generation of the UV.

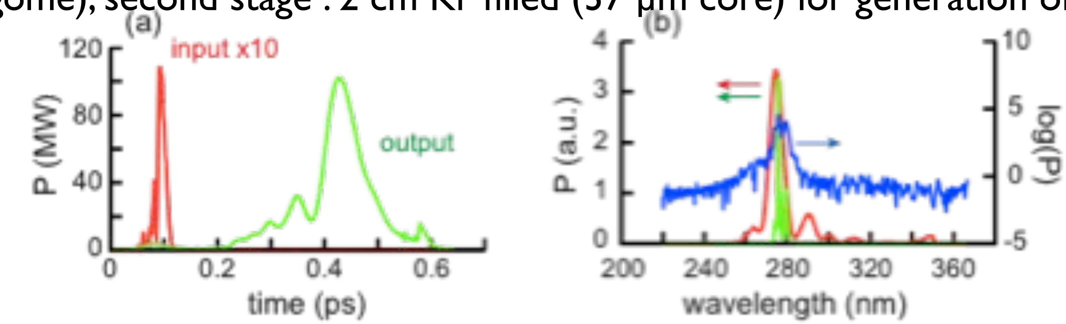

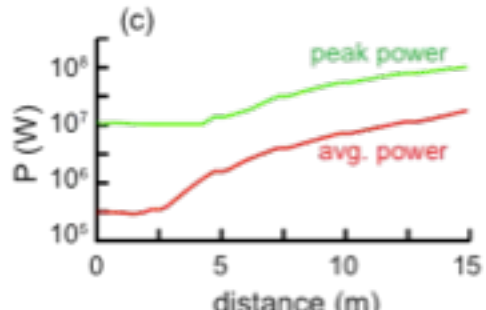

Seeding of SPARC-FEL with a Tunable Fibre-based source, N. Joly et al, TUPD17, Proceedings FEL conf, Nara, Japan, 2012

Conclusion

Seeding : control of FEL performances via the seed (pulse duration... attosecond? ..., stability...)

Compactness

Use of different seeds (short wavelength, tuneable Kagome-fiber) with various frequency up-conversion schemes => short wavelengt FEL

Combination of seeds of different type (echo, TMC...)

Complementary of the seeding source and the FEL on the same site

Combination of different seeds : ex of LUNEX5

free electron **L**aser **U**sing a **N**ew accelerator for the **E**xploitation of **X**-ray radiation of **5**th generation

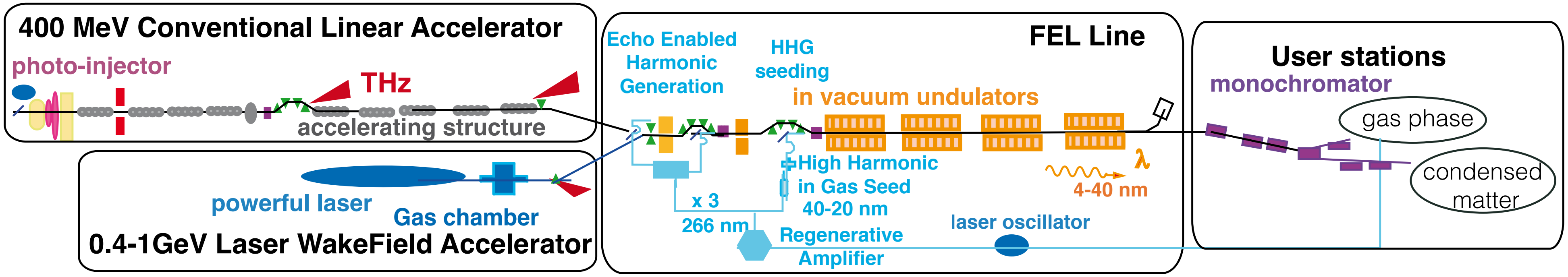

40-4 nm, 20 fs and shorter

Beyond third generation light source (undulator spontaneous emission, partial transverse coherence),

progress towards advanced fourth generation (4G+) light sources (coherent emission, temporal and transverse coherence, femtoseconde pulses, high brilliance) via the latest free electron laser seeding schemes and electron photon interaction, to be validated by pilot user experiments,

=> *Demonstration of echo at short wavelength*

=> *FEL physics*

=> *Advanced design of FEL source for improved performances, associated with cost and size reduction*

and towards fifth generation (5G) (Conventional Linac replaced by a LWFA), FEL being viewed as a qualifying LWFA application *: evaluation of the LWFA performances in «operation-like» conditions (cf EuRRONAc objectives)*

Complementarity CLA / LWFA :

CLA high repetition rate, high reliability, LWFA : ultra-short electron bunch, compacity